

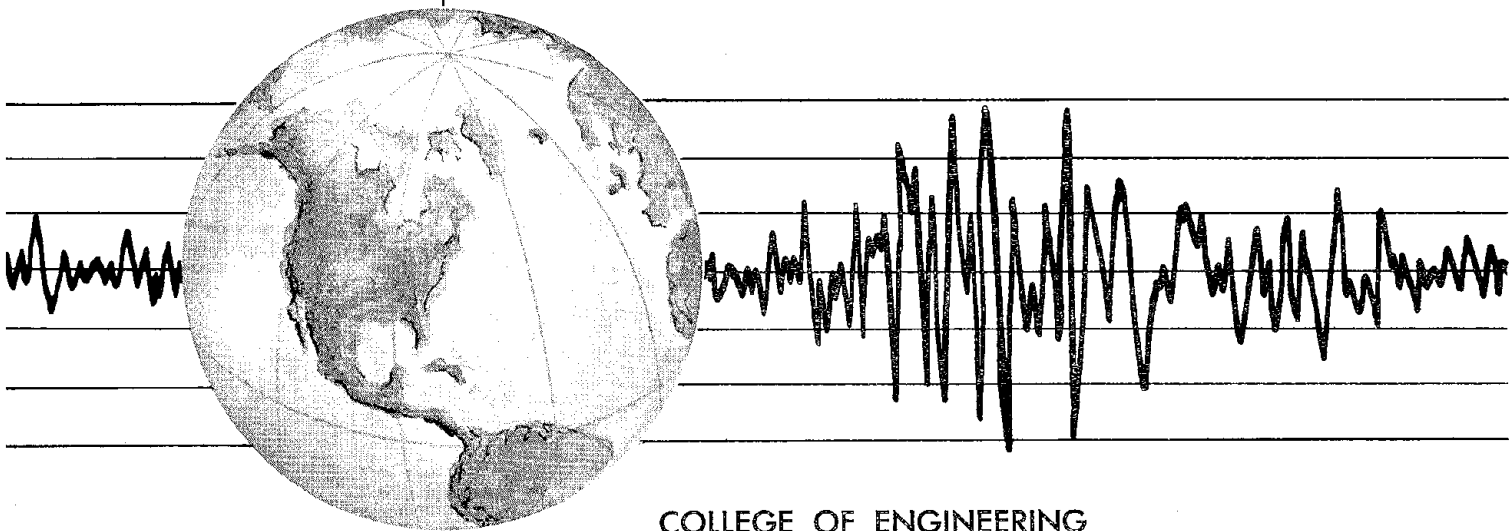
REPORT NO.
UCB/EERC-78/08
MAY 1978

EARTHQUAKE ENGINEERING RESEARCH CENTER

A LABORATORY STUDY OF THE FLUID-STRUCTURE INTERACTION OF SUBMERGED TANKS AND CAISSONS IN EARTHQUAKES

by
ROBERT C. BYRD

Report to Sponsors:
NOAA, Office of Sea Grant
The State Resources Agency of California



COLLEGE OF ENGINEERING
UNIVERSITY OF CALIFORNIA • Berkeley, California

A LABORATORY STUDY OF THE FLUID-STRUCTURE
INTERACTION OF SUBMERGED TANKS AND
CAISSONS IN EARTHQUAKES

by

Robert C. Byrd

Report to

NOAA, Office of Sea Grant
Department of Commerce, Washington, D.C.

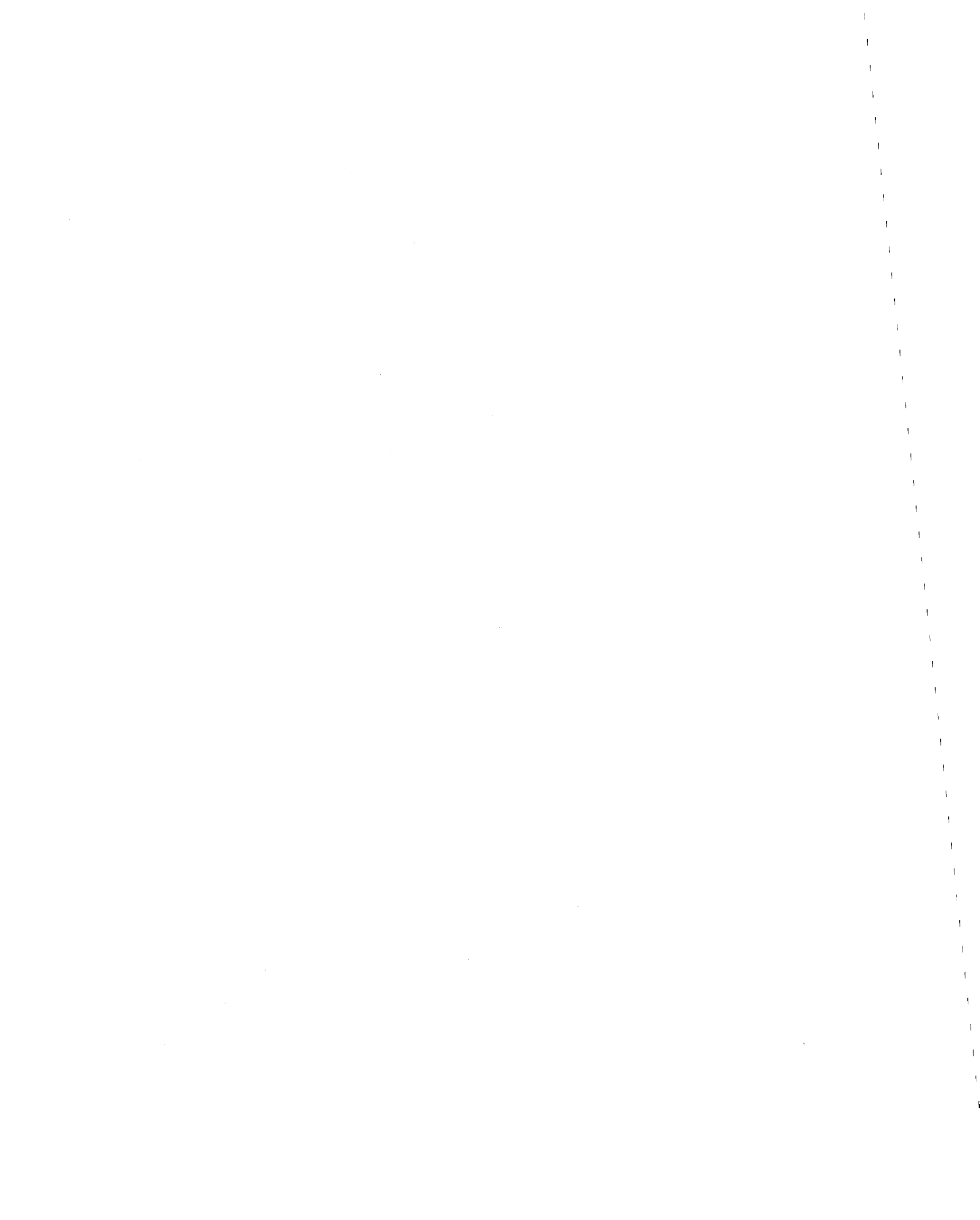
and

The State Resources Agency
of California

Report No. UCB/EERC-78/08
Earthquake Engineering Research Center
University of California
Berkeley, California

May 1978

BIBLIOGRAPHIC DATA SHEET	1. Report No. UCB/EERC-78/08	2.	3. Recipient's Accession No. 1284957
4. Title and Subtitle A Laboratory Study of the Fluid-Structure Interaction of Submerged Tanks and Caissons in Earthquakes		5. Report Date May 1978	
7. Author(s) Robert C. Byrd		6.	
9. Performing Organization Name and Address Earthquake Engineering Research Center University of California, Richmond Field Station 47th Street and Hoffman Blvd. Richmond, California 94804		8. Performing Organization Rept. No.	
		10. Project/Task/Work Unit No. R/E-14	
		11. Contract/Grant No. 04-6-158-44110	
12. Sponsoring Organization Name and Address Sea Grant College Program University of California, San Diego La Jolla, California 92093		13. Type of Report & Period Covered	
		14.	
15. Supplementary Notes			
<p>16. Abstracts</p> <p>An experimental study comparing the results of measurements of forces on a submerged tank model due to earthquake excitation is presented. The experimental results are compared with analytical solutions for the case where the model is submerged in water of depth equal to 2.5 times the tank height and for the case where the depth exactly equals the height.</p> <p>Details are presented for the design of a 1 to 100 scale model of a circular cylindrical structure which is 34 meters in height with a mass of approximately 250,000 tons. The model includes a foundation system which simulates elastic half-space soil stiffness in three degrees of freedom.</p> <p>The experimental results are presented in the form of inertia coefficients measured in harmonic motion at varying amplitudes and over a frequency range of 0.3 Hz to 2 Hz in prototype scale. Coefficients are presented for horizontal, vertical, rotational, and horizontal-rotational coupling. The relationship between these coefficients and the physics of the fluid-structure interaction are discussed in detail.</p> <p>The study leads to the following conclusions concerning earthquake induced forces on large submerged, gravity-type structures:</p> <ul style="list-style-type: none"> a. Available analytical techniques provide good estimates of hydrodynamic inertia force coefficients for submerged structures of simple form. b. A correct estimate of foundation dampening is likely to be the most critical point in calculating the hydrodynamic forces on a submerged gravity structure. c. Foundation stiffness only influences the hydrodynamic force by changing the resonant frequency. d. Frequency dependence in the inertia coefficients is not likely to be an important consideration. e. Coupling in the hydrodynamic inertia forces between the horizontal and rotational modes is not likely to be an important consideration in structural design. f. Hydrodynamic dampening will not be an important factor for deeply submerged structures but may be significant in near surface and surface-piercing structures. <p>17c. COSATI Field/Group</p>			
18. Availability Statement Release Unlimited		19. Security Class (This Report) UNCLASSIFIED	21. No. of Pages 167
		20. Security Class (This Page) UNCLASSIFIED	22. Price \$1.00



ABSTRACT

An experimental study comparing the results of measurements of forces on a submerged tank model due to earthquake excitation is presented. The experimental results are compared with analytical solutions for the case where the model is submerged in water of depth equal to 2.5 times the tank height and for the case where the depth exactly equals the height.

Details are presented for the design of a 1 to 100 scale model of a circular cylindrical structure which is 34 meters in height with a mass of approximately 250,000 tons. The model includes a foundation system which simulates elastic half-space soil stiffness in three degrees of freedom.

The experimental results are presented in the form of inertia coefficients measured in harmonic motion at varying amplitudes and over a frequency range of 0.3 Hz to 2 Hz in prototype scale. Coefficients are presented for horizontal, vertical, rotational, and horizontal-rotational coupling. The relationship between these coefficients and the physics of the fluid-structure interaction are discussed in detail.

The study leads to the following conclusions concerning earthquake induced forces on large submerged, gravity-type structures:

- a. Available analytical techniques provide good estimates of hydrodynamic inertia force coefficients for submerged structures of simple form.
- b. A correct estimate of foundation dampening is likely to be the most critical point in calculating the hydrodynamic forces on a submerged gravity structure.

c. Foundation stiffness only influences the hydrodynamic force by changing the resonant frequency.

d. Frequency dependence in the inertia coefficients is not likely to be an important consideration.

e. Coupling in the hydrodynamic inertia forces between the horizontal and rotational modes is not likely to be an important consideration in structural design.

f. Hydrodynamic dampening will not be an important factor for deeply submerged structures but may be significant in near surface and surface-piercing structures.

ACKNOWLEDGEMENT

This work is a result of research sponsored by NOAA, Office of Sea Grant, Department of Commerce, Under Grant No. 04-6-158-44110, Project No. R/E-14, and by the State Resources Agency of California. The author sincerely appreciates their willingness to fund this program sufficiently to allow for the development of a structural model of high quality--thereby greatly simplifying the analysis and insuring the success of the study.

Professor C. J. Garrison of the Naval Postgraduate School, Monterey, California, was kind enough to perform the diffraction theory calculations for comparison with these experiments. This work has been a major contribution to the scope of this study.

The author is indebted to the faculty investigators for this research project, Professors Ben C. Gerwick, Jr., Joseph Penzien, and Robert L. Wiegel, for providing the necessary advice and guidance during the progress of this research and to Professor William C. Webster for many helpful suggestions in preparing the experiment and performing the analysis. Professor Jorg Imberger helped significantly in developing the proper data analysis techniques.

Special thanks are extended to Professor Wiegel who served as dissertation committee chairman and advisor throughout the author's progress through the doctoral program.

It would not have been possible to conduct this investigation without the able assistance of Mr. Fukij Nilrat in designing the model and carrying out the experiments and without the excellent facilities and personnel of the Earthquake Engineering Research Center.

This work is not copyrighted and is available for reproduction
for non-commercial purposes by anyone.

TABLE OF CONTENTS

	Page
ABSTRACT.	i
ACKNOWLEDGEMENTS.	iii
TABLE OF CONTENTS	v
LIST OF FIGURES	viii
LIST OF TABLES.	xi
LIST OF SYMBOLS AND DEFINITIONS	xii
 1. INTRODUCTION.	 1
1.1 Review of Analytical Procedures.	1
1.2 Objectives and Scope of the Investigation.	3
2. DYNAMICS OF OFFSHORE GRAVITY STRUCTURES IN EARTHQUAKES.	5
2.1 The Equations of Motion.	5
2.2 Scaling of Forces.	6
2.2.1 Forces in Horizontal Motion	7
2.2.2 Forces in Vertical Motion	10
2.3 The Virtual Mass Representation of Fluid Effects . . .	11
2.3.1 Hydrodynamic Pressure	12
2.3.2 The Complex Frequency Response Representation	13
2.3.3 The Acceleration Response Function.	15
2.3.4 The Hydrodynamic Pressure Response Function	16

	Page
3. THE SUBMERGED TANK EXPERIMENT	18
3.1 Model Design	18
3.1.1 The Elastic Foundation.	18
3.1.2 Model Shell and Instrumentation	20
3.2 Experimental Arrangement and Test Procedures.	22
3.3 Data Analysis.	23
4. THE EXPERIMENTAL RESULTS.	39
4.1 General Model Response	39
4.2 Virtual Mass	40
4.3 Hydrodynamic Pressure Force.	42
5. SUMMARY AND DISCUSSION.	69
5.1 Inertia Coefficients	69
5.1.1 Comparison with Theoretical Values.	69
5.1.2 Frequency Dependence.	70
5.1.3 Horizontal-Rotational Coupling.	70
5.2 Hydrodynamic Pressure Force.	71
5.2.1 Parameter Sensitivity	71
5.2.2 Phase Angle	72
5.3 Foundation Forces in Random Excitation	72
6. CONCLUSIONS	86
REFERENCES.	87
APPENDICES	
A. RESPONSE OF ELASTIC FOUNDATIONS.	89
B. MODEL FOUNDATION DESIGN.	98
C. DISCRETE DYNAMIC TIME SERIES ANALYSIS.	106

	Page
D. CONTAPE--PROGRAM LISTING	119
E. MASSCAL--PROGRAM LISTING	123
F. SUBTANK--PROGRAM LISTING	132

LIST OF FIGURES

Figure	Page
1. 1: Prototype System and Model Idealization for the Submerged Tank Experiment	4
3. 1: Prototype Horizontal Foundation Stiffness (K_{xx}^b) Versus Soil Shear Modulus (G)	27
3. 2: Prototype Vertical Foundation Stiffness (K_{zz}^b) versus Soil Shear Modulus (G)	28
3. 3: Prototype Rotational Foundation Stiffness ($K_{\theta\theta}^b$) Versus Soil Shear Modulus	29
3. 4: A Typical Foundation Spring	30
3. 5: A Foundation Spring Instrumented as a Load Cell	31
3. 6: Foundation Load Cell Arrangement	32
3. 7: Instrumentation Arrangement	33
3. 8: Model Internal Arrangement	34
3. 9: The Submerged Tank Model, Side View	35
3.10: The Submerged Tank Model, Top View	36
3.11: The Experiment Arrangement	37
3.12: The Model Basin as Filling Begins	38
4. 1: Uncoupled Resonant Response of the Model, $h/H = 2.5$	45
4. 2: Horizontal Inertia Coefficient, $h/H = 2.5$	46
4. 3: Horizontal Inertia Coefficient, $h/H = 2.0$	47
4. 4: Horizontal Inertia Coefficient, $h/H = 1.5$	48
4. 5: Horizontal Inertia Coefficient, $h/H = 1.0$	49
4. 6: Vertical Inertia Coefficient, $h/H = 2.5$	50
4. 7: Vertical Inertia Coefficient, $h/H = 2.0$	51

Figure	Page
4. 8: Vertical Inertia Coefficient, $h/H = 1.5$	52
4. 9: Rotational Inertia Coefficient, $h/H = 2.5$	53
4.10: Rotational Inertia Coefficient, $h/H = 2.0$	54
4.11: Rotational Inertia Coefficient, $h/H = 1.5$	55
4.12: Rotational Inertia Coefficient, $h/H = 1.0$	56
4.13: Coupled Inertia Coefficient, $h/H = 2.5$	57
4.14: Coupled Inertia Coefficient, $h/H = 2.0$	58
4.15: Coupled Inertia Coefficient, $h/H = 1.5$	59
4.16: Coupled Inertia Coefficient, $h/H = 1.0$	60
4.17: Vertical Inertia Force Representation	61
4.18: Calculated Versus Measured Horizontal Hydrodynamic Force Amplitude, $h/H = 2.5$	62
4.19: Calculated Versus Measured Horizontal Hydrodynamic Force Amplitude, $h/H = 2.0$	63
4.20: Calculated Versus Measured Horizontal Hydrodynamic Force Amplitude, $h/H = 1.5$	64
4.21: Calculated Versus Measured Horizontal Hydrodynamic Force Amplitude, $h/H = 1.0$	65
4.22: Calculated Versus Measured Vertical Hydrodynamic Force Amplitude, $h/H = 2.5$	66
4.23: Calculated Versus Measured Vertical Hydrodynamic Force Amplitude, $h/H = 2.0$	67
4.24: Calculated Versus Measured Vertical Hydrodynamic Force Amplitude, $h/H = 1.5$	68
5. 1: Horizontal Inertia Coefficient (C_{xx}^m) Mean Values Versus Relative Depth (h/H)	76
5. 2: Vertical Inertia Coefficient (C_{zz}^m) Mean Values Versus Relative Depth (h/H)	77
5. 3: Rotational Inertia Coefficient ($C_{\theta\theta}^m$) Mean Values Versus Relative Depth (h/H)	78



Figure	Page
5. 4: Coupled Inertia Coefficient ($C_{\theta x}^m$) Mean Values Versus Relative Depth (h/H)	79
5. 5: Variation in Hydrodynamic Force with Changes in Virtual Mass	80
5. 6: Variation in Hydrodynamic Force with Changes in Foundation Stiffness	81
5. 7: Variations in Hydrodynamic Force with Changes in Foundation Dampening	82
5. 8: Hydrodynamic Force Phase Angle Relative to Foundation Acceleration for Various Values of Foundation Dampening	83
5. 9: Comparison of Measured and Calculated Horizontal Shear Force in the Model for the El Centro (1940) Earthquake, h/H = 2.5	84
5.10: Calculated Horizontal Shear Force in the Model for the El Centro (1940) Earthquake (a) Neglecting Hydrodynamic Dampening (b) With Foundation Dampening Equal to 5% of Critical (c) With Foundation Dampening Equal to 15% of Critical, h/H = 2.5	85

APPENDIX FIGURES

A1: A Gravity Structure in an Exaggerated Displaced Configuration	95
A2: Gravity Structure--Foundation System Idealization	96
A3: Foundation Forces on a Rigid Disk	97
B1: Typical Lumped Mass Idealization of a Foundation Spring, 55 - DOF	103
B2: A Typical Calibration Curve for a Very Stiff Foundation Spring/Load Cell, Horizontal Direction (in English Units)	104
B3: Model Idealization for Foundation Stiffness Evaluation	105
C1: Pressure Gauge Locations for Horizontal Force Determination	117
C2: Pressure Gauge Locations for Vertical Force Determination	118

LIST OF TABLES

Table	Page
3.1: Model Foundation Condition Summary	25
3.2: Submerged Tank Model Dimensions and Characteristics	25
3.3: Instrumentation Specifications	26
4.1: Model Resonant Response Frequencies	44
4.2: Model Dampening Summary	44
5.1: Comparison of Mean Values of Experimentally and Theoretically Determined Inertia Coefficients for the Range of Frequencies of the Experiment	75

APPENDIX TABLES

B1: Foundation Load Cell Calibration Information	102
C1: Data Channel Lists for the Master and Working Tapes	113
C2: Time Series Recorded on Model Response Tapes	116

LIST OF SYMBOLS AND DEFINITIONS

$[A]$	= structure projected area matrix
a	= amplitude of ground motion = u_g , etc.
a_o	= dimensionless frequency parameter for soil stiffness evaluation = $\omega R/C_s$
$[c]$	= foundation dampening matrix
$[C^m]$	= hydrodynamic inertia coefficient matrix = $\rho K_w A$
C_i	= foundation dampening in mode i , neglecting coupling = C_{ii}^b
C_{ij}^b	= foundation dampening in mode i due to motion in mode j
C_{ij}^m	= inertia coefficient for force in mode i due to motion in mode j
C_i^*	= hydrodynamic dampening in mode i , neglecting coupling
C_{il}^*	= hydrodynamic dampening in mode i associated with relative motion between structure and foundation
C_{i0}^*	= hydrodynamic dampening in mode i associated with rigid motion of the structure with the foundation
C_s	= shear wave velocity in the soil
\bar{C}	= total dampening for a given mode, neglecting coupling = $C_i + C_i^*$
D	= structure diameter
F_i	= total force in mode i
F_{ij}	= force in mode i due to motion in mode j
F_{Di}	= hydrodynamic force in mode i due to drag
F_{Ii}	= hydrodynamic force in mode i due to inertia effects

F_{wi}	= hydrodynamic force in mode i due to wave generation
\vec{F}_i^b	= complex frequency dependent force on the structure base in mode i
f_i^b	= time dependent force on the structure base in mode i
G	= soil shear modulus of elasticity
g	= acceleration of gravity - 9.807 m/sec^2
H	= structure height
H'	= effective height of the pressure distribution due to wave generation
h	= water depth
ΔH	= depth of submergence = $h - H$
$[K]$	= foundation stiffness matrix
$[K_d]$	= hydrodynamic drag coefficient matrix
$[K_m^{-1}] = [C^m]$	= hydrodynamic inertia coefficient matrix
$[K_w]$	= wave making coefficient matrix
K_i	= foundation stiffness in mode i neglecting coupling = K_{ii}^b
K_{ij}^b	= foundation stiffness in mode i due to motion in mode j
k	= wave number = $2\pi/\lambda$
L	= foundation spring length
$[M]$	= structure mass matrix
$[M^*]$	= "virtual" or "added" mass matrix due to surrounding fluid = $\rho[C^m] [V]$
M_i	= structure mass in mode i
M_{i1}^*	= virtual mass in mode i associated with relative motion between the structure and foundation
M_{i0}^*	= virtual mass in mode i associated with rigid motion of structure with the foundation
M_{ij}^*	= virtual mass in mode i for motion in mode j

- \bar{M} = total mass for a given mode, neglecting coupling
 $= M_i + M_{ii}^*$
- P_{wi} = pressure due to wave generation by structure motion in mode i
- p^* = time dependent hydrodynamic pressure force
- \bar{p}^* = complex frequency dependent hydrodynamic pressure force
- P_I^*, P_R^* = imaginary and real parts, respectively of the complex hydrodynamic force
- p_i = time dependent hydrodynamic pressure force due to motion in mode i
- \bar{p}_i = total complex frequency dependent hydrodynamic pressure due to motion in mode i
- \bar{p}_{i1} = complex hydrodynamic pressure due to relative motion in mode i between the structure and foundation
- \bar{p}_{i0} = complex hydrodynamic pressure due to rigid motion of the structure and foundation in mode i
- R = structure radius
- R_g = radius of gyration of the displaced volume of water around its center of gravity
 $= \left(\frac{R^2}{4} + \frac{H^2}{12} \right)^{\frac{1}{2}}$, for a circular cylinder
- $\{r\}$ = time dependent displacement vector, relative to the foundation
- $\{r_t\}$ = time dependent total displacement
- S_{ij} = foundation spring stiffness in mode i for displacement in mode j
- t = time
- $\{u_g\}$ = time dependent foundation displacement vector, relative to a fixed reference
- $\{u_w\}$ = time dependent water partical displacement, relative to a fixed reference
- u_g = horizontal component of foundation displacement
- $[v]$ = volume matrix
- v_g = vertical component of foundation displacement

X_s	= horizontal location of the foundation springs from the center of gravity
\bar{X}	= complex frequency dependent horizontal displacement amplitude, relative to the foundation
x	= time dependent horizontal displacement, relative to the foundation
z	= time dependent vertical displacement, relative to the foundation
Z_{cg}	= vertical location of structure center of gravity
Z_s	= vertical location of foundation spring attachment point from the center of gravity
ρ	= mass density of water
ρ_s	= mass density of soil
ξ_i	= foundation dampening in mode i, percent of critical
ξ_i^*	= hydrodynamic dampening in mode i, percent of critical
θ	= angular displacement relative to the foundation
θ_g	= angular component of foundation displacement
ϕ	= linear velocity potential or phase angle, depending on context
σ	= dimensionless frequency parameter $= \frac{\omega^2 \sqrt{DH}}{g}$
λ	= length of generated waves
ω	= radial frequency $= 2\pi/T, \text{ where } T \text{ is the period in seconds}$

1. INTRODUCTION

The progress of offshore development on the North American west coast, in Alaska and around the Pacific Ocean in general in recent years has made it increasingly likely that large volume, gravity-type structures will be desirable in the near future in some applications in areas of high seismic activity. Since this type structure has had little or no prior history in this environment, it was considered desirable to conduct a series of experiments in as realistic conditions as possible in a laboratory to confirm or deny currently used analytic procedures for calculating earthquake forces. The overall purpose of this study is to reduce the uncertainty associated with the fluid-structure interaction aspect of these calculations by answering some of the questions concerning the inertia coefficients.^{1*}

1.1 Review of Analytical Procedures

The details of the analytical procedures will not be discussed in this paper, but it is appropriate to give some consideration to the techniques which are generally used in engineering applications and to the types of problems which they solve. These procedures can be lumped broadly into three categories.

- a. closed form (or continuum) solutions,
- b. diffraction theory based on the use of Green's functions,
- c. variational methods (finite element).

Diffraction and variation methods can be considered as closed-form solutions under some circumstances², but in application they

* Superscripts refer to the corresponding items under 'References'.

involve discretization of the system and are essentially numerical procedures. Wehausen and Laitone³ provide a detailed discussion of the basis for all of these procedures, examples of the application of diffraction theory are shown by Garrison and Chow⁴ and by Hogben and Standing⁵, Bai⁶ and Zienkiewicz and Newton⁷ show examples of fluid problem solutions applying the variational principle to finite elements. Liaw and Chopra⁸ also present a variational method solution for the fluid problem along with a closed-form solution for comparison. Petrauskas⁹ presents a similar closed-form solution.

The assumptions that are generally common to these methods are:

- a. small amplitude displacements such that linear boundary conditions may be assumed,
- b. inviscid fluid (irrotational flow),
- c. incompressible fluid (except as shown in Refs. 7 and 8).

However, the effects of compressibility can be shown to be negligible for the type of structure and motion presently being considered).

Solutions to the fluid problem under these circumstances can be considered as "linear potential flow" solutions, and it can be shown by comparison of the results under similar conditions that the solutions by any of these methods are comparable, as one would hope. All methods are not, however, available under all circumstances with closed-form solutions being limited to simple geometries and diffraction and closed-form solutions being limited to harmonic motions, linear superposition notwithstanding.

It has been shown that all of these methods yield good results under conditions in waves which satisfy their assumptions (see Refs. 6, 9 and 10, for examples). The experiments presented in this report

have attempted to test these assumptions under realistic earthquake conditions. Diffraction calculations were performed by Garrison specifically for comparison with these experiments in the fully submerged condition and a closed-form solution after Liaw was performed for the condition where the structure penetrated the surface.

1.2 Objectives and Scope of the Investigation

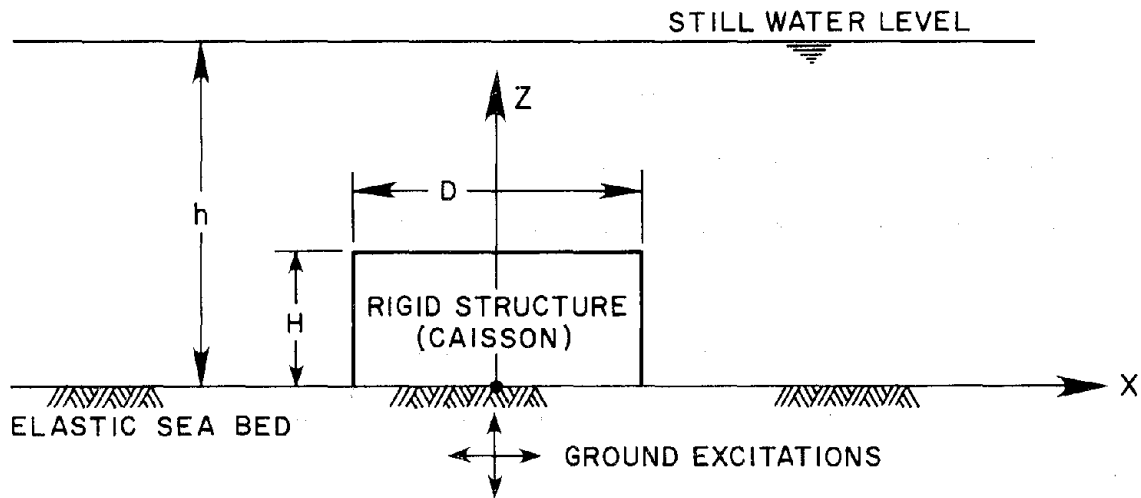
The study has concerned itself with examining the following factors:

- a. The general degree to which analytic procedures can accurately predict hydrodynamic earthquake forces.
- b. The existence of significant frequency dependence over the range of frequencies of interest for earthquakes.
- c. The influence of coupling between modes within the hydrodynamic inertia forces.
- d. The sensitivity of the hydrodynamic forces to changes in the various coefficients.

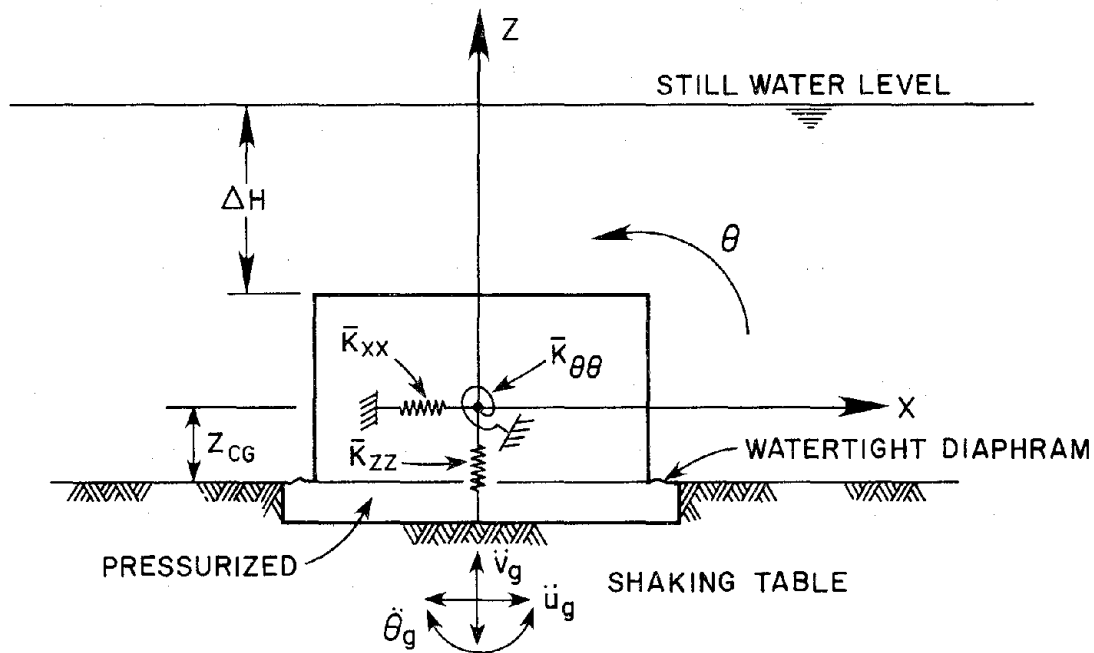
It was desirable to stay as general and simple as possible in selecting a prototype system to model so that the results would be interpretable and broadly applicable--while retaining enough realism to make the effort worthwhile. The following system was selected to satisfy these ends:

- a. A circular cylindrical tank, or gravity structure caisson without a superstructure, of approximately 250,000 tons with a height approximately equal to its radius.
- b. An elastic but firm foundation.
- c. A water depth of approximately 100 meters.

The idealized prototype system is shown in Fig. 1.1.



(a) PROTOTYPE SYSTEM



(b) MODEL IDEALIZATION

FIGURE 1.1: PROTOTYPE SYSTEM AND MODEL IDEALIZATION FOR THE SUBMERGED TANK EXPERIMENT

2. DYNAMICS OF OFFSHORE GRAVITY STRUCTURES IN EARTHQUAKES

2.1 The Equation of Motion

It is appropriate to consider briefly the general equation of motion for a structure in the marine environment, in this case generally following the matrix notation of Penzien:¹¹

$$\begin{aligned}
 [M] \{\ddot{r}_t\} + [C] \{\dot{r}\} + [K] \{r\} = \\
 \rho [K_m - 1] [V] \{\ddot{u}_w - \ddot{r}_t\} \\
 + \rho [V] \{\ddot{u}_w\} \\
 + \rho [K_w] [A] \{\dot{u}_w - \dot{r}_t\} \\
 + \rho [K_d] [A] \{|\dot{u}_w - \dot{r}_t| (\dot{u}_w - \dot{r}_t)\} \dots \dots (2.1)
 \end{aligned}$$

In the general case for an offshore gravity structure, we would be concerned about flexibility in the platform and legs, but we can usually treat the base as being rigid. Since we are only considering the base response in this study we will only concern ourselves with the rigid body response modes. Therefore, we can define:

- $[A]$ = structure projected area matrix,
- $[C]$ = foundation damping matrix,
- $[K]$ = foundation stiffness matrix,
- $[K_d]$ = hydrodynamic drag coefficient matrix,
- $[K_m - 1] = [C^m]$ = hydrodynamic inertia coefficient matrix,
- $[K_w]$ = wave making coefficient matrix,
- $[M]$ = structure mass matrix,
- $\{r\}$ = displacement vector, relative to the moving foundation,
- $\{r_t\}$ = total displacement = $\{r\} + \{u_g\}$,

$\{u_g\}$ = foundation displacement vector, relative to a fixed reference,

$\{u_w\}$ = instantaneous water particle displacement relative to a fixed reference,

$[V]$ = volume matrix.

The experimental work to be discussed was conducted under conditions of initially still water, and we may, therefore, drop water particle motions which are normally caused by waves from further consideration.

2.2 Scaling of Forces

At this point, one should consider the relative magnitudes of the various forces acting on the structure in an earthquake, as defined by Eq. 2.1. We must, therefore, further define the conditions under which we will seek a solution.

Physical considerations indicate that there are six parameters (excluding viscosity) which influence the earthquake forces on marine structures. These are (see Fig. 1.1):

a = amplitude of ground motion = u_g , etc.,

ω = radial frequency of the motion = $2\pi/T$, where T is the period in seconds,

h = water depth,

D = diameter of the structure = $2R$,

H = height of the structure,

g = acceleration of gravity = 9.807 m/sec^2 .

2.2.1 Forces in Horizontal Motion

Examination of the right-hand side of Eq. 2.1 shows that there are three types of forces: (a) inertial, (b) drag, and (c) wave making. If we assume harmonic motion, we can describe the magnitude of these forces with the following approximate relationships for the horizontal mode of motion:

$$F_x = F_{Ix} + F_{Dx} + F_{Wx}$$

and,

$$F_{Ix} = \rho(K_{mx} - 1) \ddot{V} \doteq \rho \frac{\pi D^2}{4} H a \omega^2 \quad \dots \dots \dots (2.2)$$

$$F_{Dx} = \rho K_{Dx} A |\dot{u}| \dot{u} \doteq \rho D H a^2 \omega^2 \quad \dots \dots \dots (2.3)$$

$$F_{Wx} = \rho K_{Wx} A \dot{u} \doteq D H' P_{Wx} \quad \dots \dots \dots (2.4)$$

where: ρ = mass density of the water,

P_w = pressure on the structure due to waves being generated by the structure motion,

H' = effective height of the pressure distribution on the structure.

MacCamy and Fuchs² have shown that there are two components of pressure due to a structure oscillating horizontally in a fluid; (a) one associated with the inertia force term and due to local disturbance of the fluid by the structure, (b) a second in phase with the velocity and due to creation of progressive waves of the same frequency as the oscillations and which transmit energy from the system. The progressive wave pressure term has been shown to extend to an effective depth approximately equal to the wave length, λ .

If we assume a wave amplitude approximately equal to the amplitude of the ground motion, we can describe the velocity potential for the

linear progressive wave as follows:¹²

$$\phi = \frac{a\omega}{k} \frac{\cosh(kZ)}{\cosh(kh)} \sin(kx - \omega t) \dots \dots \dots (2.5)$$

where: $k = \frac{2\pi}{\lambda} = \frac{\omega^2}{g} \tanh(kh)$

The amplitude of the wave making pressure term then becomes:

$$p_{wx} \doteq \rho \frac{\partial \phi}{\partial t} = \frac{\rho a \omega^2}{k} \dots \dots \dots (2.6)$$

We can assume that for all practical cases involving gravity structures and earthquakes,

$$kh \gg 2\pi.$$

Therefore,

$$k = \frac{2\pi}{\lambda} = \frac{\omega^2}{g} \dots \dots \dots (2.7)$$

and

$$\lambda = \frac{2\pi g}{\omega^2} \dots \dots \dots (2.8)$$

We may now rewrite Eq. 2.4 as follows:

$$F_{wx} \doteq \frac{\rho a \omega^2}{k} DH' \doteq \rho a g DH' \dots \dots \dots (2.9)$$

Defining,

$$\Delta H = h - H = \text{depth of submergence.}$$

Then, Eq. 2.9 becomes,

$$F_{wx} \doteq \rho a g D(\lambda - \Delta H), \dots \dots \dots (2.10)$$

where the wave force amplitude is recognized to be positive only.

We are now in position to consider the relative magnitude of the various forces for horizontal motion. Dividing the sum of the forces

by the inertia term we now have:

$$\begin{aligned} \frac{F_x}{F_{Ix}} &\doteq \frac{4\rho DH a^2 \omega^2}{\rho \pi D^2 H a \omega^2} + 1 + \frac{4\rho a g D(\lambda - \Delta H)}{\rho \pi D^2 H a \omega^2} \\ &\doteq \frac{a}{D} + 1 + \frac{g(\lambda - \Delta H)}{DH \omega^2} \dots \dots \dots (2.11) \end{aligned}$$

It is immediately clear that the drag term will not be important, since we are generally considering amplitudes of ground motion much less than one meter and structure diameters of approximately 100 meters. It would appear that structure member diameter would have to be in the order of one or two meters before drag would need to be considered in earthquake motion. This agrees with the general range of importance for drag in waves as found by other investigations.⁵

Consideration of the wave making term shows a somewhat more complex situation. We can, however, see immediately from Eq. 2.10 that energy will not be dissipated by wave making for any structure where the depth of submergence exceeds the wave length, or:

$$\Delta H \geq \frac{2\pi g}{\omega^2} \dots \dots \dots (2.12)$$

For the case where structure height equals water depth ($\Delta H = 0$), the wave making force ratio in Eq. 2.11 becomes:

$$\begin{aligned} \frac{F_{Wx}}{F_{Ix}} &\doteq \frac{g\lambda}{DH\omega^2} = \frac{2\pi g^2}{DH\omega^4} \\ &= \frac{2\pi}{\sigma^2} \dots \dots \dots (2.13) \end{aligned}$$

where,

$$\sigma = \frac{\omega^2 \sqrt{DH}}{g} \dots \dots \dots (2.14)$$

We can conclude that where the dimensionless frequency parameter, σ , is large, little energy will be dissipated through wave making, regardless of the depth of submergence, ΔH . However, a considerable amount of energy could be dissipated by wave making at low frequencies and shallow submergence depths.

2.2.2 Forces in Vertical Motion

The forces due to vertical motion of the structure can be written approximately as:

$$F_z = F_{Iz} + F_{Dz} + F_{Wz}$$

and,

$$F_{Iz} = \rho(K_{mz} - 1) \ddot{V} \doteq \rho \frac{\pi D^2}{4} Ha \omega^2 \dots \dots \dots (2.15)$$

$$F_{Dz} = \rho K_{Dz} A |\dot{V}| \dot{V} \doteq \rho \frac{\pi D^2}{4} a^2 \omega^2 \dots \dots \dots (2.16)$$

$$F_{Wz} = \rho K_{Wz} A \dot{V} \doteq \frac{\pi D^2}{4} P_{Wz} \dots \dots \dots (2.17)$$

We note that the wave pressure force again is intended to describe the effect of waves propagating from the system. Unfortunately, we do not have a convenient expression to describe this quantity. However, we can define the region in which it is likely to become important by noting that the wave length of the highest frequency wave which could propagate completely from the vicinity of the disturbance caused by structure motion would be equal to the diameter of the structure, i.e.

$$\lambda_{\text{critical}} = D \dots \dots \dots (2.18)$$

This follows from the relationships between wave length, propagation speed, and frequency in deep water.¹² We can now define a critical

frequency above which we would expect energy loss due to wave making to decrease rapidly:

$$\omega_{\text{critical}} = \left(\frac{2\pi g}{D} \right)^{\frac{1}{2}} \quad \dots \dots \dots (2.19)$$

Examination of the ratio of drag to inertia force yields

$$\frac{F_{DZ}}{F_{IZ}} = \frac{a}{H} \quad \dots \dots \dots (2.20)$$

Once again we can conclude that the drag force will be negligible for most gravity structures.

2.3 The Virtual Mass Representation of Fluid Effects

We can now rewrite the equation of motion in simplified form as:

$$[M] \{\ddot{r}_t\} + [C] \{\dot{r}\} + [K] \{r\} = - [M^*] \{\ddot{r}_t\} - [C^*] \{\dot{r}_t\}, \quad \dots \dots \dots (2.21)$$

with notation as before except:

$[M^*]$ = matrix of the "virtual" or "added" mass of the surrounding water

$$= \rho [C^m] [V]$$

$[C^*]$ = coefficient of equivalent hydrodynamic damping, due primarily to wave making at shallow water depths.

$$\doteq \rho [K_w] [A]$$

The purpose of this investigation was primarily to shed additional light on the virtual mass matrix $[M^*]$ under earthquake conditions and to compare the findings with analytical methods for computing these effects.

The term "virtual mass" is used in this report in the same context as "added mass". Virtual mass is favored as a term for describing the inertial effect of the surrounding fluid because, depending on the usage, the effect is not always additive.

It is now convenient to dispense with the matrix notation and write Eq. 2.21 as three independent mode equations:

$$M_x \ddot{x}_t + C_x \dot{x}_t + K_x x_t = -M_{xx}^* \ddot{x}_t - M_{x\theta}^* \ddot{\theta}_t - C_x^* \dot{x}_t \dots (2.22)$$

$$M_z \ddot{z}_t + C_z \dot{z}_t + K_z z_t = -M_{zz}^* \ddot{z}_t - C_z^* \dot{z}_t \dots (2.23)$$

$$M_\theta \ddot{\theta}_t + C_\theta \dot{\theta}_t + K_\theta \theta_t = -M_{\theta\theta}^* \ddot{\theta}_t - M_{\theta x}^* \ddot{x}_t - C_\theta^* \dot{\theta}_t \dots (2.24)$$

It would be expected that the coupled virtual mass terms $M_{x\theta}^*$ and $M_{\theta x}^*$ are approximately equal and that they are not particularly large. This last hypothesis will be supported by the test results which we shall discuss later. The rotational acceleration, $\ddot{\theta}_t$, is also very small in the experimental system and we would expect that the coupled force term would drop out of Eq. 2.22.

2.3.1 Hydrodynamic Pressure

Before we proceed with the discussion of the submerged tank experiment, it is enlightening to consider the fundamentals of the virtual mass representation of fluid effects on structures. The following discussion will be limited to the rigid body mode of horizontal motion on a flexible foundation; interested readers are referred to Chapter 2 of Liaw and Chopra⁸ for a discussion of the effects of structure flexibility modes on virtual mass.

The uncoupled equation for horizontal motion including fluid effects can be written (see Fig. 1.1):

$$M_x \ddot{x}(t) + C_x \dot{x}(t) + K_x x(t) = -M_x \ddot{u}_g(t) - P_x^*(t) \dots (2.25)$$

where $P_x^*(t)$ represents the force in the horizontal mode of oscillation associated with the hydrodynamic pressure, $p_x(z, \phi, t)$. This quantity is described by the Laplace equation in cylindrical coordinates,

$$\frac{\partial^2 P}{\partial r^2} + \frac{1}{r} \frac{\partial P}{\partial r} + \frac{1}{r^2} \frac{\partial^2 P}{\partial \phi^2} + \frac{\partial^2 P}{\partial z^2} = 0 \quad (2.26)$$

which, after applying appropriate boundary conditions, can be solved for the dynamic pressure distribution on the surface of simply shaped structures which pierce the surface.^{8,9} If such a solution is available, then

$$P_x^*(t) = \int_0^H \int_0^{2\pi} p_x(z, \phi, t) R \cos \phi d\phi dz \quad (2.27)$$

2.3.2 The Complex Frequency Response Representation

One characteristic of linear systems with time independent physical properties is that they respond to simple harmonic excitation with simple harmonic motion of the same frequency, once steady-state conditions have been achieved. The amplitude and phase relationship of this response is frequency dependent in general. This frequency dependence is conveniently described by the use of complex frequency response functions. The complex response function $x(t)$ is written as $\bar{X}(\omega)$ and has the property that when the excitation is the real part of $e^{i\omega t}$, the response is the real part of $\bar{X}(\omega) e^{i\omega t}$.

Applying this to the hydrodynamic pressure from Eq. 2.27, we have for the pressure on the surface of an oscillating structure

$$p_x(z, \phi, t) = \bar{p}_x(z, \phi, \omega) e^{i\omega t} \quad (2.28)$$

and for the kinematic quantities in Eq. 2.25,

$$\begin{aligned} \ddot{x}(t) &= \bar{\ddot{X}}(\omega) e^{i\omega t} \\ \dot{x}(t) &= -i \frac{\bar{\ddot{X}}(\omega)}{\omega} e^{i\omega t} \\ x(t) &= -\frac{\bar{\ddot{X}}(\omega)}{\omega^2} e^{i\omega t} \end{aligned} \quad (2.29)$$

where all are expressed in terms of the complex acceleration response function.

It is now convenient to describe the dynamic pressure on the surface of the cylinder in terms of total structure acceleration, assuming that linear superposition applies, and ground acceleration is $\ddot{u}_g = e^{i\omega t}$,

$$p_x(z, \phi, t) = [\bar{p}_{xo}(z, \phi, \omega) + \bar{p}_{xl}(z, \phi, \omega) \bar{\bar{x}}(\omega)] e^{i\omega t} \dots (2.30)$$

Replacing the time dependent pressure in Eq. 2.27 with Eq. 2.30, we have:

$$p_x^*(t) = \left[\int_0^H \int_0^{2\pi} \bar{p}_{xo}(z, \phi, \omega) R \cos \phi d\phi dz + \bar{\bar{x}}(\omega) \int_0^H \int_0^{2\pi} \bar{p}_{xl}(z, \phi, \omega) R \cos \phi d\phi dz \right] e^{i\omega t} \dots (2.31)$$

We can now see that the first term on the right of Eq. 2.31 represents the complex hydrodynamic "mass" associated with the rigid motion of the structure on its foundation and the second term represents "mass" associated with the relative motion between the structure and the foundation.

It is more physically relevant to describe these complex "mass" terms as a real virtual mass and a real dampening which is associated with the wave making component of pressure acting on the structure. The terms in Eq. 2.31 become,

$$\int_0^H \int_0^{2\pi} \bar{p}_{xo}(z, \phi, \omega) R \cos \phi d\phi dz = M_{xo}^*(\omega) - \frac{iC_{xo}^*(\omega)}{\omega} \dots (2.32a)$$

$$\int_0^H \int_0^{2\pi} \bar{p}_{xl}(z, \phi, \omega) R \cos \phi d\phi dz = M_{xl}^*(\omega) - \frac{iC_{xl}^*(\omega)}{\omega} \dots (2.32b)$$

We note that in the case of horizontal motion the terms for rigid and relative motion are the same for a rigid structure on an elastic foundation, however, in general they are not.

Returning to the notation used in Eq. 2.22, we can now describe the hydrodynamic forces of Eq. 2.27 as

$$\begin{aligned} P_x^*(t) &= \left[\{M_{xx}^*(\omega) + M_{xx}^*(\omega) \ddot{X}(\omega)\} - \frac{i}{\omega} \{C_x^*(\omega) + C_x^*(\omega) \ddot{X}(\omega)\} \right] e^{i\omega t} \\ &= \bar{P}_x^*(\omega) e^{i\omega t} \quad \dots \dots \dots (2.33) \end{aligned}$$

We emphasize that in the general case, the coefficients may be frequency dependent.

2.3.3 The Acceleration Response Function

Substituting Eq. 2.33 and Eq. 2.29 into Eq. 2.25, we have

$$\begin{aligned} \left[M_x \ddot{X}(\omega) - \frac{iC_x \ddot{X}(\omega)}{\omega} - \frac{K_x \ddot{X}}{\omega^2} \right] e^{i\omega t} &= \left[-M_x - M_{xx}^*(\omega) - M_{xx}^*(\omega) \ddot{X}(\omega) \right. \\ &\quad \left. + \frac{iC_x^*(\omega)}{\omega} + \frac{iC_x^*(\omega) \ddot{X}(\omega)}{\omega} \right] e^{i\omega t} \dots \dots \dots (2.34) \end{aligned}$$

This expression can be solved for $\ddot{X}(\omega)$, which represents the acceleration amplification factor for horizontal motion. The solution yields:

$$\ddot{X}(\omega) = \frac{\{\bar{M}(-\omega^2\bar{M} + K) - C^*\bar{C}\} + i\{-\frac{C^*}{\omega}(-\omega^2\bar{M} + K) - \omega\bar{C}\bar{M}\}}{\omega^2\bar{M}^2 - 2\bar{M}K + \frac{K^2}{\omega^2} + \bar{C}^2} \dots \dots \dots (2.35)$$

where directional and frequency dependent notation have been dropped in the coefficients and where

$$\bar{M} = M_x + M_{xx}^*$$

and,

$$\bar{C} = C_x + C_x^* \quad \dots \dots \dots (2.36)$$

2.3.4 The Hydrodynamic Pressure Response Function

We can now describe the hydrodynamic pressure in terms of the acceleration response function as

$$\begin{aligned} \bar{P}^*(\omega) &= \{M^* + M^* \ddot{X}_R(\omega) + \frac{C^*}{\omega} \dot{X}_I(\omega)\} + i\{M^* \ddot{X}_I(\omega) - \frac{C^*}{\omega} - \frac{C^*}{\omega} \ddot{X}_R(\omega)\} \\ &= P_R^*(\omega) + i P_I^*(\omega) \quad \dots \dots \dots (2.37) \end{aligned}$$

where \ddot{X}_R and \ddot{X}_I are the magnitudes of the real and imaginary parts of Eq. 2.35, respectively.

We can now describe a convenient expression for the steady-state harmonic pressure force function of Eq. 2.31 in terms of structure system characteristics and hydrodynamic coefficients. Recalling that the response to the real part of the excitation $e^{i\omega t}$ is the real part of $\bar{P}_x^*(\omega) e^{i\omega t}$ (Eq. 2.33), we can state the harmonic pressure response as

$$P^*(t) = P_R^*(\omega) \cos(\omega t) - P_I^*(\omega) \sin(\omega t) \quad \dots \dots \dots (2.38)$$

This expression represents hydrodynamic pressure force per unit of ground acceleration. For the cases where dampening due to wave making can be ignored, this expression in its entirety becomes:

$$\begin{aligned} P^*(t) &= \left\{ M^* + \frac{M^*(-\omega^2 \bar{M}^2 + \bar{M}K)}{\omega^2 \bar{M}^2 - 2\bar{M}K + \frac{K^2}{\omega^2} + C^2} \right\} \cos(\omega t) \\ &+ \left\{ \frac{\omega M^* \bar{M}C}{\omega^2 \bar{M}^2 - 2\bar{M}K + \frac{K^2}{\omega^2} + C^2} \right\} \sin(\omega t) \quad \dots \dots \dots (2.39) \end{aligned}$$

where,

\bar{M} = total mass as in Eq. 2.35,

M^* = hydrodynamic virtual mass, the real part of Eq. 2.32,

C = foundation damping only,

$= 2\xi_n \bar{\omega}_n M_n$ where ξ_n is percent of critical damping, $\bar{\omega}_n$ is the natural frequency of the system in that mode, and M_n is the dry mass of the structure,

K = foundation stiffness,

ω = radial frequency of the excitation.

The magnitude of the hydrodynamic pressure force is

$$|\bar{P}^*(\omega)| = (P_R^{*2} + P_I^{*2})^{\frac{1}{2}} \quad \dots \dots \dots (2.40)$$

and the phase angle relative to ground acceleration is

$$\phi = \text{ARCTAN} \left(\frac{P_I^*}{P_R^*} \right) \quad \dots \dots \dots (2.41)$$

It should be noted that an expression for vertical pressure force can be developed in a similar manner. The differences occur because the virtual mass and dampening terms as described in Eq. 2.32a and 2.32b are not equal for the vertical case. These differences must be considered in the pressure response function, Eq. 2.37, and when developing the acceleration response function, Eq. 2.35. The nature of the vertical virtual mass terms will be discussed further in Chapter 4.

3. THE SUBMERGED TANK EXPERIMENT

Before proceeding into the details of the submerged tank model and experiment, we shall take a closer look at the reduced equations of motion as stated in Eqs. 2.22 - 2.24. We have previously stated that the coupled terms can be dropped from Eq. 2.22. With this simplification we can rewrite all of the equations for solution:

$$M_{xx}^* \ddot{x}_t = -M_x \ddot{x}_t - C_x \dot{x} - K_x x - C_x^* \dot{x}_t \quad \dots \quad (3.1)$$

$$M_{zz}^* \ddot{z}_t = -M_z \ddot{z}_t - C_z \dot{z} - K_z z - C_z^* \dot{z} \quad \dots \quad (3.2)$$

$$M_{\theta\theta}^* \ddot{\theta}_t + M_{\theta x}^* \ddot{x}_t = -M_\theta \ddot{\theta}_t - C_\theta \dot{\theta} - K_\theta \theta - C_\theta^* \dot{\theta} \quad \dots \quad (3.3)$$

3.1 Model Design

The general intent of the model design for the experiment was, simply stated, to be able to measure or at least accurately estimate all of the coefficients and kinematic quantities in Eq. 3.1 - 3.3 which are required for solution for the virtual mass terms in $[M^*]$, while allowing the possibility of varying the foundation stiffness in a controlled manner.

The design was simplified by the fact that the prototype was axisymmetric, therefore requiring only three degrees of freedom in a two-dimensional plane (see Fig. 1.1).

3.1.1 The Elastic Foundation

The single most challenging feature in the model design was to simulate an elastic foundation such that an appropriate relationship could be maintained between horizontal and rotational stiffness and

therefore provide a more realistic framework in which to access the importance of hydrodynamic coupling and the possible influence of nonlinearities. An elastic half-space formulation for foundation impedances was chosen from which to derive the stiffness coefficients.¹³ An appropriate mean stiffness value for the frequency range tested was chosen in each case. APPENDIX A contains the details of the foundation impedances considerations and the approximations which were necessary to select appropriate stiffness coefficients. The results of this analysis are shown in Figures 3.1 - 3.3. The approximate equivalent prototype stiffnesses for the three foundation conditions examined are indicated on these figures. It was unnecessary to maintain a consistent relationship between the vertical stiffness and stiffness in the other two modes, since no coupling was anticipated with the vertical mode. The vertical stiffnesses used were somewhat greater than required by the elastic half-space model for the respective horizontal and rotational stiffness. This resulted from construction considerations. Elastic coupling in the foundation was also eliminated so that analysis of hydrodynamic coupling would be simpler (see APPENDIX B).

The early stages of foundation design included plans for adding viscous damping to the foundation in approximate agreement with that called for by the elastic half-space model. Careful consideration of the dynamics of the system (see Eq. 2.35) revealed, however, that added foundation dampening would only mask the effect of hydrodynamic dampening, if any existed. Therefore, this feature was excluded from the final model design. The completed model was found to have approximately 0.8% of critical dampening in all three modes in the dry condition, as will be discussed in Chapter 4.

Control of the foundation stiffness was accomplished by the

design of compound cantilever springs, an example of which is shown in Fig. 3.4. The details of the stiffness analysis of these load cells and their operation in the model are contained in APPENDIX B. As is demonstrated, these cells could be assembled to give an appropriate stiffness in the axial direction and in shear, and produced no rotational coupling when assembled in the model with the model center of gravity adjusted vertically to the midpoint of the four load cells. The load cells were instrumented with full bridge strain gauge rosettes for force measurements in both the axial and shear directions, as shown in Fig. 3.5. Each load cell was calibrated on a dynamometer for its exact stiffness in the two directions and for force-strain relationships. Examples of these calibrations for the three conditions are contained in APPENDIX B. Table 3.1 contains a summary of the mean stiffness values of the three conditions and their approximate equivalent secant stiffness modulus (G/S_u) for the prototype system.

Fig. 1.1 shows the model idealization of the prototype system. Fig. 3.6 shows the general arrangement of the load cells on the model base, with typical dimensions indicated.

3.1.2 Model Shell and Instrumentation

The shell of the model was designed to be simple and rigid. The cylindrical portion was rolled from a 25 mm thick aluminum plate. The top and bottom plates were of 19 mm thick aluminum and were fitted with neoprene gaskets to form watertight seals to the cylinder. The bottom gasket extended out from the model and attached to the foundation plate on which the model was mounted. This gasket completed the watertight seal and was flexible enough to allow free movement of the model. The details of this arrangement are shown in Fig. 3.7.

The model shell was suspended on the foundation load cells from the top of the bottom plate, Fig. 3.8, with the upper part of each load cell being attached to an aluminum center post which was in turn attached to the shaking table. All of the model structural parts were reinforced to the fullest extent to hold deformations to a minimum.

The final weight balance in the model was accomplished by attaching lead weights at appropriate locations such that a mass distribution which was considered reasonable for a structure of this nature could be achieved. Table 3.2 shows the final dimensions and weight characteristics of the model and an equivalent prototype on a scale of 1:100.

Four different types of instrumentation were installed in the model:

- a. accelerometers for recording total accelerations in the three degrees of freedom of the model and horizontally and vertically on the foundation. Angular acceleration was recorded on the shaking table itself.
- b. displacement transducers for relative displacements of the model from the foundation.
- c. full bridge strain gauge rosettes on each load cell, one each for horizontal and vertical directions, calibrated to read foundation spring forces directly.
- d. pressure sensors in one quadrant, arranged at Gaussian quadrature points for integration of forces.

The general arrangement of the instrumentation is shown in Figs. 3.7 and 3.8. Table 3.3 lists the details and specification for the actual instruments used. The actual model with cover and foundation

support removed is shown in Figs. 3.9 and 3.10.

The model interior was pressurized to an equivalent hydraulic head exceeding the actual water depth by approximately 30 cm. during all tests to protect the instrumentation.

3.2 Experimental Setup and Test Procedures

Testing of the submerged tank model was conducted in two test series on the earthquake simulator, located at the Earthquake Engineering Research Center, Richmond Field Station, University of California, Berkeley. The facility contains a 6-by-6-meter, shaking table with a load carrying capacity of approximately 60 metric tons. The table can be excited harmonically either horizontally, vertically, or both simultaneously at frequencies up to approximately 30 Hz. It has a maximum horizontal stroke amplitude of approximately 15 cm and can achieve accelerations of approximately 1 g ($g = 980.7 \text{ cm/sec}^2$) within the stroke limitation. Random excitations can be induced in the table from magnetic tape input. The facility has direct recording capabilities for 128 digitized data channels to computer compatible magnetic tape.

A rigid bulkhead was constructed to surround the shaking table, and a flexible membrane was placed over the table and bulkhead to form the test basin. Figure 3.11 shows the experiment arrangement and Fig. 3.12 shows the basin and model as filling begins.

The test procedure for each foundation condition and water depth was approximately as follows:

- a. shock tests for natural frequencies,
- b. vertical and horizontal harmonic tests over the range of frequencies from 3 to 19 Hz, using at least two different values of

acceleration in most cases, up to a maximum of about 0.5 g when conditions allowed,

c. vertical and horizontal random excitation with maximum acceleration of approximately 0.3 g.

This procedure was also carried out for the dry condition for calibration purposes.

Four water depths were tested in this study, ranging from level with the model top to a maximum of 2.5 times the height of the model, a depth of 85 centimeters.

3.3 Data Analysis

Referring to Eq. 3.1 - 3.3, the tests yielded the following information in our effort to solve for the virtual mass terms:

- a. direct measurement of the total structure acceleration, $\{\ddot{r}_t\}$,
- b. direct measurement of foundation acceleration, $\{\ddot{u}_g\}$,
- c. direct measurement of structure relative displacement, $\{r\}$,
- d. direct measurement of structure mass, $[M]$,
- e. determination of material damping in each mode from the dry shock tests, $[C]$,
- f. direct measurement of foundation stiffness, $[K]$,
- g. determination of damping due to hydrodynamic effects from the submerged shock tests, $[C^*]$.

The only remaining quantities needed in order to proceed with the solution were the velocities, and these were calculated from the acceleration and displacement time series using numerical integration and differentiation schemes.

In theory Eqs. 3.1 and 3.2 could be solved at any point in the response time series for M_{xx}^* and M_{zz}^* , since they are satisfied for all time and regardless of the nature of the motion. In fact, linear regression techniques¹⁴ must be applied using a large number of data points before reliable results can be achieved. Multiple regression¹⁵ was used in solving Eq. 3.3 for $M_{\theta\theta}^*$ and $M_{\theta x}^*$.

The details of the time series analysis and virtual mass calculations are contained in APPENDIX C. The computer program used to convert the raw experimental data to model response is listed in APPENDIX D. The program used to analyze the model response and calculate the virtual mass is listed in APPENDIX E.

TABLE 3.1: MODEL FOUNDATION CONDITION SUMMARY (MODEL UNITS)

COND. NO.	K_x (N/m)	K_z (N/m)	K_θ (N-m/RAD)	APPROX. PROTOTYPE SECANT MODULUS (G/Su)	
				HORIZ. & ROT.	VERTICAL
1	2.9×10^6	5.2×10^6	3.2×10^5	2500	3000
2	1.9×10^6	4.8×10^6	2.1×10^5	1600	3000
3	5.3×10^5	1.5×10^6	5.2×10^4	500	1000

TABLE 3.2: SUBMERGED TANK MODEL DIMENSIONS AND CHARACTERISTICS

	MODEL	PROTOTYPE (SCALE 1:100)
HEIGHT (H)	34.3 cm	34.3 m
DIAMETER (D)	80.3 cm	80.3 m
C.G. HEIGHT	13.4 cm	13.4 m
MASS	249.8 kg	249,800 TONS
RADIUS OF GYR.	26.2 cm	26.2 m
CONSTRUCTION	MACHINED ALUMIMUM	RIGID

TABLE 3.3: INSTRUMENTATION SPECIFICATIONS

TYPE	MANUFACTURE	MODEL	RANGE AS USED	APPROX. ACCURACY
ACCELEROMETERS	STATHAM	A39TC-5-350	± 2.5 g	1.0 %
DISPLACEMENT TRANSDUCERS	HEWLETT-PACKARD	a) 7DCDT-500 b) 7DCDT-100	± 1.270 cm. ± 0.254 cm.	0.5 % 0.5 %
FORCE TRANSDUCERS (HORIZ. AND VERT.)	*	*	± 1000 N	$\pm 2\%$ (STATIC)
HYDRODYNAMIC PRESSURE TRANSDUCERS	SUNDSTRAND DATA CONTROL, INC.	206	± 2 PSI	0.8 %
ANALOG TO DIGITAL CONVERTER	NEFF	SYSTEM-620	128 CHANNEL	0.1 %

* MANUFACTURED AT THE UNIVERSITY OF CALIFORNIA, BERKELEY, AS PER CHAPTER 3 AND APPENDIX B.

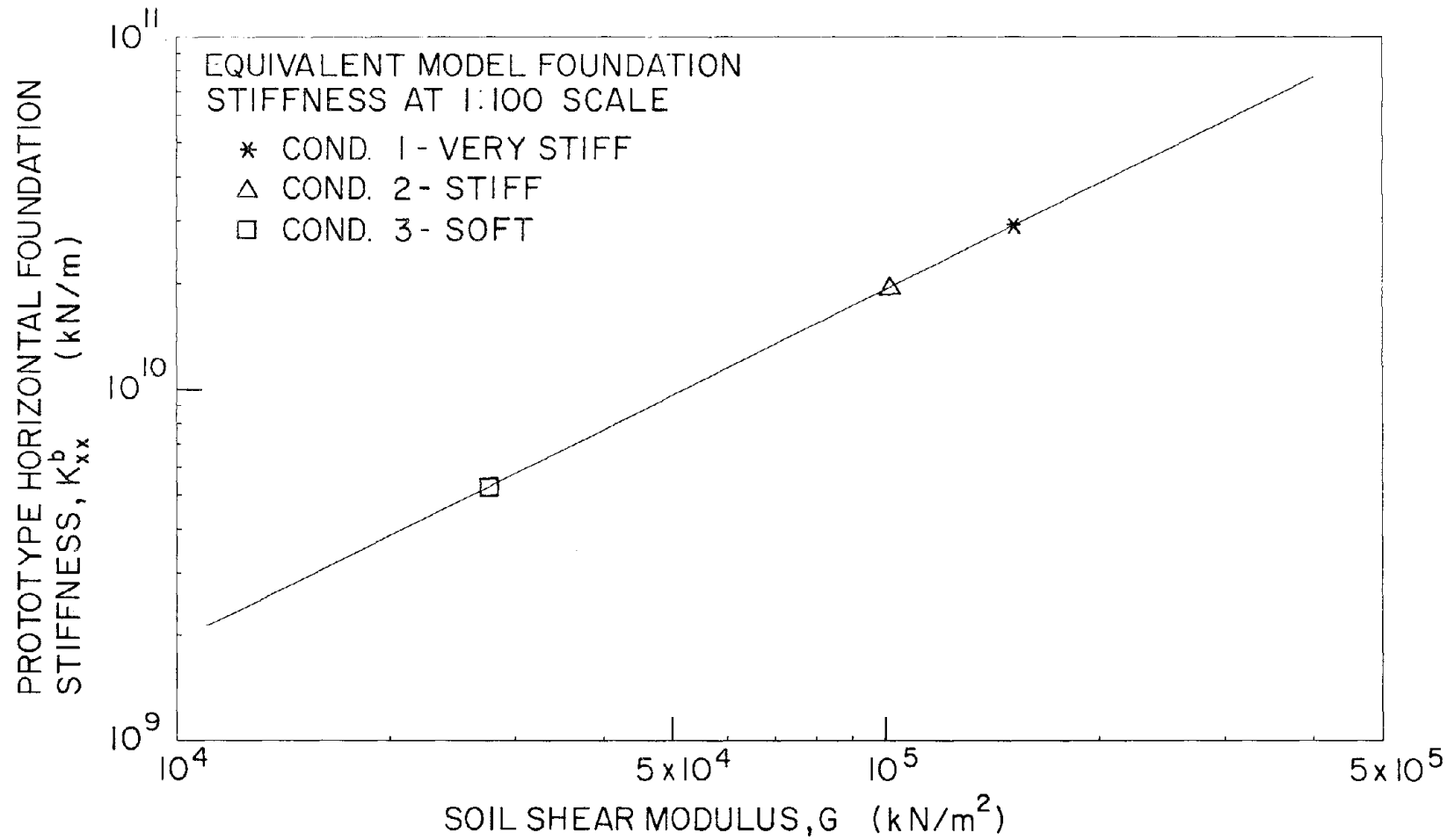


FIGURE 3.1: PROTOTYPE HORIZONTAL FOUNDATION STIFFNESS (K_{xx}^b) VERSUS SOIL SHEAR MODULUS (G)

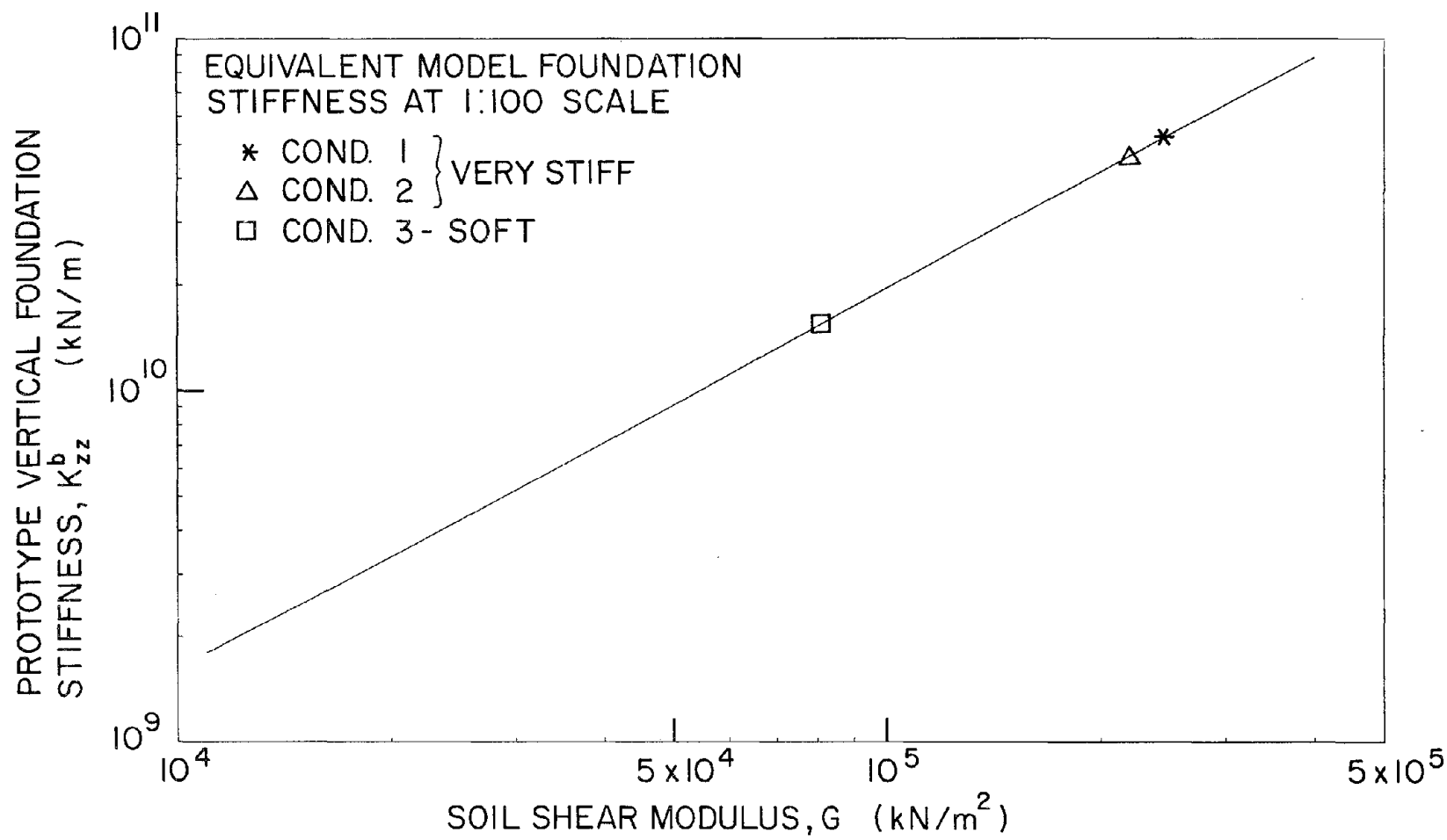


FIGURE 3.2: PROTOTYPE VERTICAL FOUNDATION STIFFNESS (K_{zz}^b) VERSUS
SOIL SHEAR MODULUS (G)

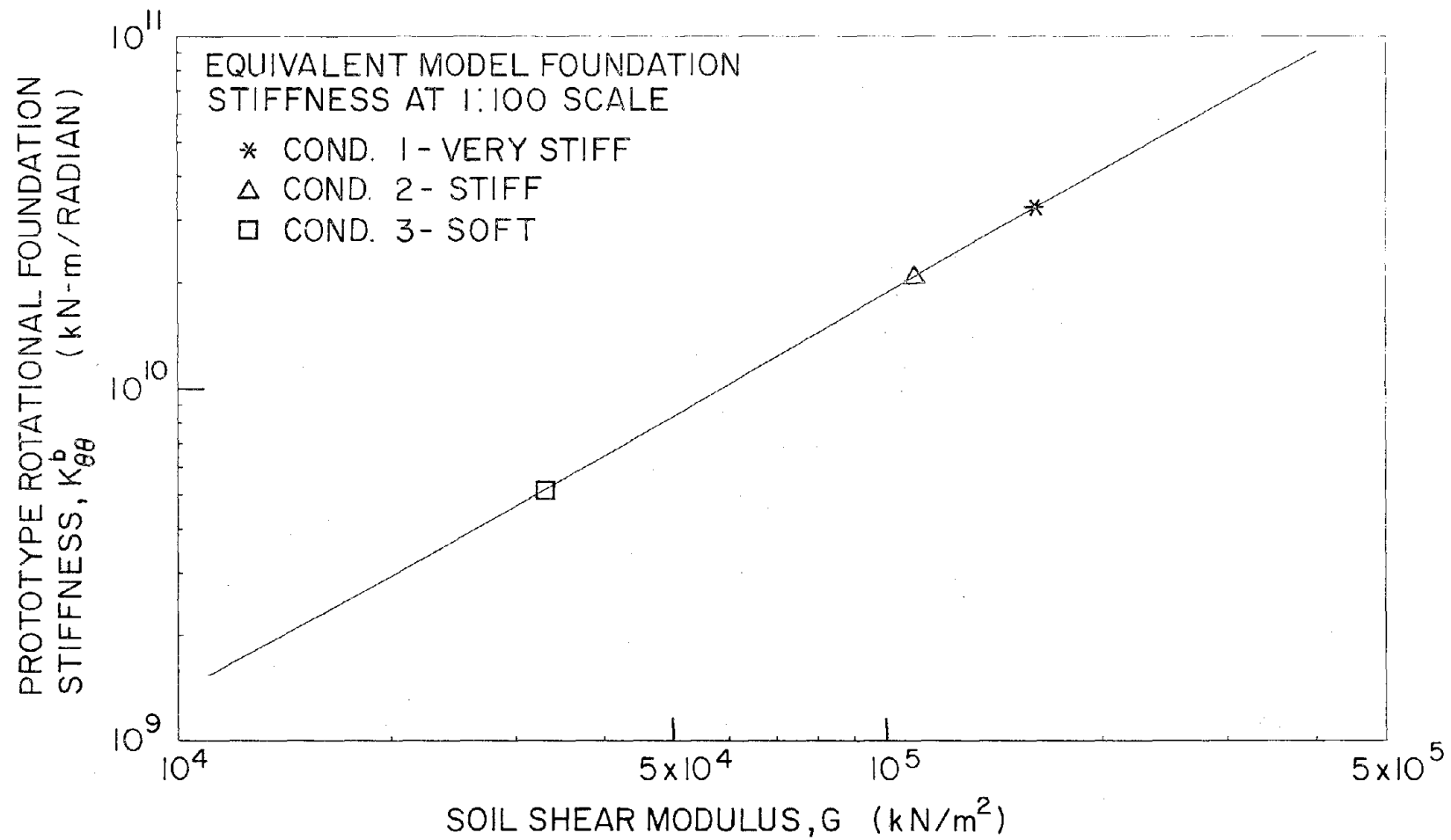


FIGURE 3.3: PROTOTYPE ROTATIONAL FOUNDATION STIFFNESS ($K_{\theta\theta}^b$) VERSUS SOIL SHEAR MODULUS

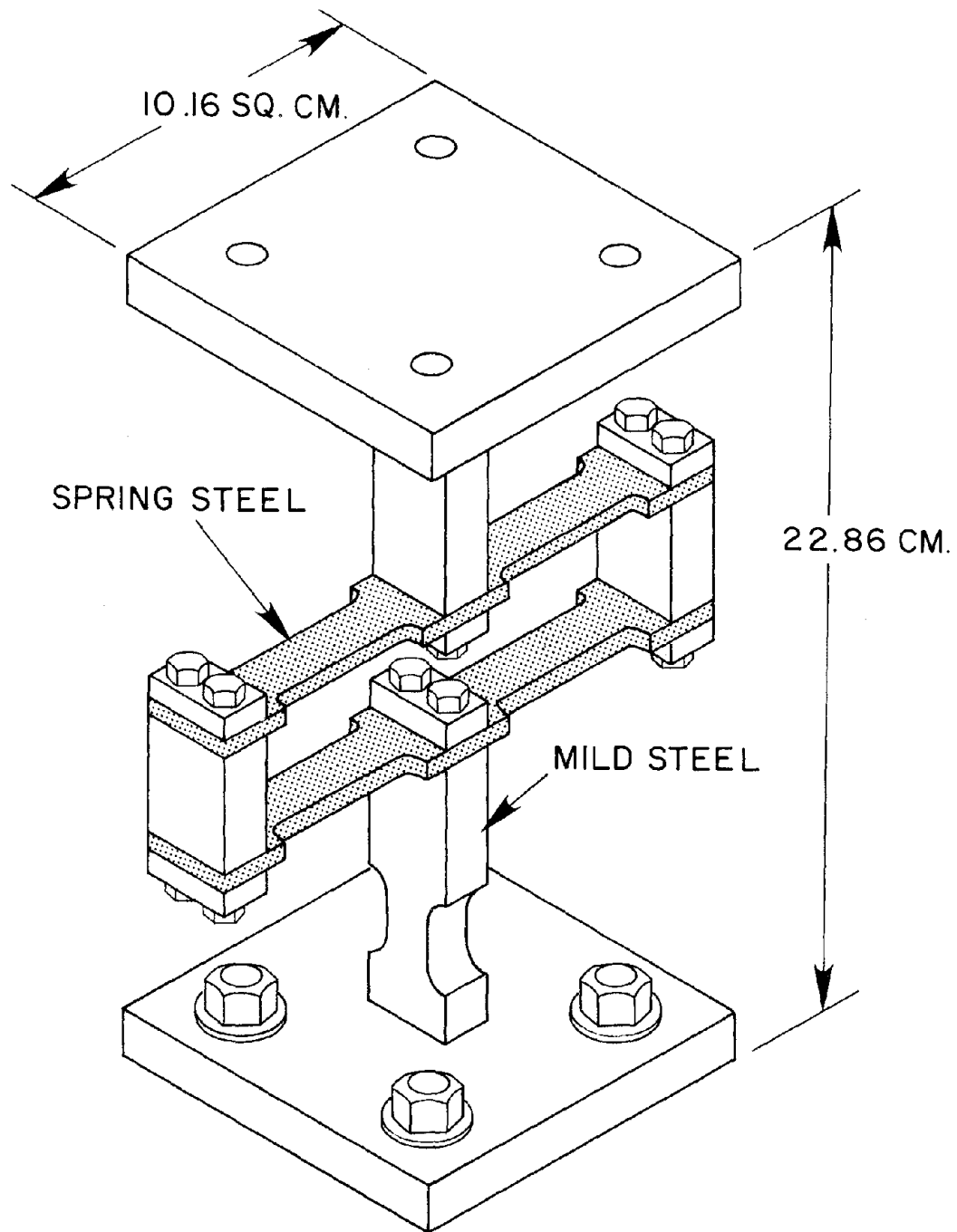


FIGURE 3.4: A TYPICAL FOUNDATION SPRING

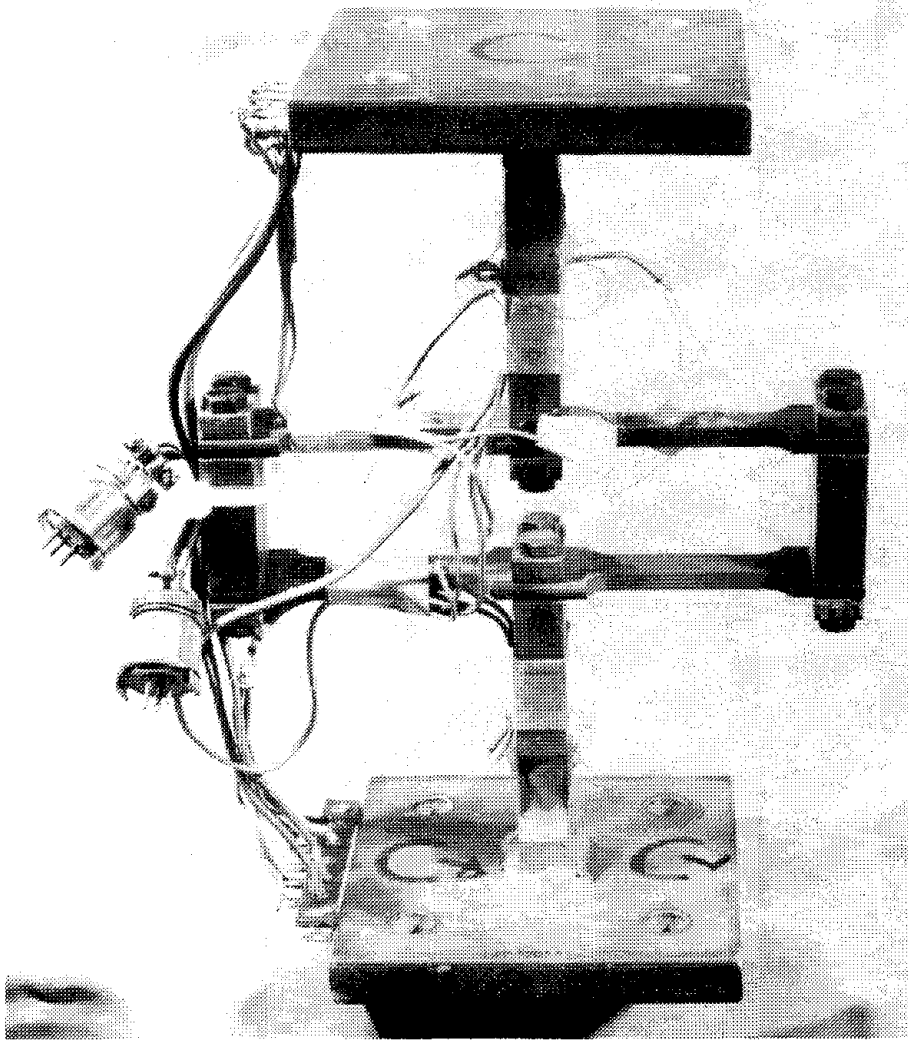


FIGURE 3.5: A FOUNDATION SPRING INSTRUMENTED AS A LOAD CELL

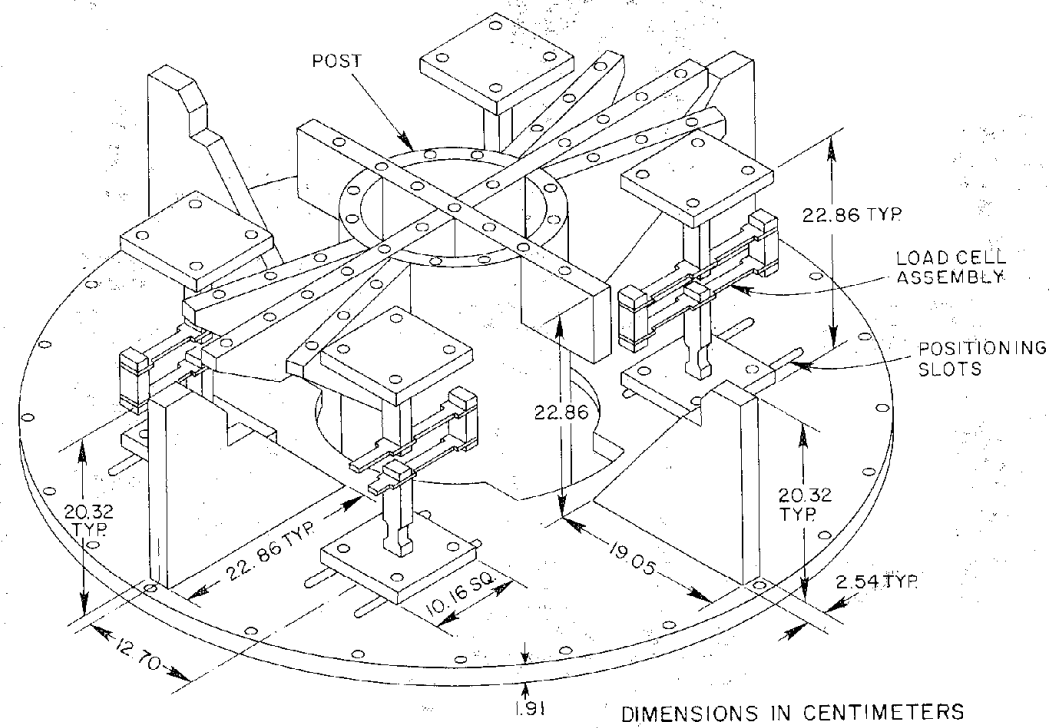


FIGURE 3.6: FOUNDATION LOAD CELL ARRANGEMENT

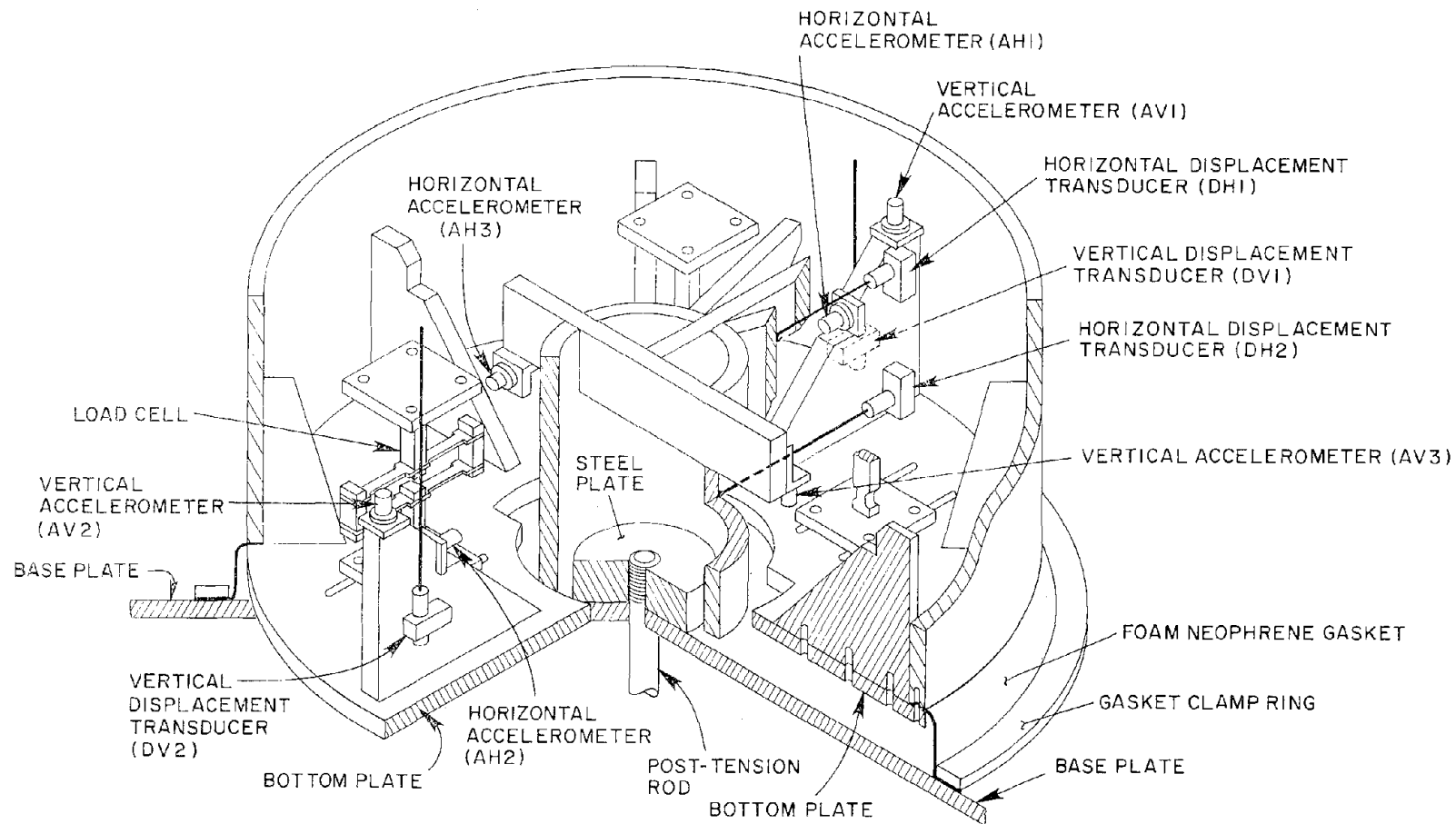


FIGURE 3.7: INSTRUMENTATION ARRANGEMENT

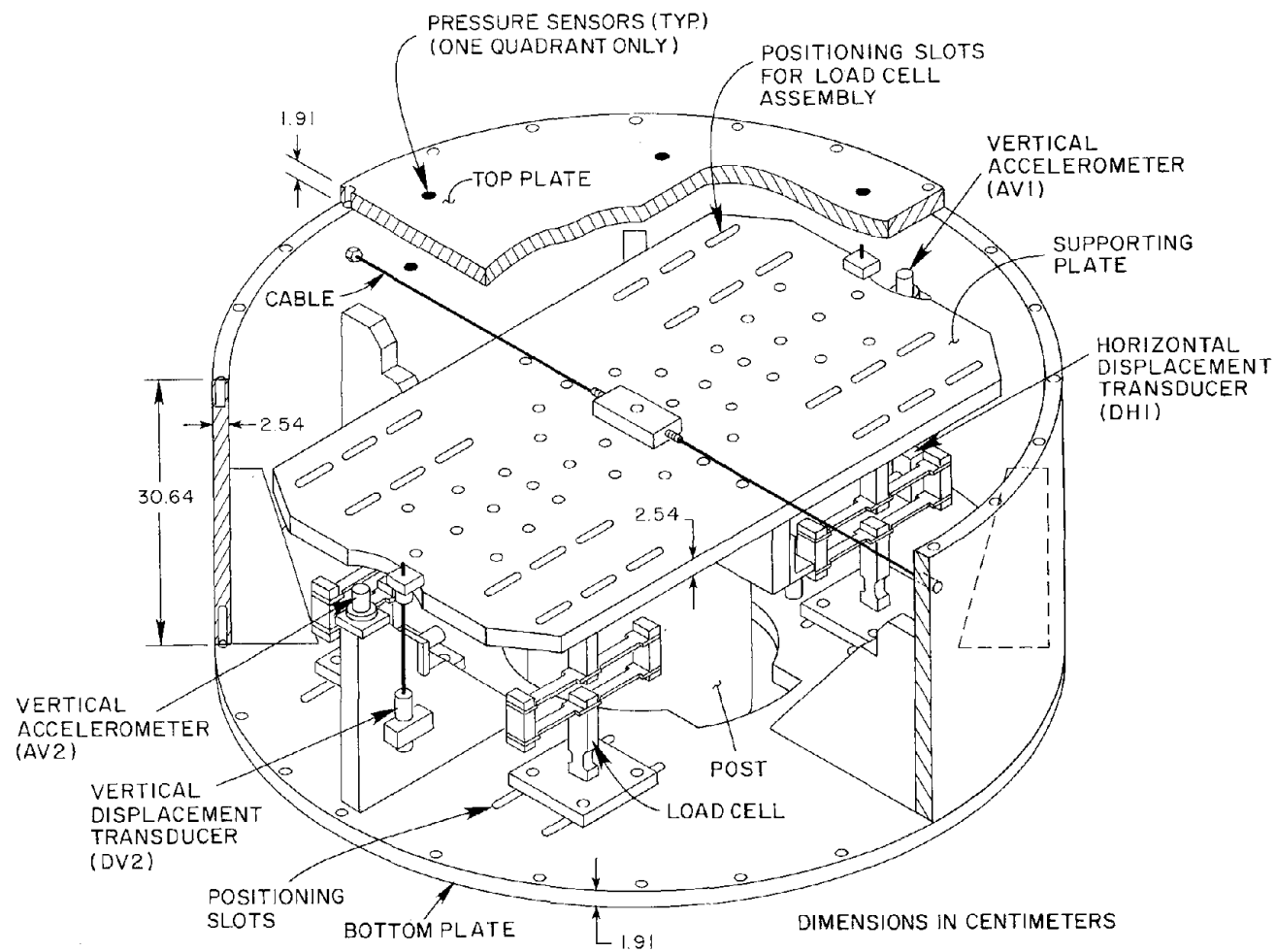


FIGURE 3.8: MODEL INTERNAL ARRANGEMENT

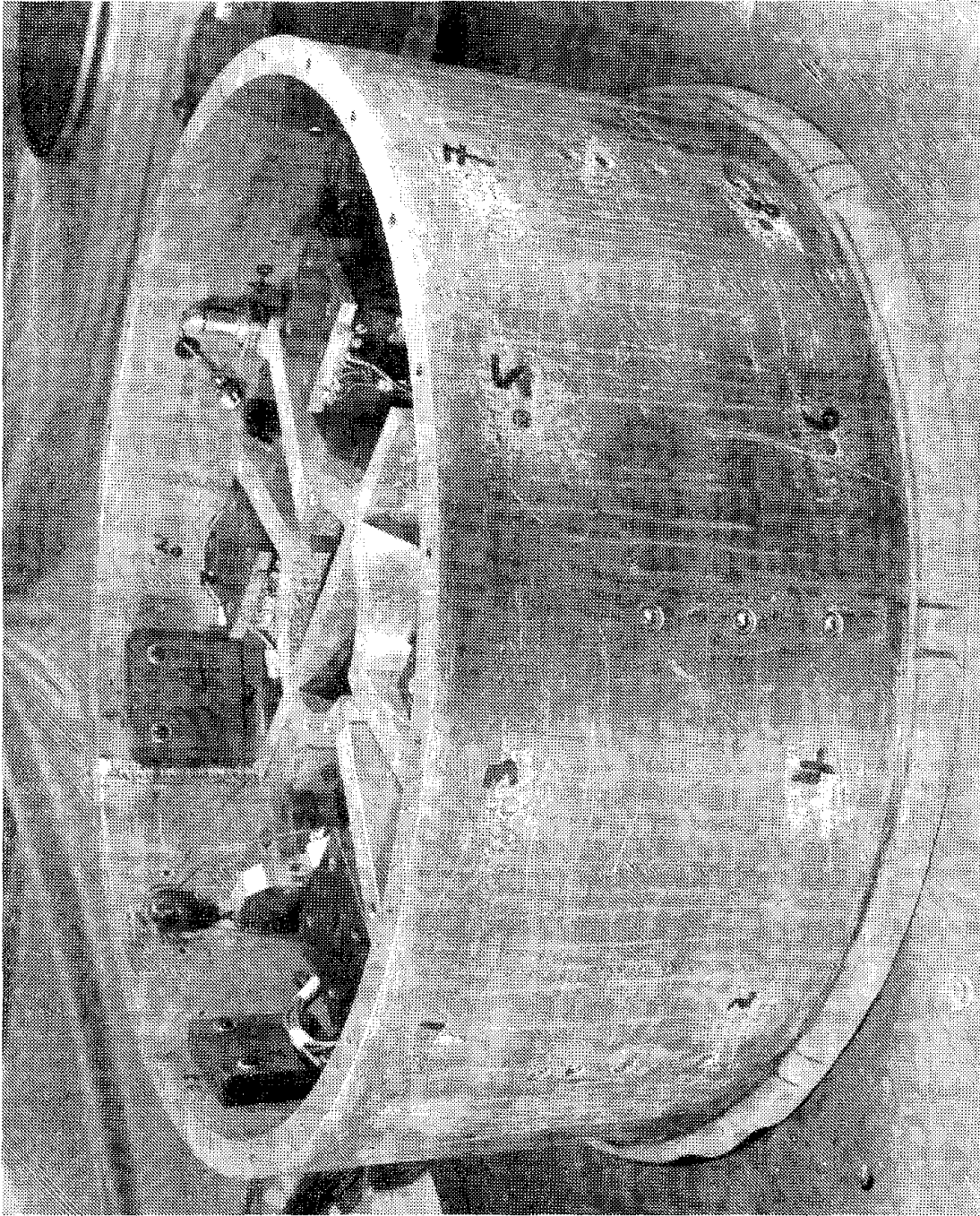


FIGURE 3.9: THE SUBMERGED TANK MODEL, SIDE VIEW

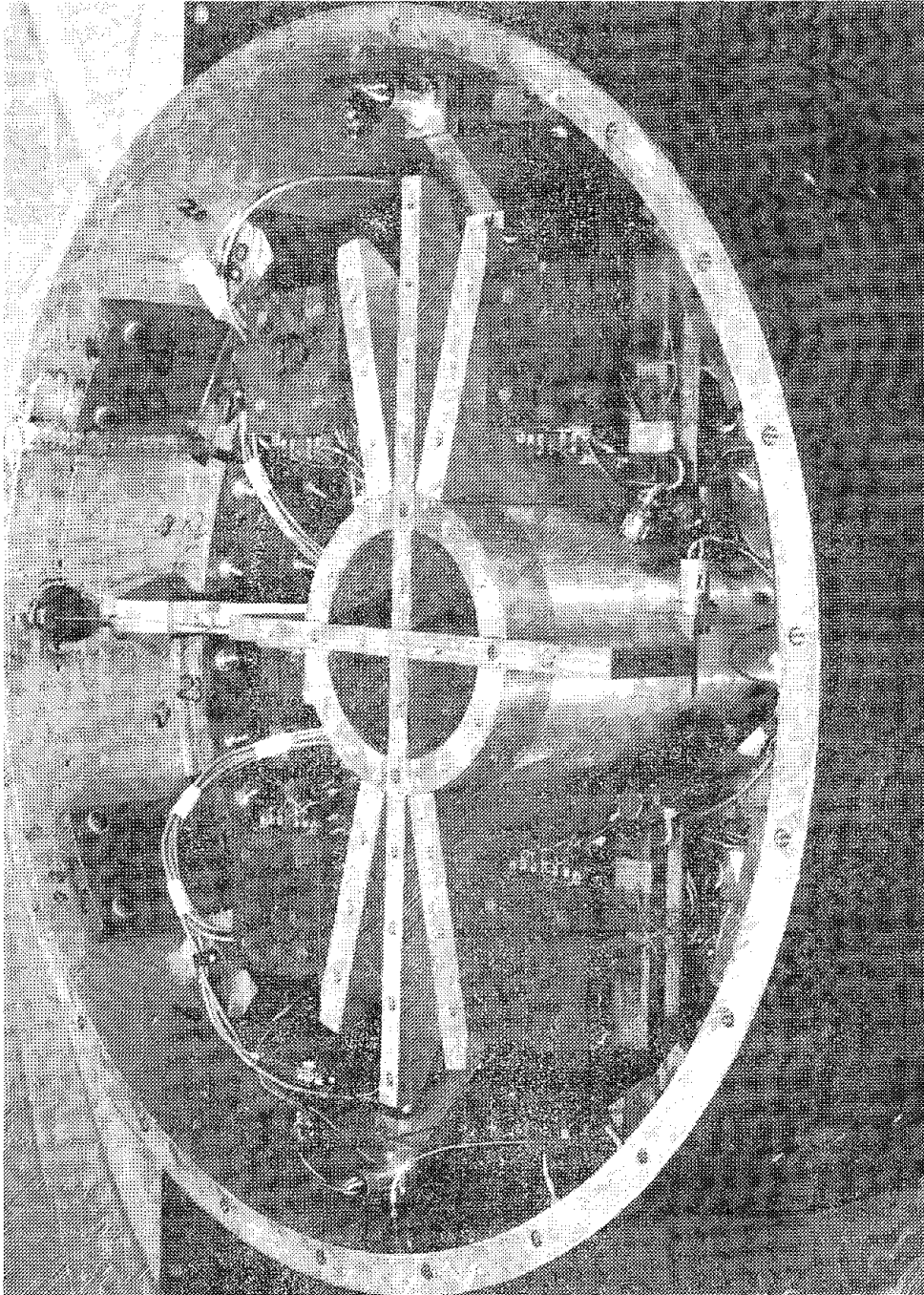


FIGURE 3.10: THE SUBMERGED TANK MODEL, TOP VIEW

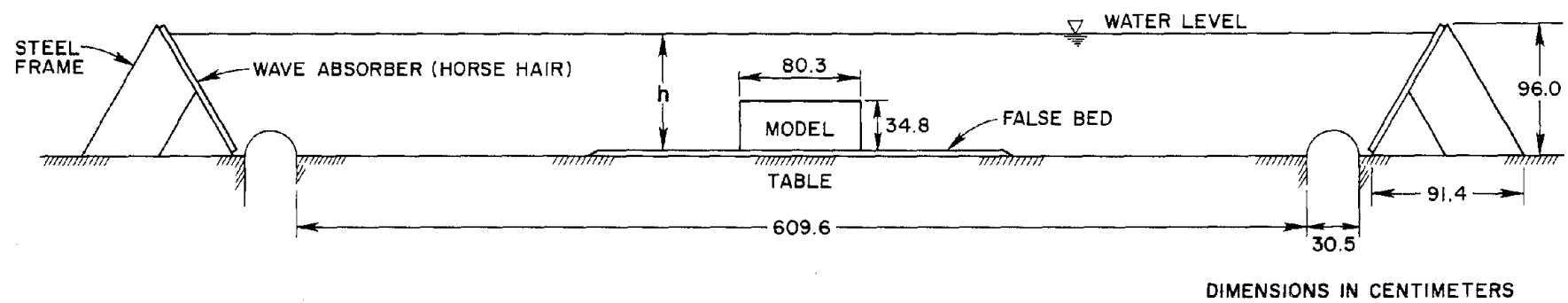


FIGURE 3.11: THE EXPERIMENT ARRANGEMENT

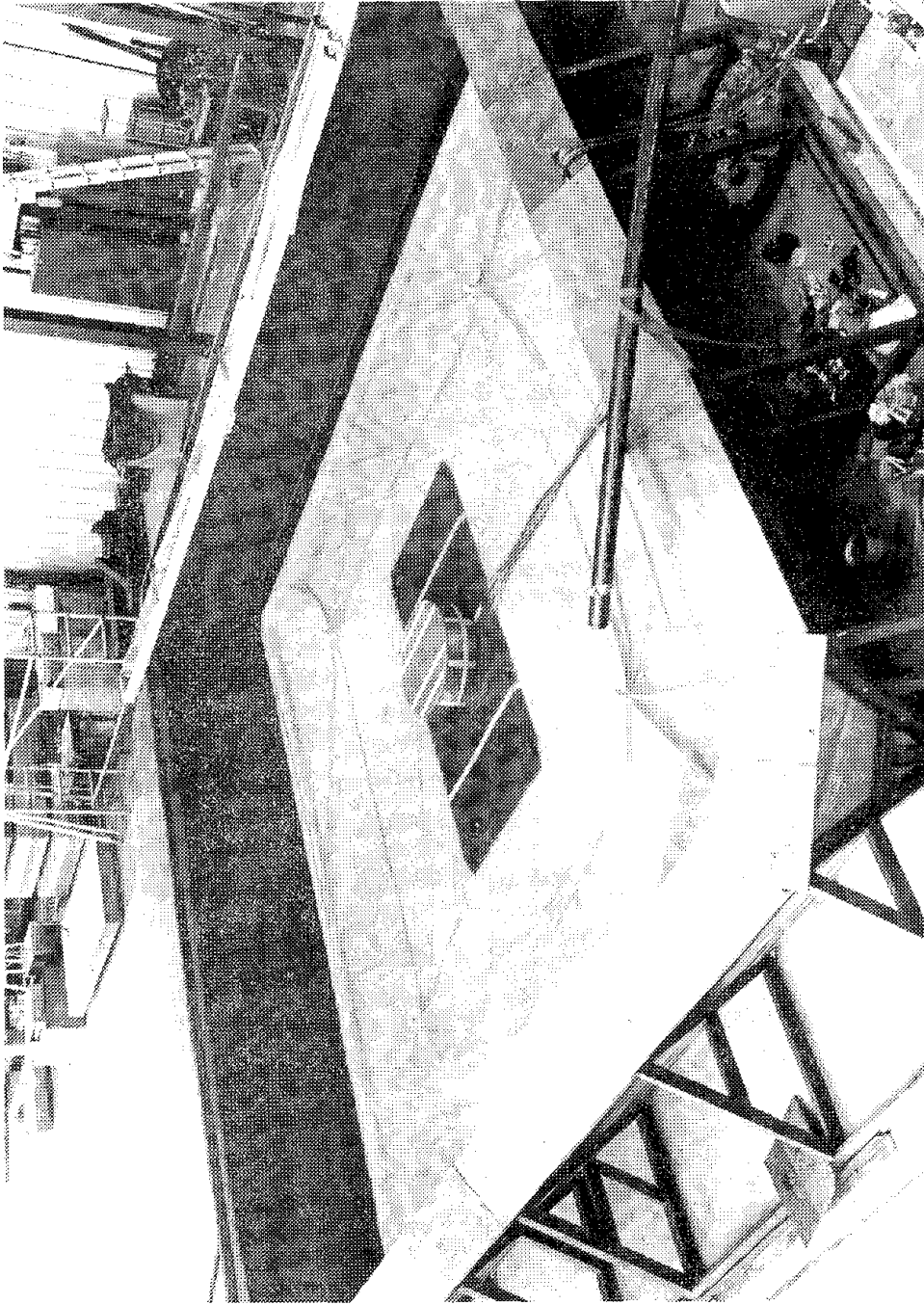


FIGURE 3.12: THE MODEL BASIN AS FILLING BEGINS

4. THE EXPERIMENTAL RESULTS

4.1 General Model Response

The resonant response for the model system in the dry state and at each of the four water depths tested is shown in Table 4.1. The record of resonant response for foundation condition No. 3 and relative water depth (h/H) equal 2.5 is shown in Fig. 4.1. It can be seen here that there is no detectable interference between the horizontal and rotational modes of oscillation when they are excited simultaneously. This figure is typical of all of the resonant data recorded. The conclusion to be drawn from this result is that hydrodynamic coupling is not strong, if it exists, and that we were justified in dropping the coupled term from the analysis of horizontal virtual mass in Eq. 3.1. Table 4.2 contains a summary of the dampening, expressed as a percent of critical dampening, derived from the model resonant response data. These values were found using the following free-vibration decay relationship:¹⁶

$$\xi = \frac{\delta_m}{2\pi m} \quad (4.1)$$

where,

m = total number of cycles

$\delta = \ln (a_n/a_{n+m})$, when a_n is the amplitude at time n and a_{n+m} the amplitude m cycles later.

This expression is exact to within the accuracy of the recorded data (approximately $\pm 2\%$).

We use the notation ξ^* when referring to hydrodynamic dampening in calculations. However, in most cases this is taken to be zero.

4.2 Virtual Mass

The results of the analysis for virtual mass in the horizontal mode are shown in Figs. 4.2 - 4.5, vertical mode in Figs. 4.6 - 4.8, rotational mode in Figs. 4.9 - 4.12, and the horizontal-rotational coupled mass in Figs. 4.13 - 4.16.

The virtual mass in these figures has been plotted versus the dimensionless frequency parameter $\omega^2 \sqrt{DH}/g$ which represents the ratio of inertia force to wave generation force in the horizontal mode, as discussed in Chapter 2.

The mass values have been normalized in the following manner:

$$C_{xx}^m = M_{xx}^* / (\rho V) \quad \dots \dots \dots (4.2a)$$

$$C_{zz}^m = M_{zz}^* / (\rho V) \quad \dots \dots \dots (4.2b)$$

$$C_{\theta\theta}^m = M_{\theta\theta}^* / (\rho V R_g^2) \quad \dots \dots \dots (4.2c)$$

$$C_{\theta x}^m = M_{\theta x}^* / (\rho V R_g) \quad \dots \dots \dots (4.2d)$$

where,

V = displaced volume of the structure

$$= \pi R^2 H$$

R_g = radius of gyration of the displaced volume
of water about its center of gravity

ρ = mass density of fresh water

The results from the diffraction theory calculations by Garrison for the relative water depth $h/H = 2.5$ and from the closed-form solution after Liaw for $h/H = 1.0$ have been included on the appropriate figures.

Our first calculation of the vertical coefficient yielded a value of approximately 1.0 at low frequencies and converged to the

theory at the natural frequencies of the various foundation conditions. This implied that there was a basic error in our formulation, since one would not expect to see frequency dependence in the coefficients which was related so closely to structure response.

This result has caused us to take a closer look at the physical system we are modeling with Eq. 2.1. We are implying by our use of a single inertia coefficient with the sum of the relative acceleration and the foundation acceleration that each of these kinematic conditions excites the same flow regime above the structure. To put it somewhat differently, we are saying that relative motion without foundation motion and foundation-structure motion without relative motion excite the same flow conditions. If one thinks in terms of an infinite rigid foundation and an incompressible fluid it is apparent that this is not true. In the latter case the structure would feel the effect of the entire mass of the water column above it during foundation vertical accelerations. This situation is shown graphically in Fig. 4.17.

We can describe the forces due to vertical ground acceleration as the summation of the force due to rigid body motion of the structure-foundation system (no relative motion)

$$F'_z = (M_z + \rho \Delta H \frac{\pi D^2}{4}) \ddot{v}_g$$

and the force due to the relative motion of the structure above

$$F''_z = (M_z + \rho C_{zz}^m H \frac{\pi D^2}{4}) \ddot{z}$$

with the total force being

$$F_z = F'_z + F''_z$$

We must now rewrite Eq. 3.2 to solve for the vertical virtual mass as follows:

$$M_{zz}^* \ddot{z} = -M_z \ddot{z}_t - \rho \Delta H^2 R \ddot{V}_g - C_z \dot{z} - K_z z - C_z^* \ddot{z} \dots (4.3)$$

The vertical mass coefficients shown have resulted from use of this formulation.

4.3 Hydrodynamic Pressure Force

Hydrodynamic pressure forces were recorded in some of the harmonic tests for comparison with the pressure force which would be predicted using the calculated virtual masses and Eq. 2.40, as discussed in Section 2.3.4.

For comparison purposes we have calculated the magnitude of the hydrodynamic force using Eq. 2.39 and the mean virtual mass values for horizontal and vertical modes. These results for each depth are shown in Figs. 4.18 - 4.24 plotted as a function of the dimensionless frequency parameter. All values shown are normalized to the $1g$ (980.7 cm/sec^2) foundation acceleration level.

Also shown on these figures are the actual magnitude of the pressure force amplitudes recorded in the testing. These forces were derived from forces measured on one quarter of the structure, as shown in APPENDIX C. The plotted values represent the average force amplitudes observed, generally taken for a minimum of 30 cycles.

Hydrodynamic and structural dampening were both very small in the model system, ranging between approximately 0.8 and 3.0 percent of critical depending on the condition. This results in the pressure force being nearly in phase with foundation acceleration and essentially real valued, except near resonance. We have, therefore, not

presented data on the pressure force phase relationship observed in the testing. We will discuss the effects of foundation dampening on the phase angle in Chapter 5 using calculated values based on Eq. 2.39.

TABLE 4.1: MODEL RESONANT RESPONSE FREQUENCIES (HZ)

FOUNDATION CONDITION		RELATIVE WATER DEPTH (h/H)				
		0 (DRY)	1.0	1.5	2.0	2.5
1	X	17.1	15.4	14.8	14.6	14.6
	Z	22.9	22.9	21.0	19.3	18.9
	θ	21.7	21.5	20.0	19.9	19.8
2	X	13.9	12.5	12.1	12.0	11.9
	Z	22.1	22.1	20.3	18.6	18.2
	θ	17.6	17.2	16.4	16.2	16.2
3	X	7.3	6.6	6.5	6.4	6.3
	Z	12.3	12.3	11.0	10.6	10.5
	θ	8.8	8.3	8.1	8.0	8.0

TABLE 4.2: MODEL DAMPENING SUMMARY (PERCENT OF CRITICAL)

FOUNDATION CONDITION	MODE	RELATIVE WATER DEPTH (h/H)				
		0 (DRY)	1.0	1.5	2.0	2.5
1	X	0.8	0.8	0.8	0.8	0.8
	Z	0.8	0.9	3.0	2.4	2.9
	θ	0.4	0.5	0.5	0.5	0.5
2	X	0.7	0.7	0.7	0.7	0.8
	Z	1.4	1.3	1.6	4.0	4.4
	θ	0.3	0.3	0.3	0.3	0.3
3	X	1.9	1.6	1.9	1.8	1.8
	Z	1.2	0.9	0.7	0.8	0.7
	θ	1.6	1.4	1.2	1.2	1.2

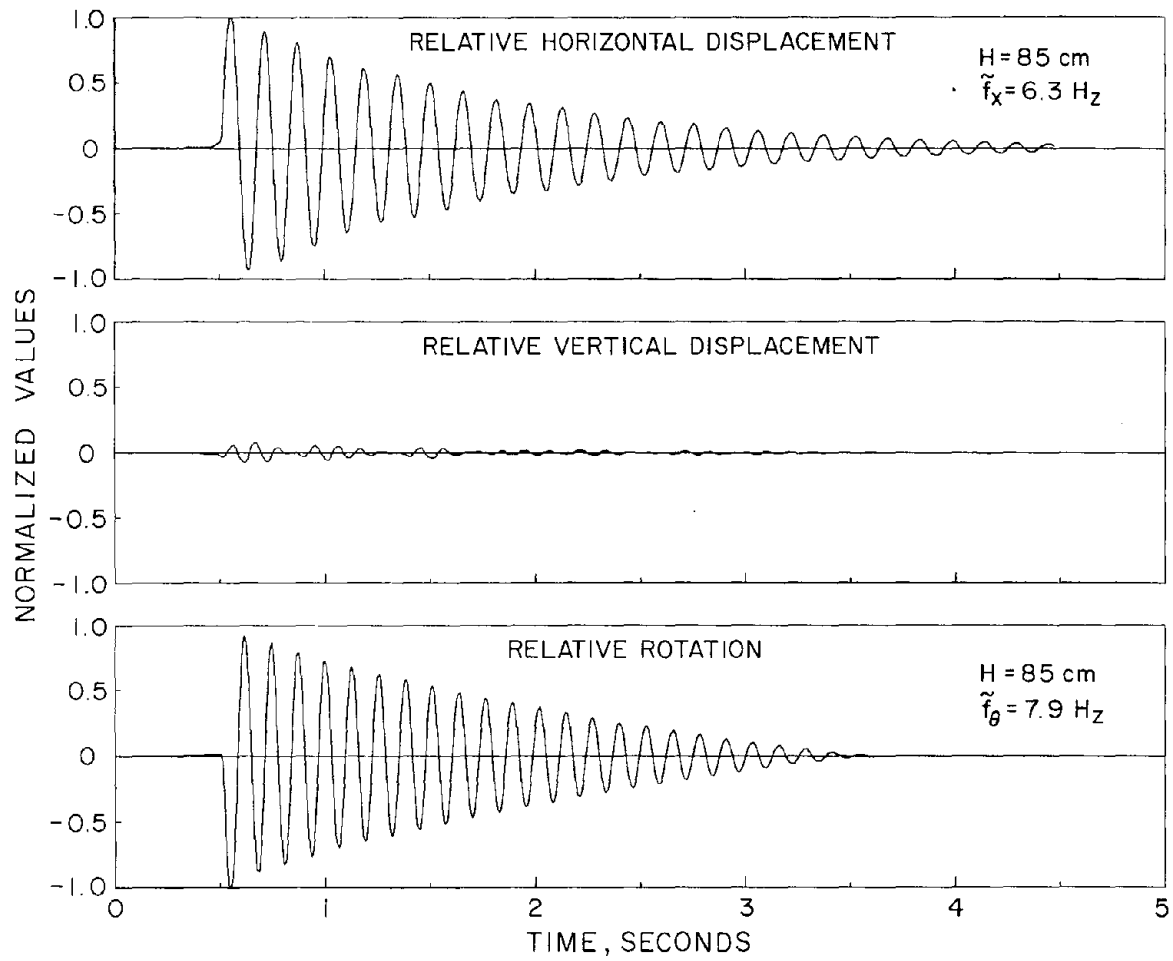


FIGURE 4.1: UNCOUPLED RESONANT RESPONSE OF THE MODEL, $h/H = 2.5$

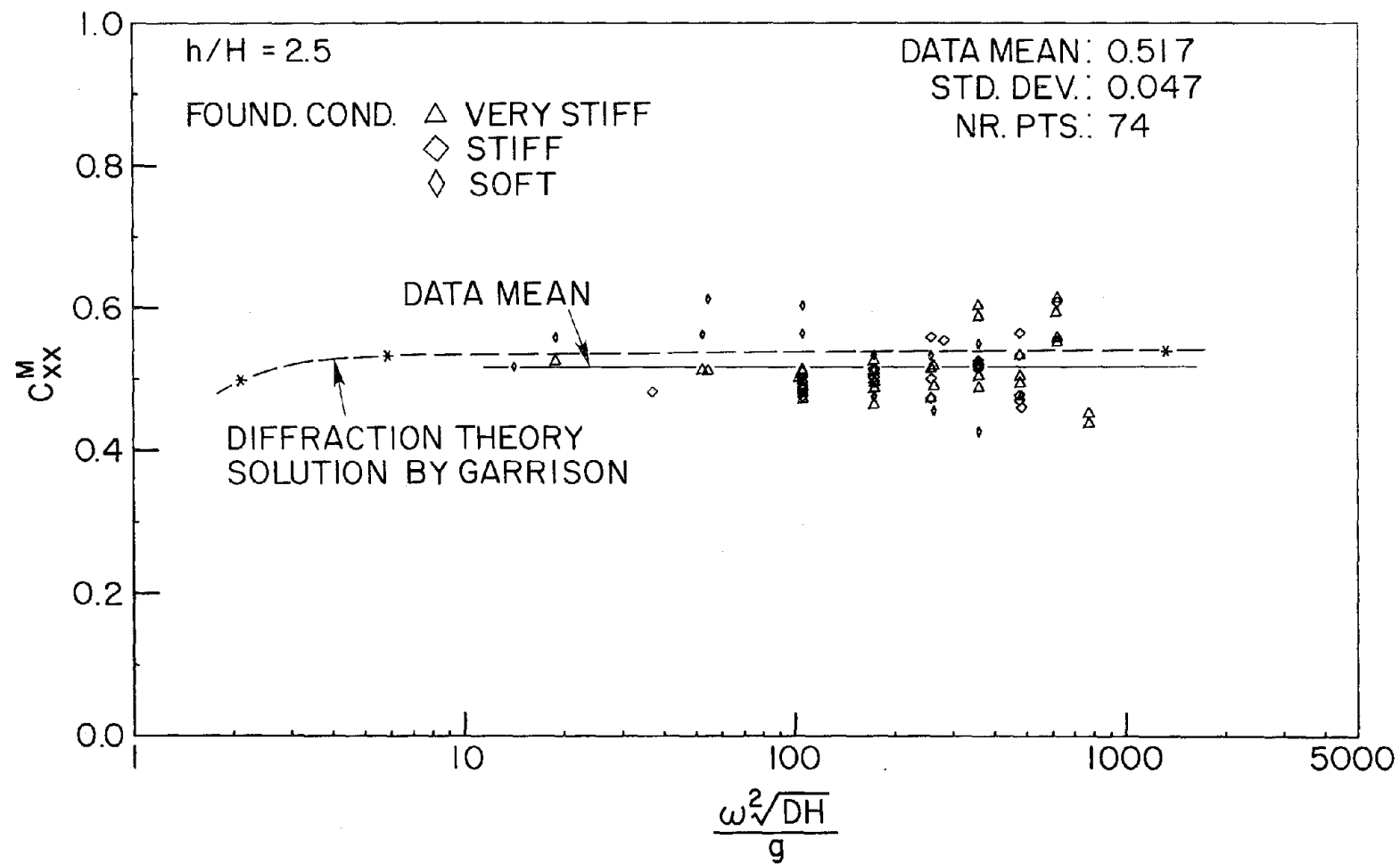


FIGURE 4.2: HORIZONTAL INERTIA COEFFICIENT, $h/H = 2.5$

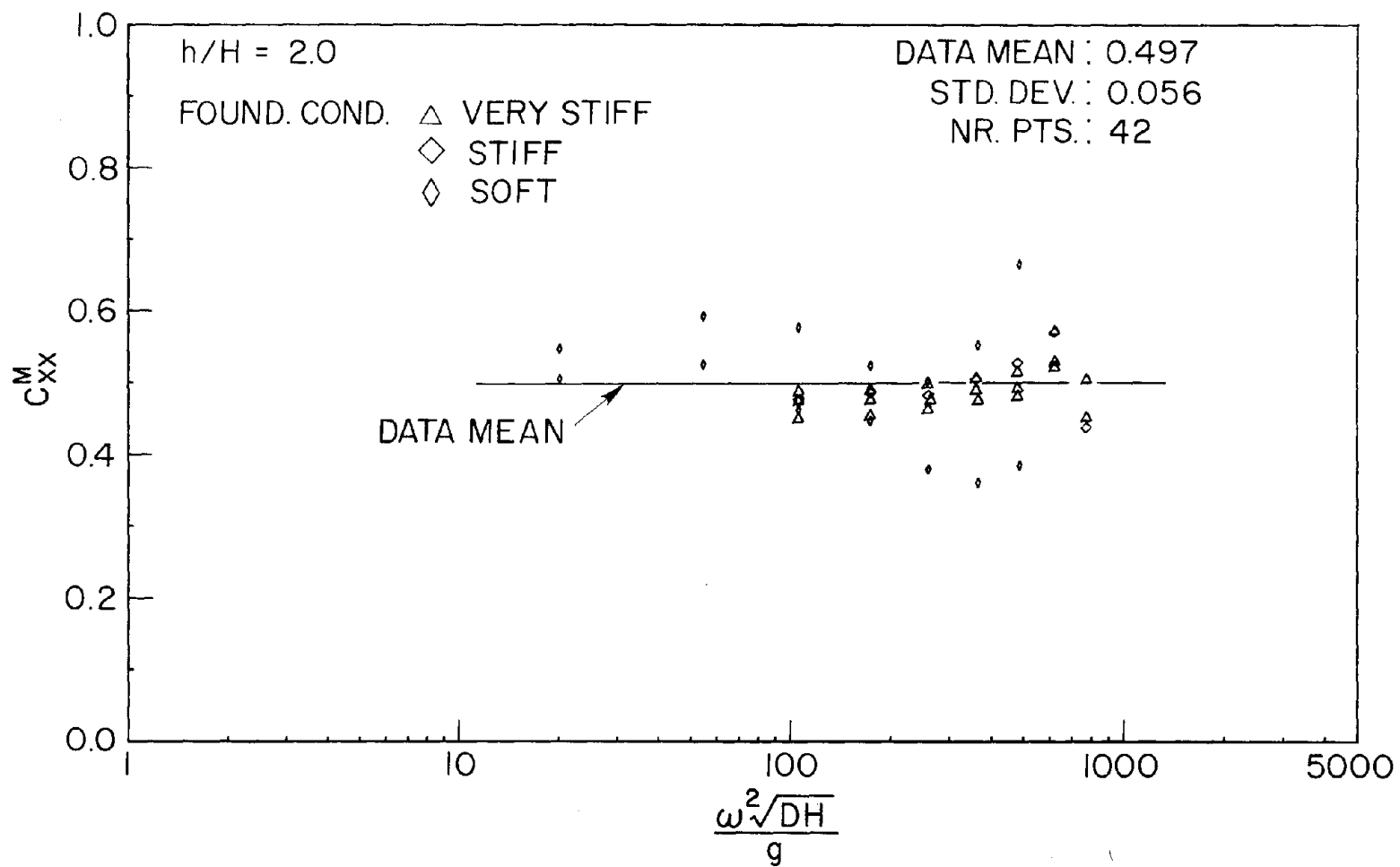


FIGURE 4.3: HORIZONTAL INERTIA COEFFICIENT, $h/H = 2.0$

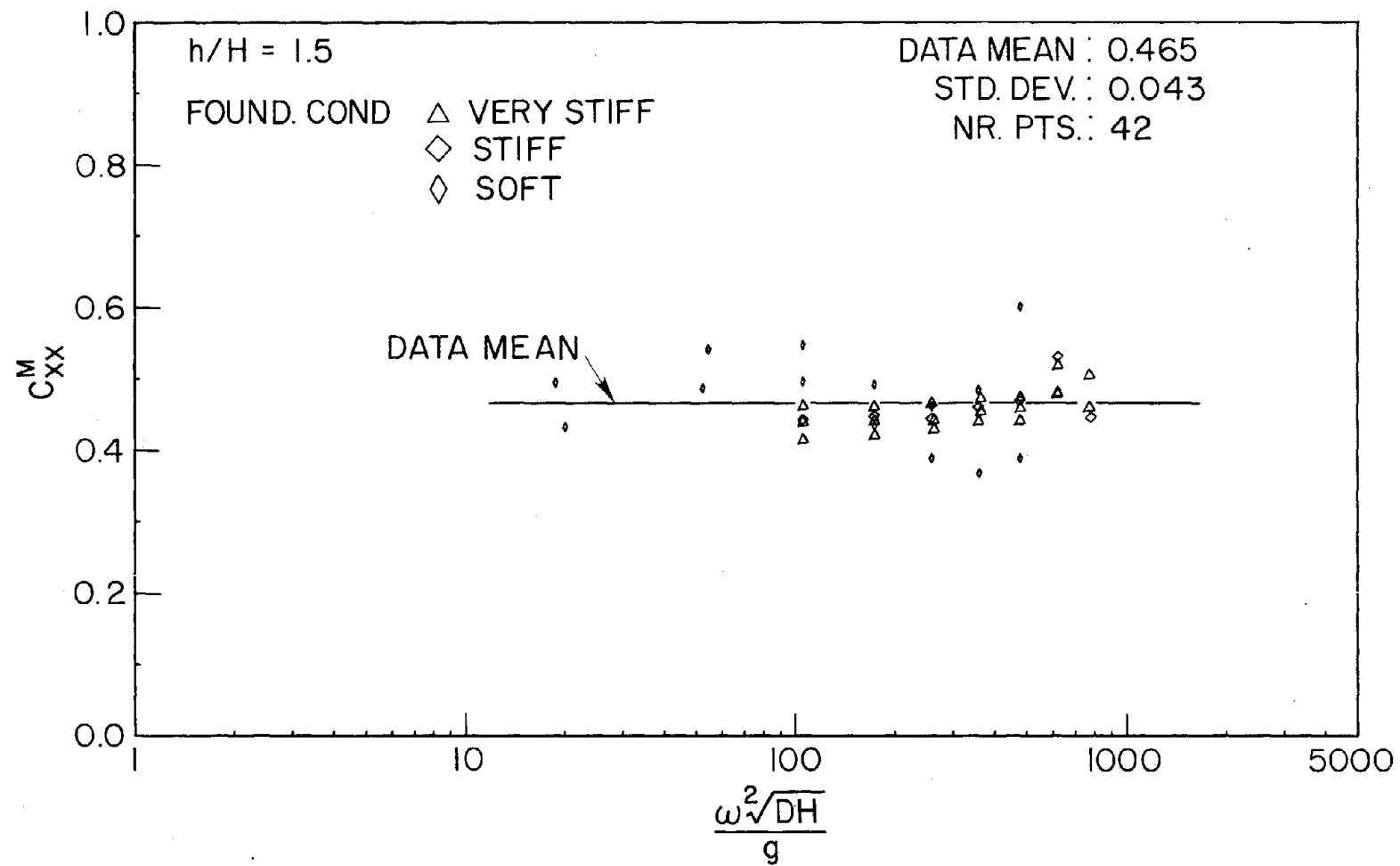


FIGURE 4.4: HORIZONTAL INERTIA COEFFICIENT, $h/H = 1.5$

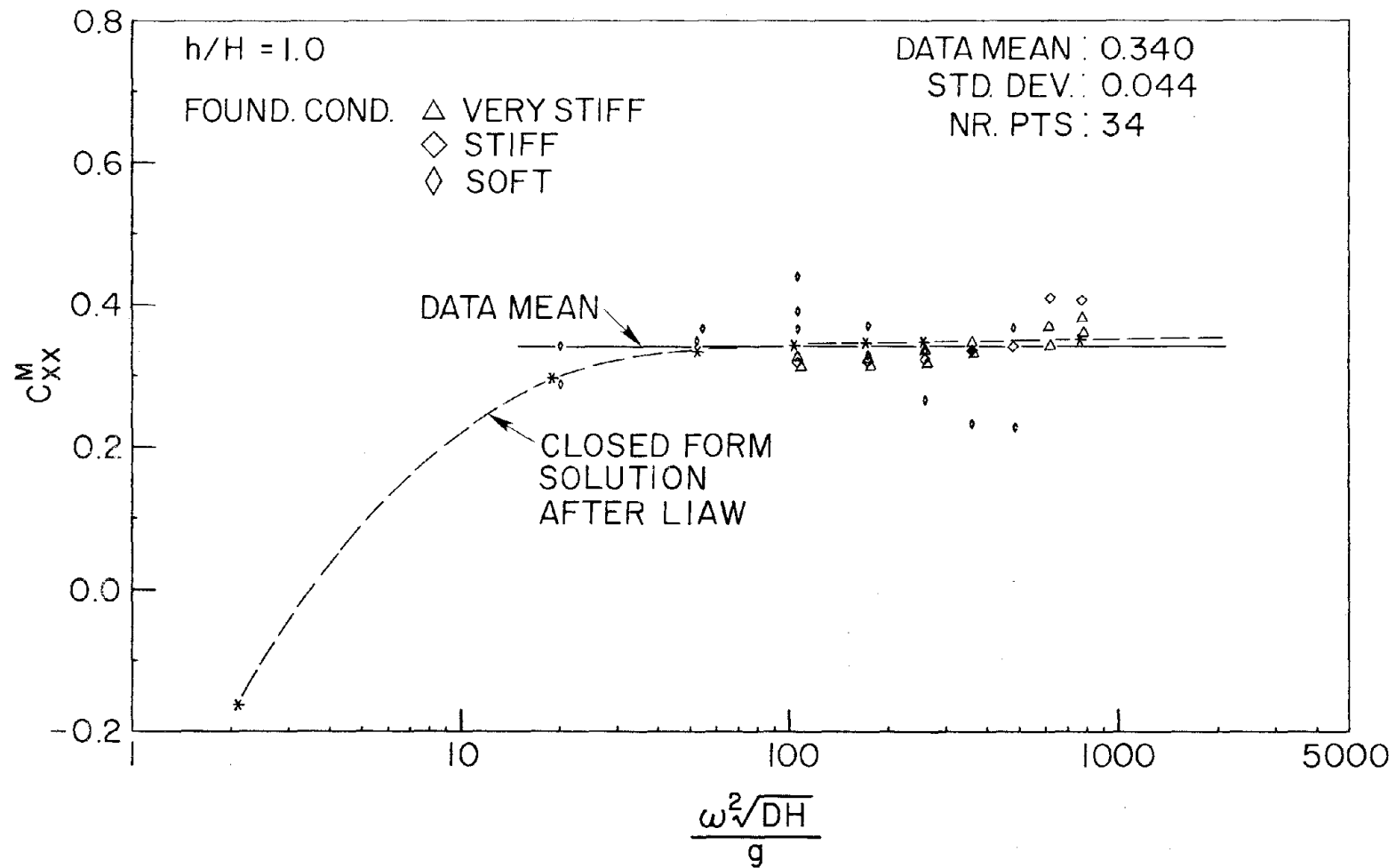


FIGURE 4.5: HORIZONTAL INERTIA COEFFICIENT, $h/H = 1.0$

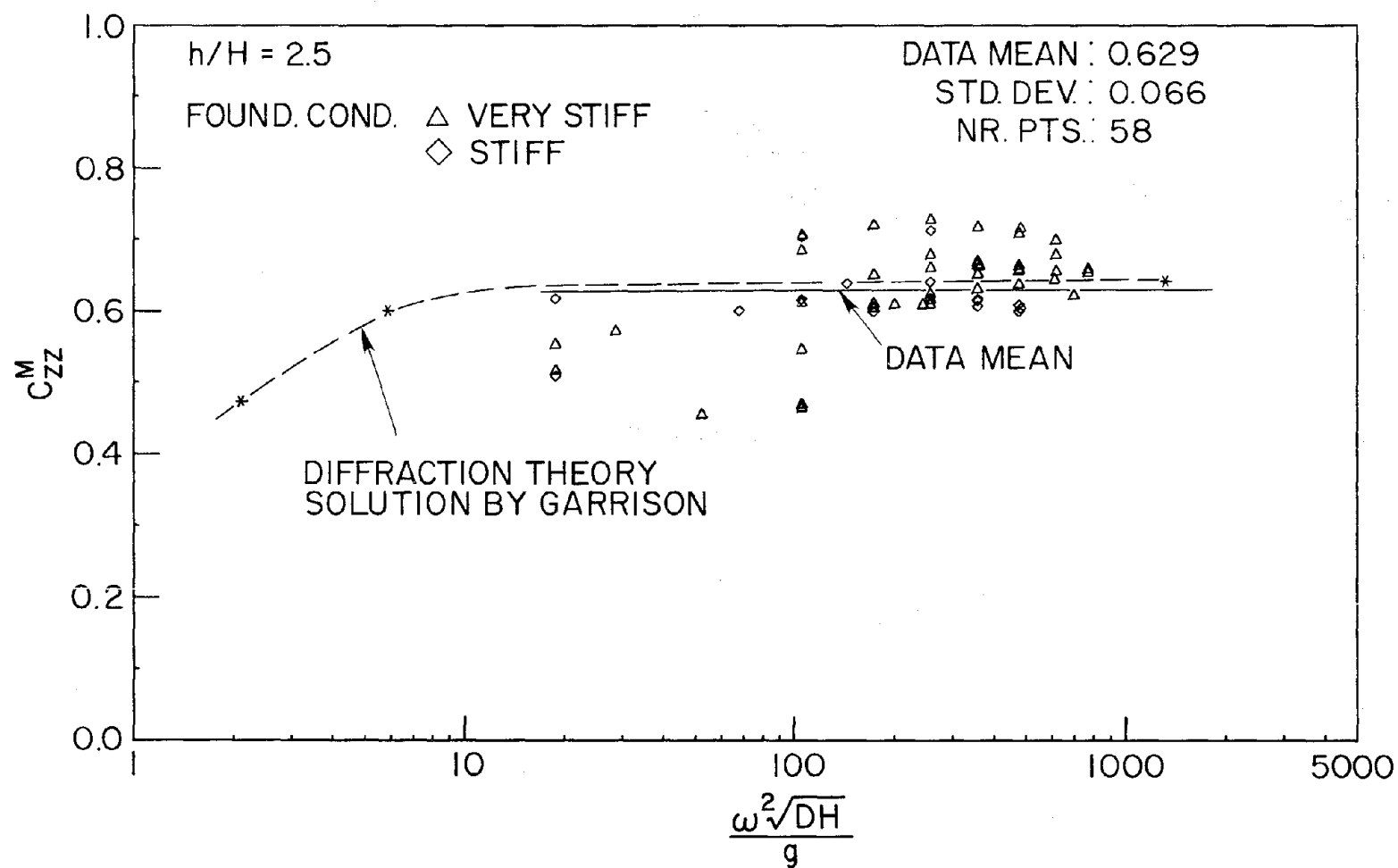


FIGURE 4.6: VERTICAL INERTIA COEFFICIENT, $h/H = 2.5$

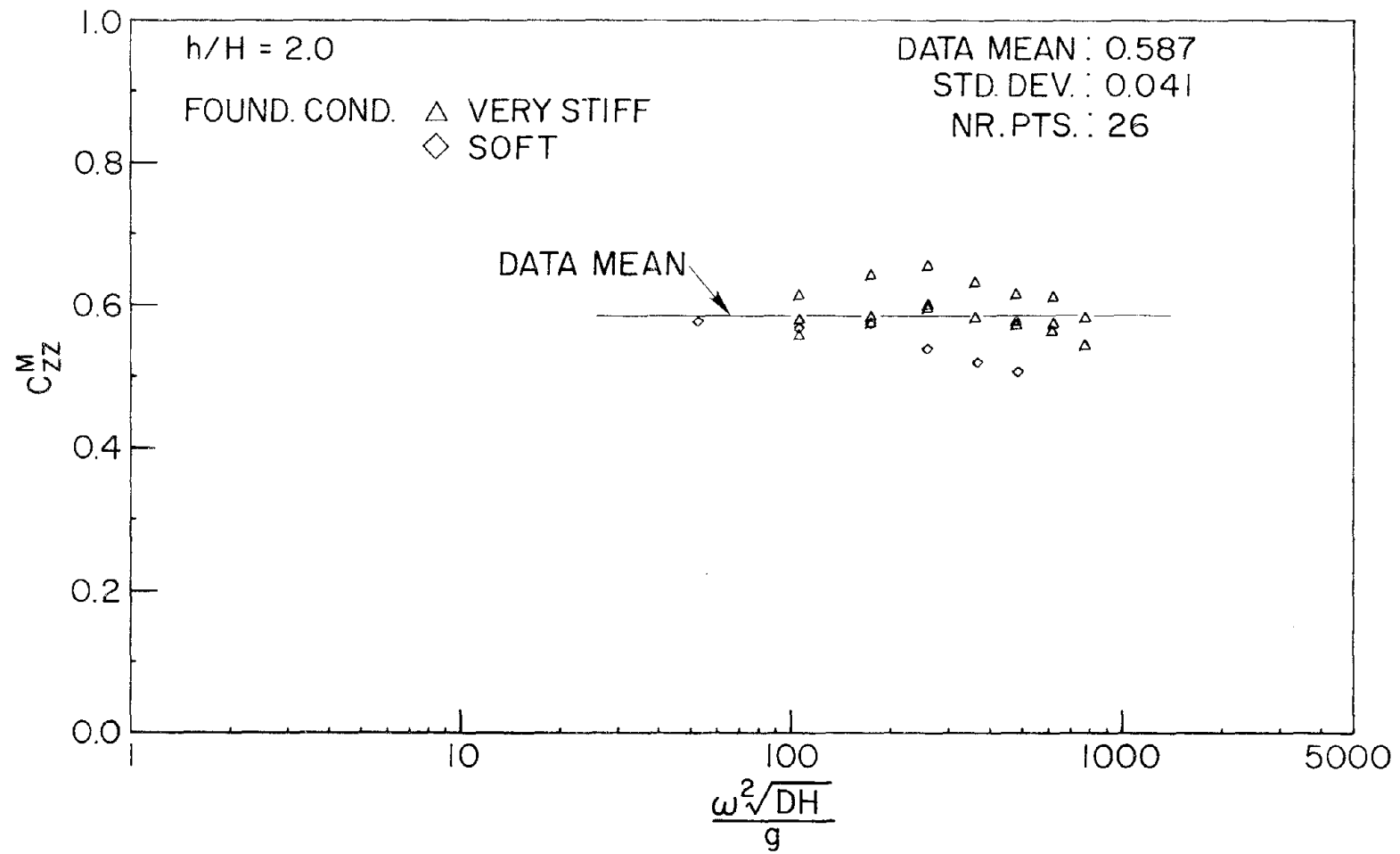


FIGURE 4.7: VERTICAL INERTIA COEFFICIENT, $h/H = 2.0$

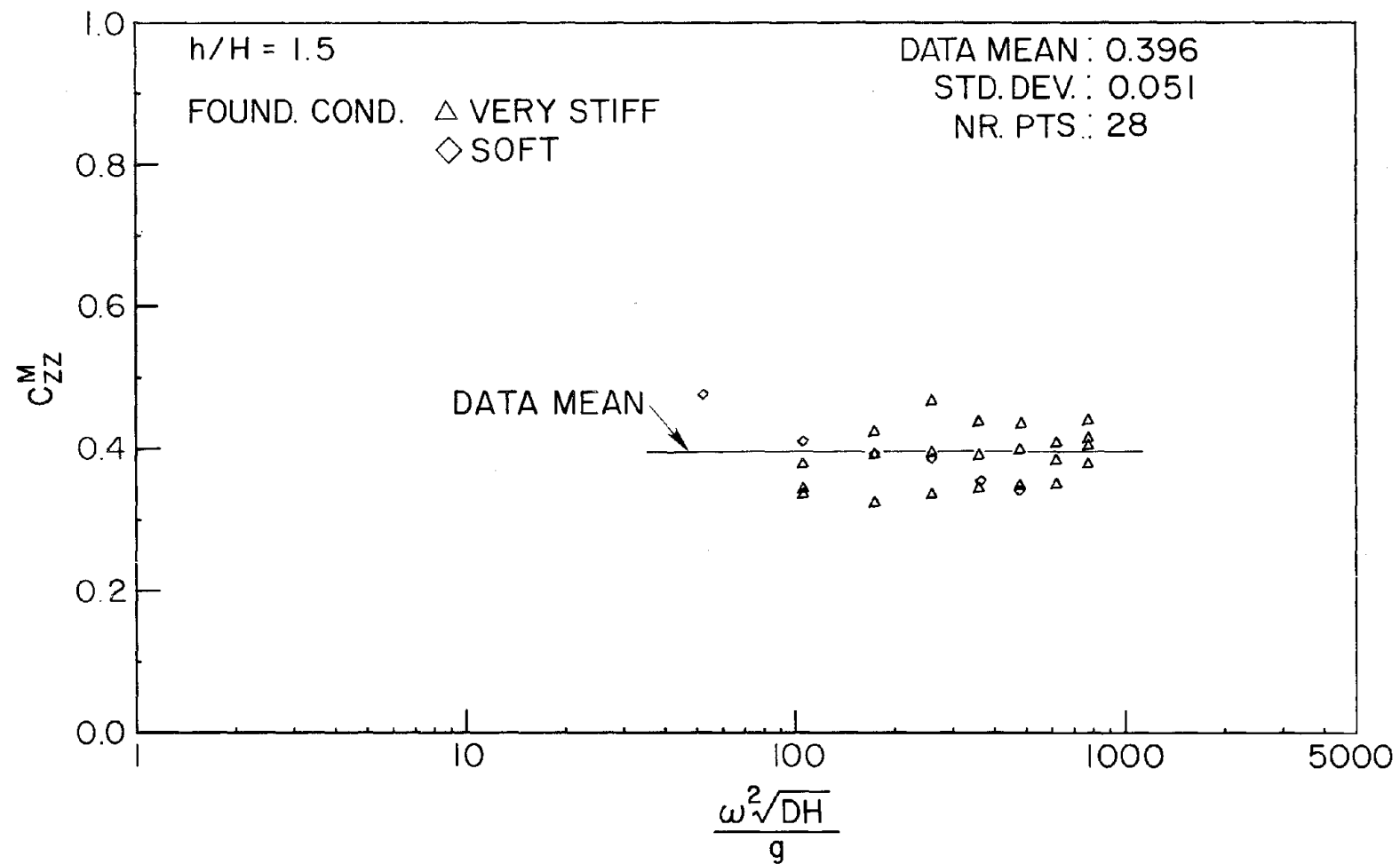


FIGURE 4.8: VERTICAL INERTIA COEFFICIENT, $h/H = 1.5$

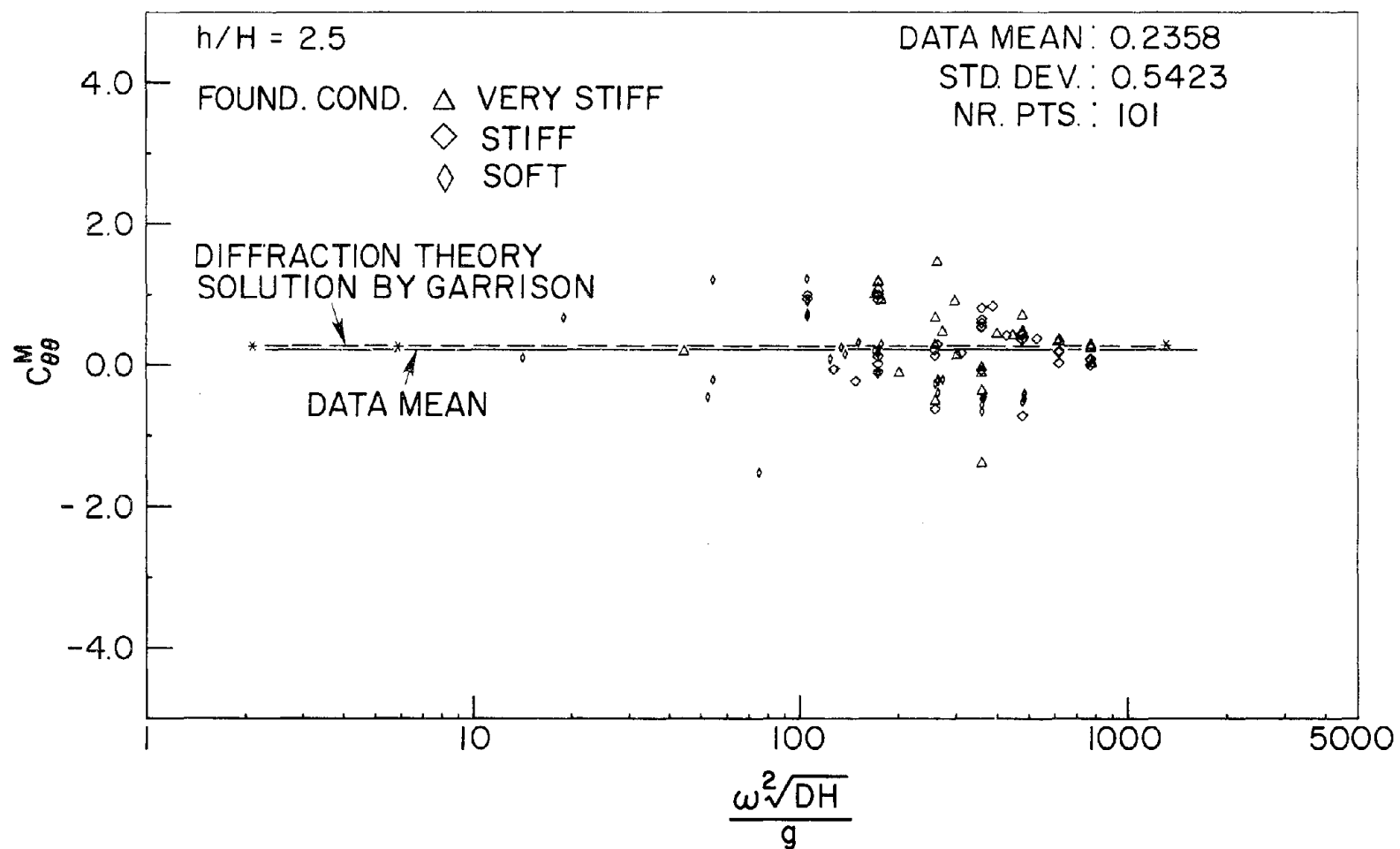


FIGURE 4.9: ROTATIONAL INERTIA COEFFICIENT, $h/H = 2.5$

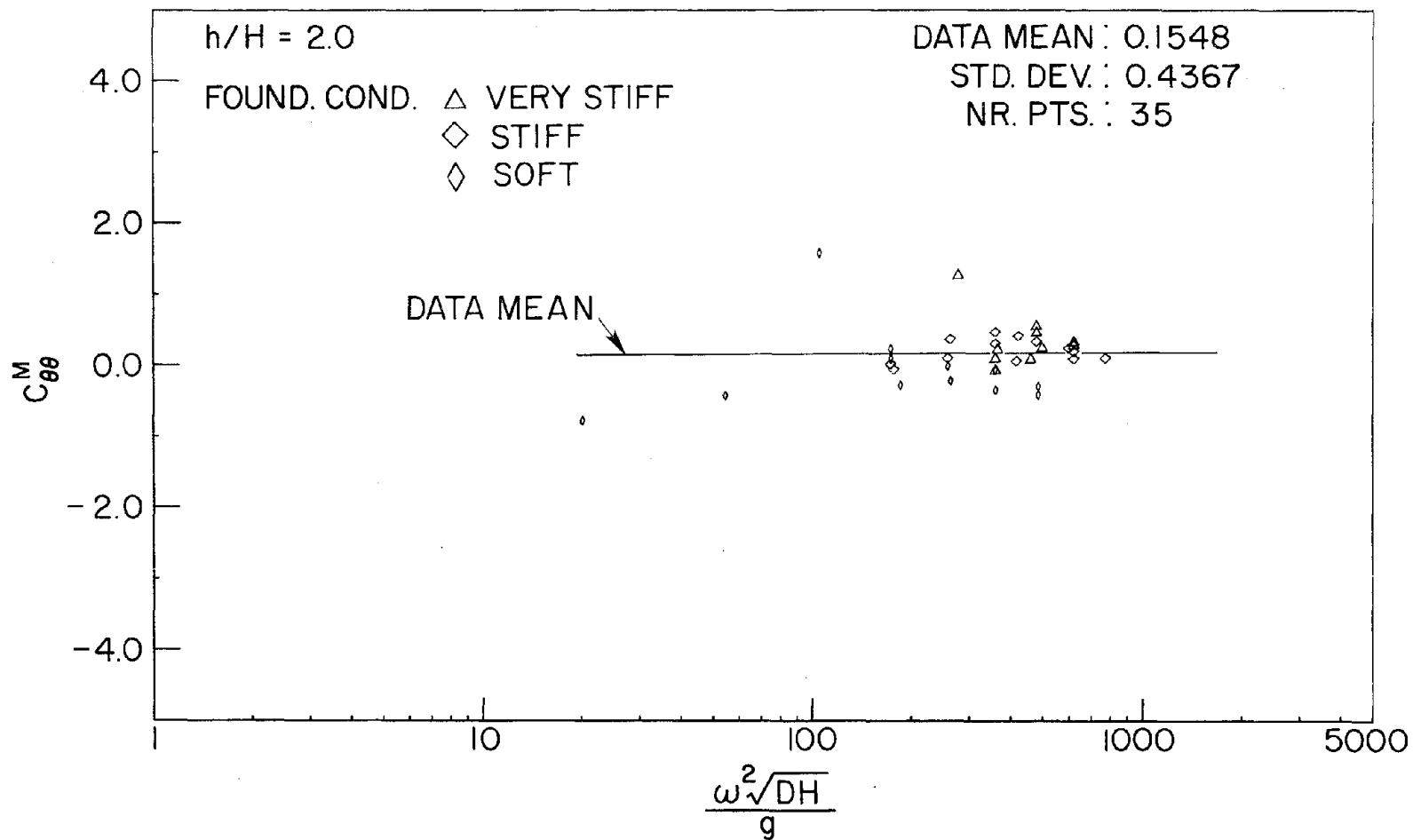


FIGURE 4.10: ROTATIONAL INERTIA COEFFICIENT, $h/H = 2.0$

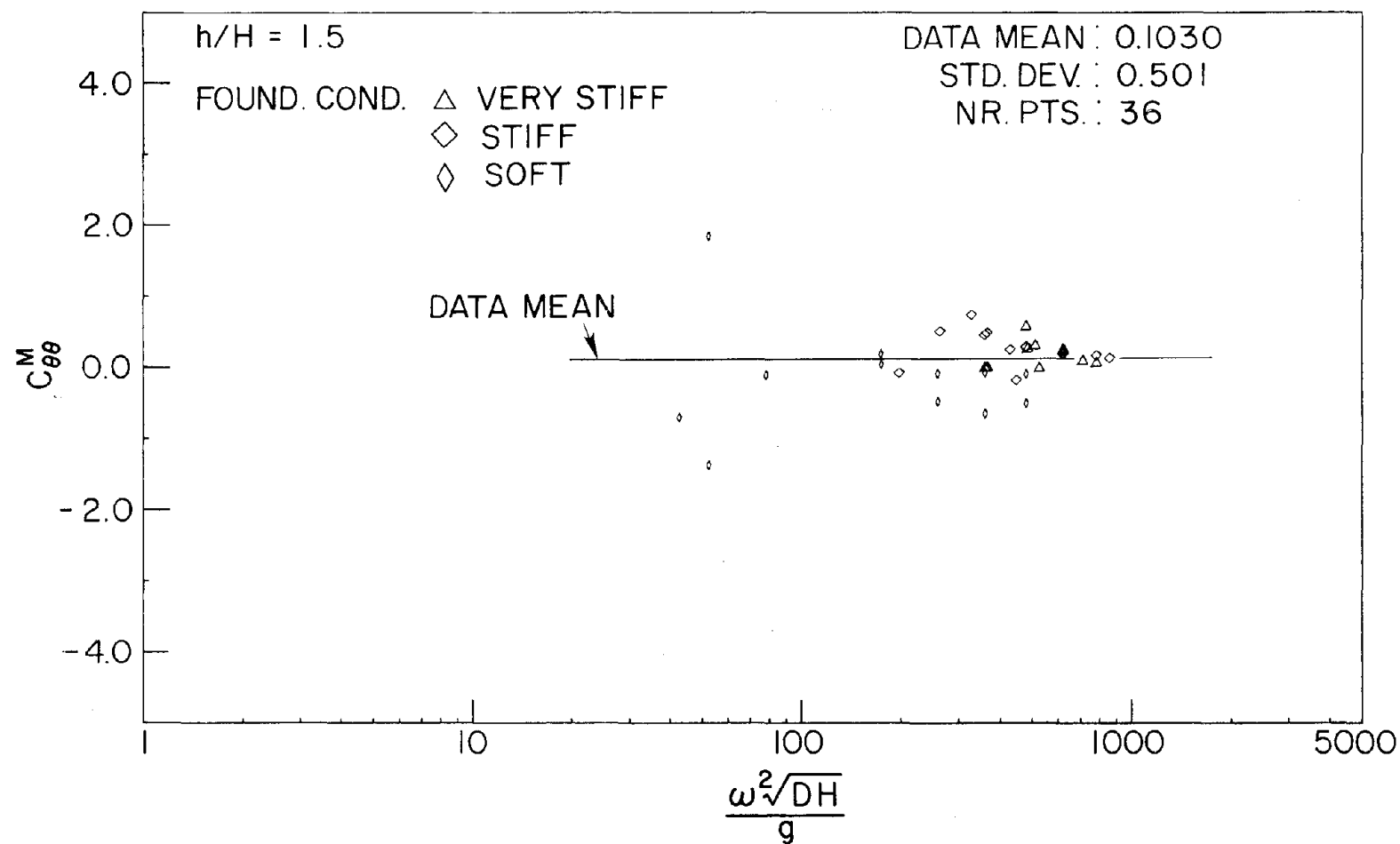


FIGURE 4.11: ROTATIONAL INERTIA COEFFICIENT, $h/H = 1.5$

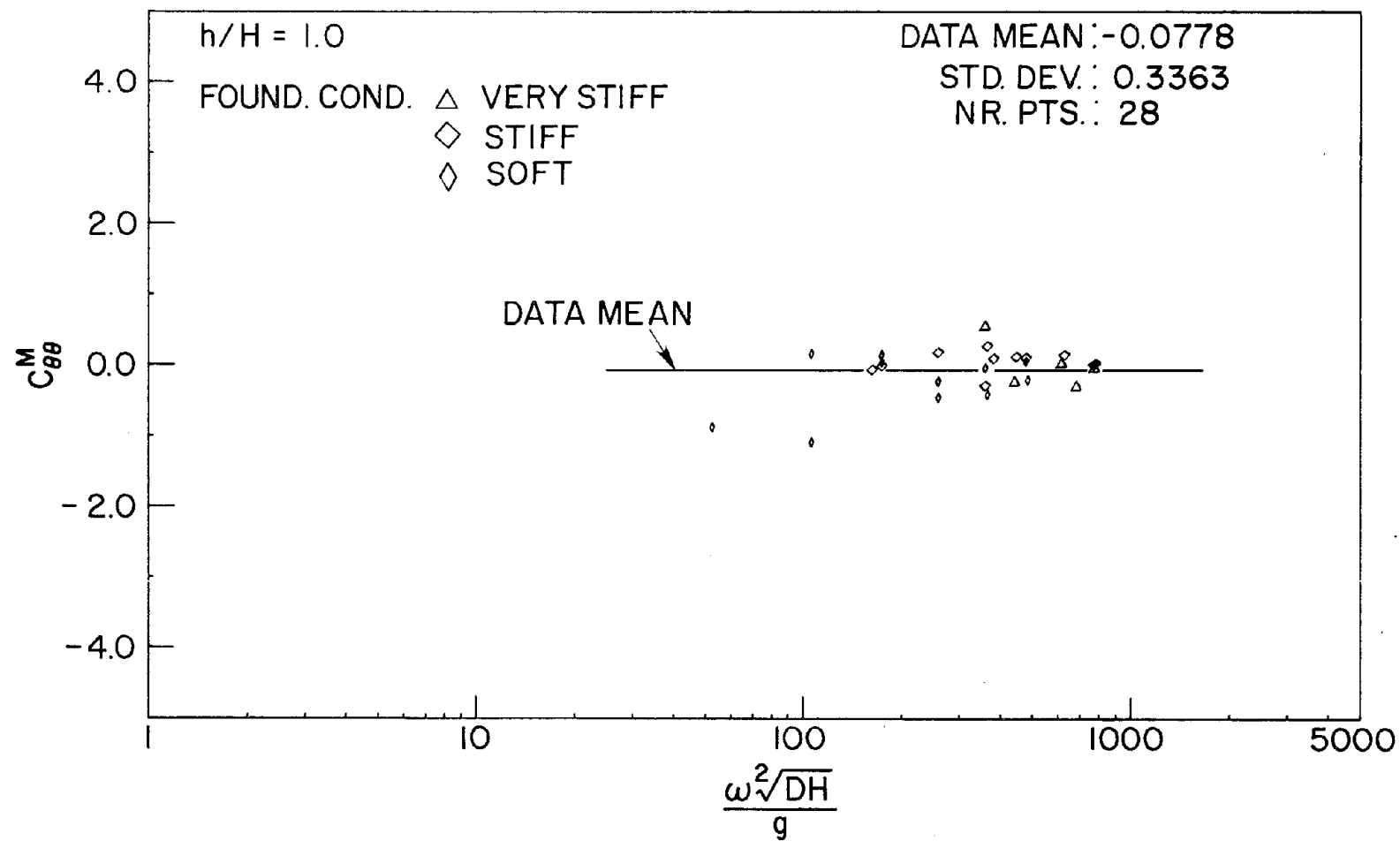


FIGURE 4.12: ROTATIONAL INERTIA COEFFICIENT, $h/H = 1.0$

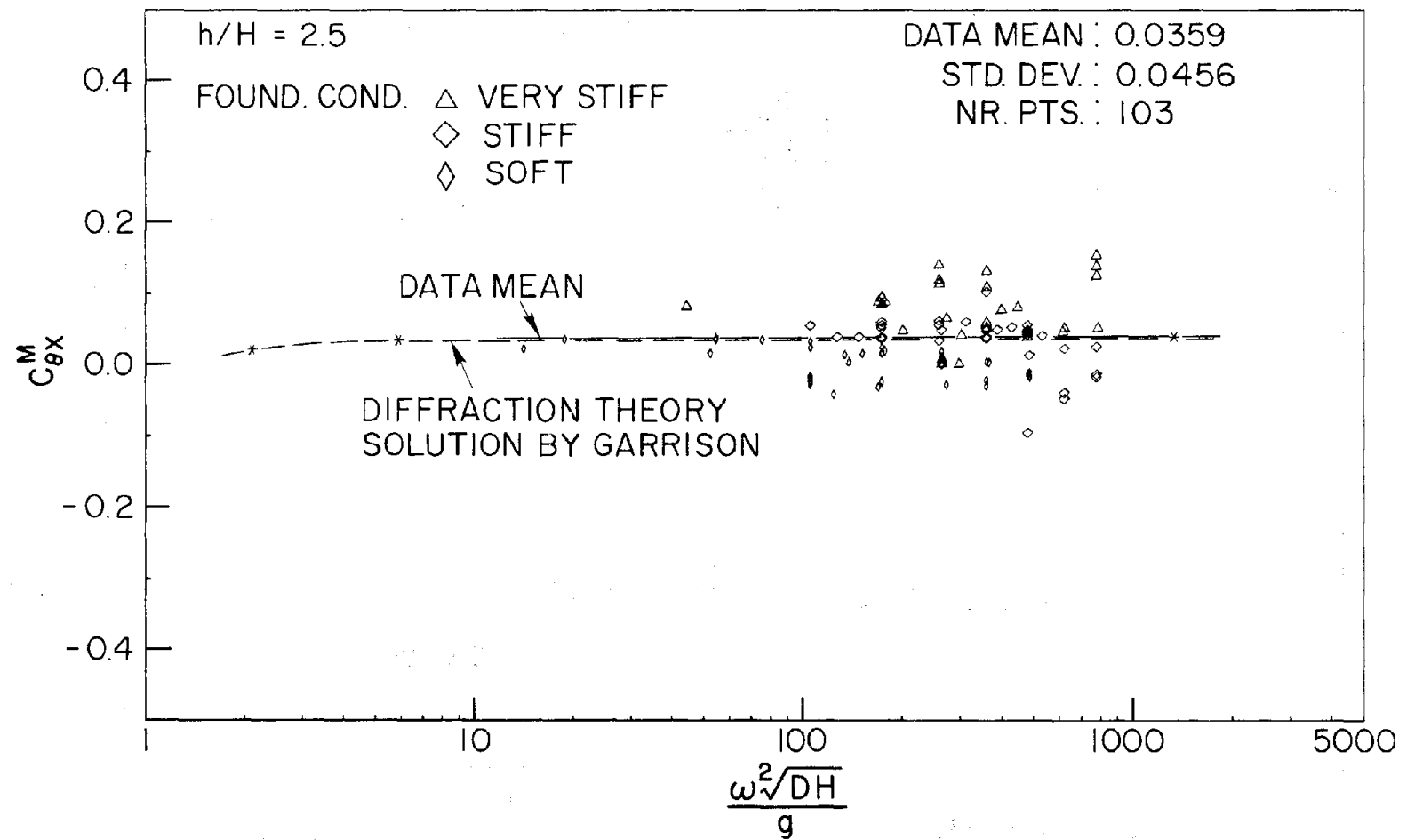


FIGURE 4.13: COUPLED INERTIA COEFFICIENT, $h/H = 2.5$

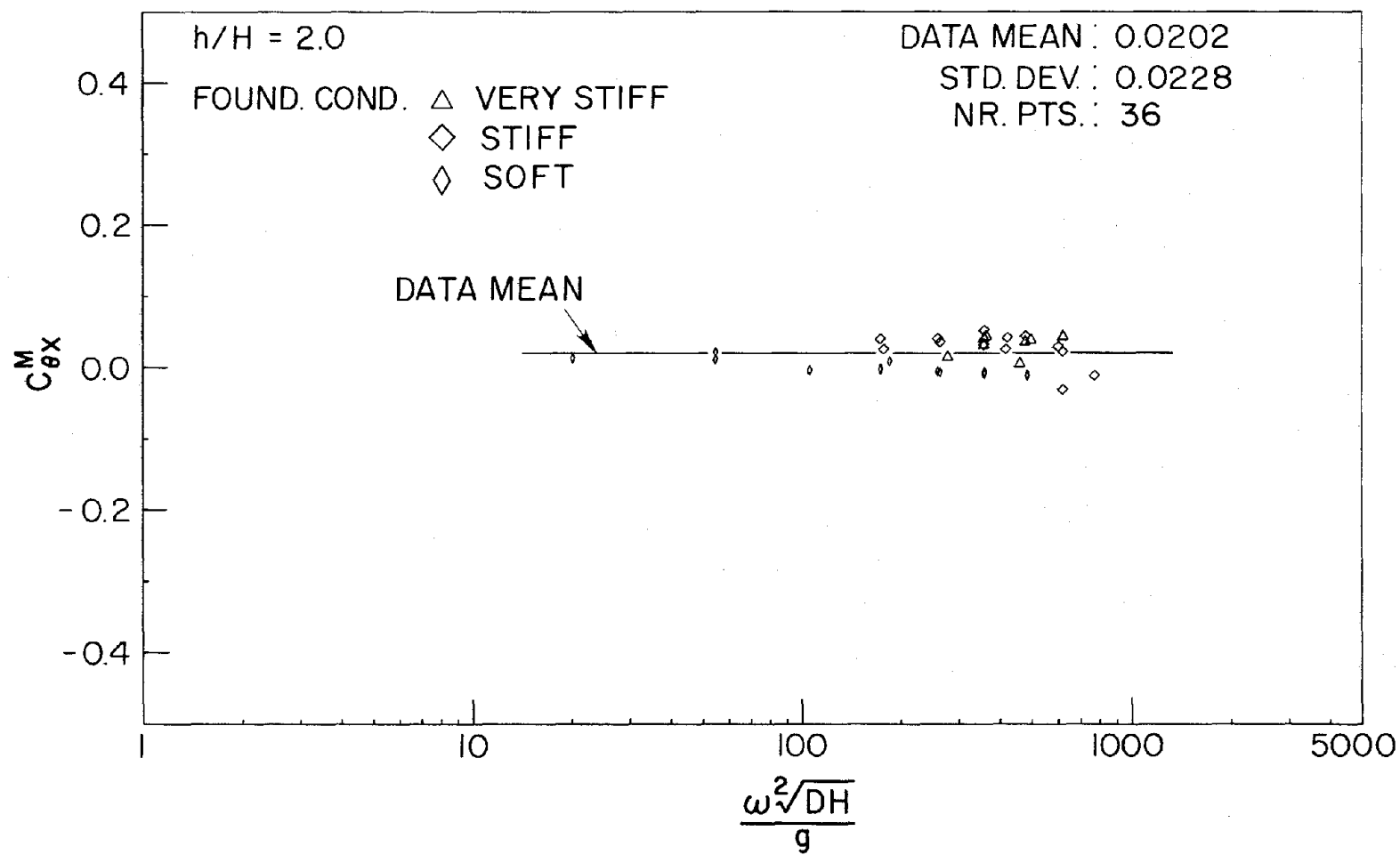
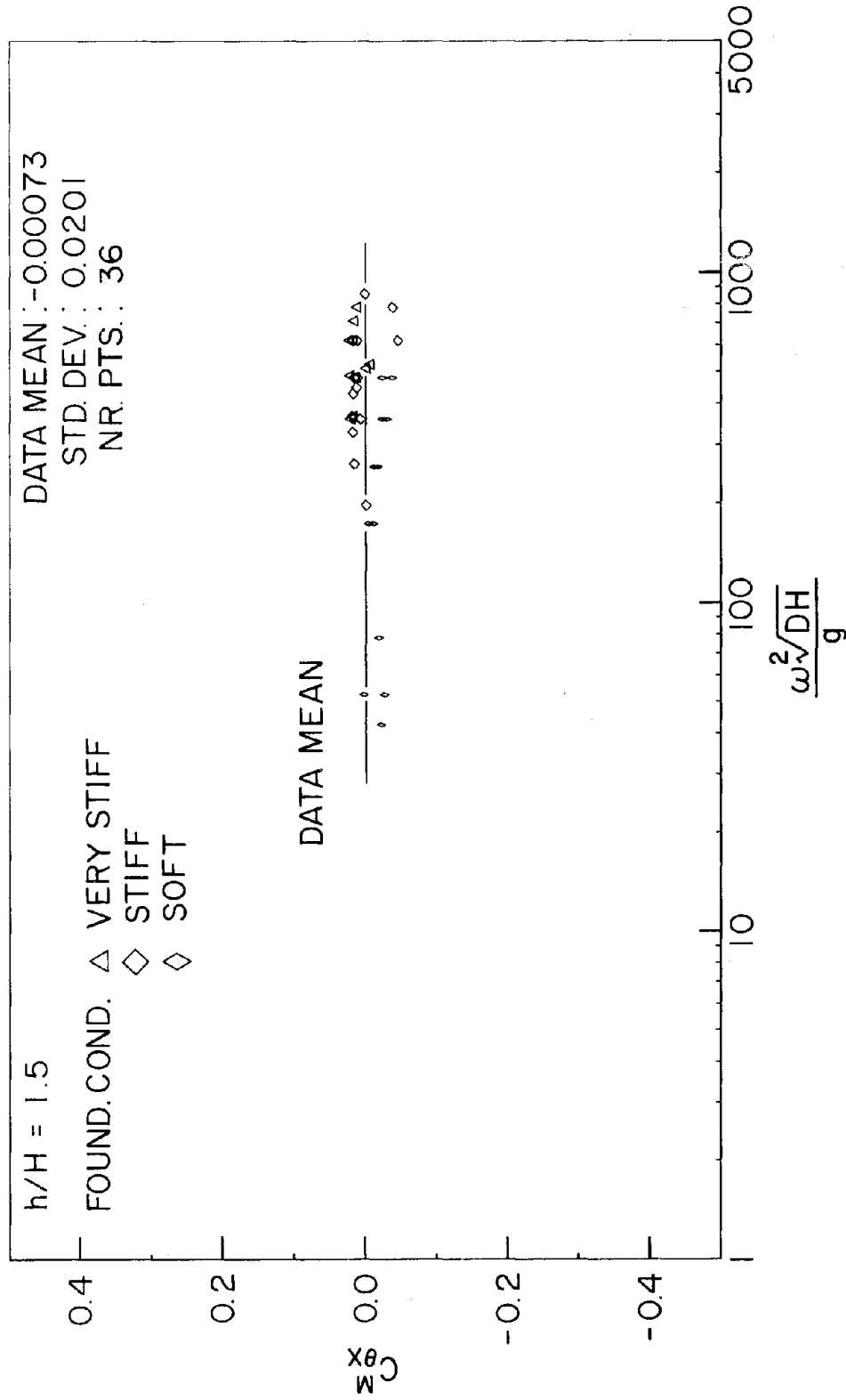


FIGURE 4.14: COUPLED INERTIA COEFFICIENT, $h/H = 2.0$

FIGURE 4.15: COUPLED INERTIA COEFFICIENT, $h/H = 1.5$

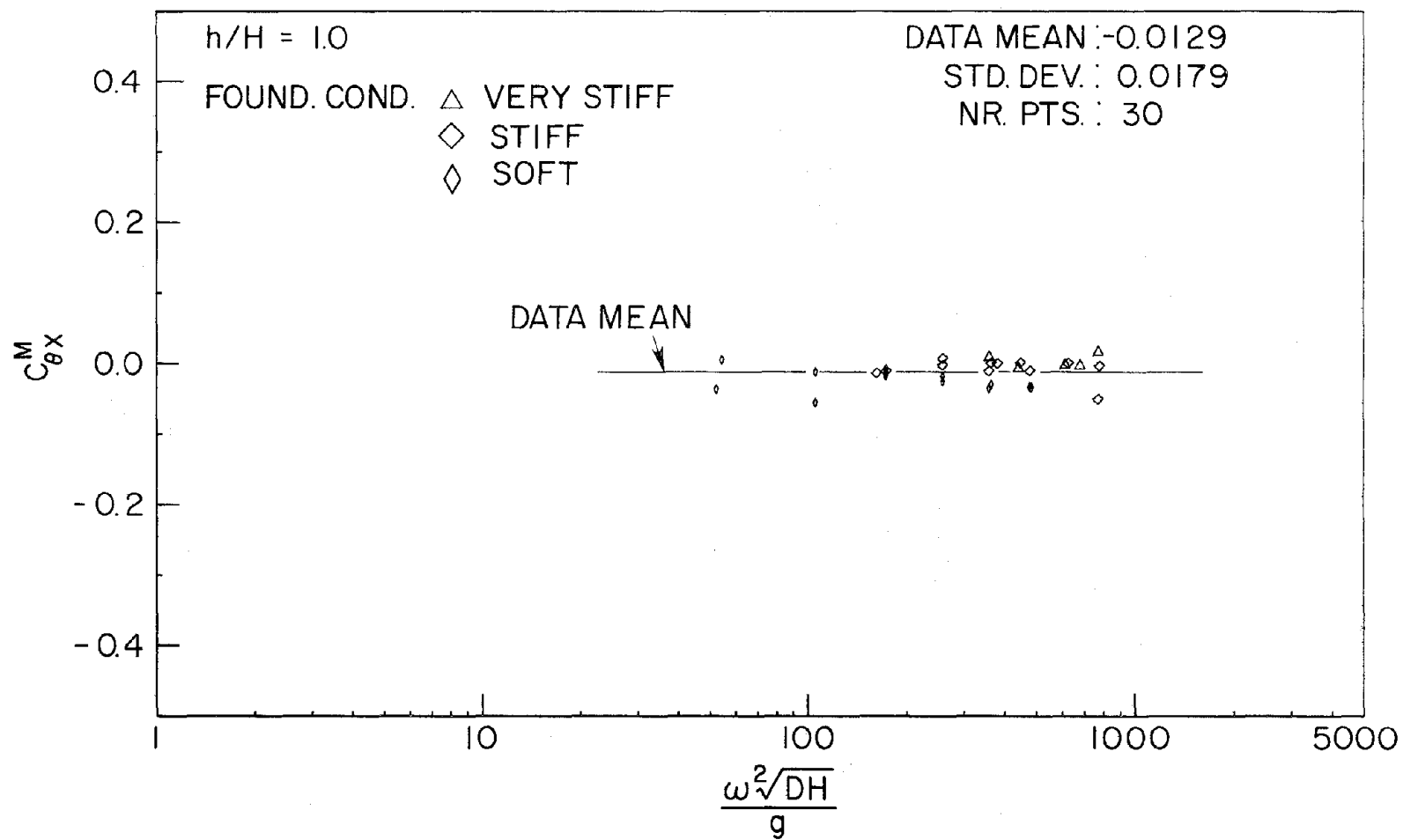
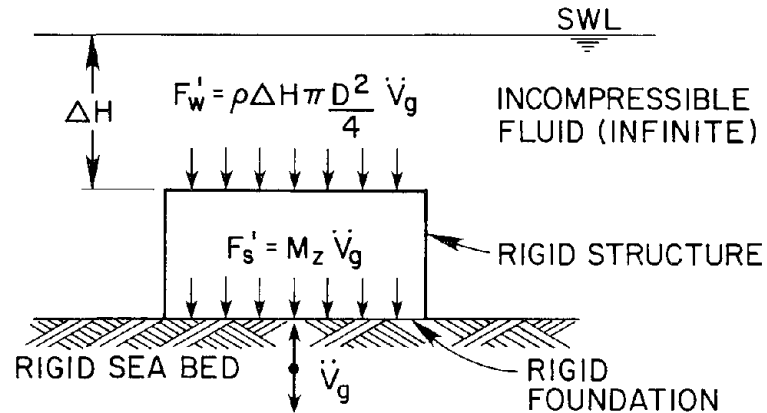


FIGURE 4.16: COUPLED INERTIA COEFFICIENT, $h/H = 1.0$

(1) FOUNDATION EXCITATION ONLY

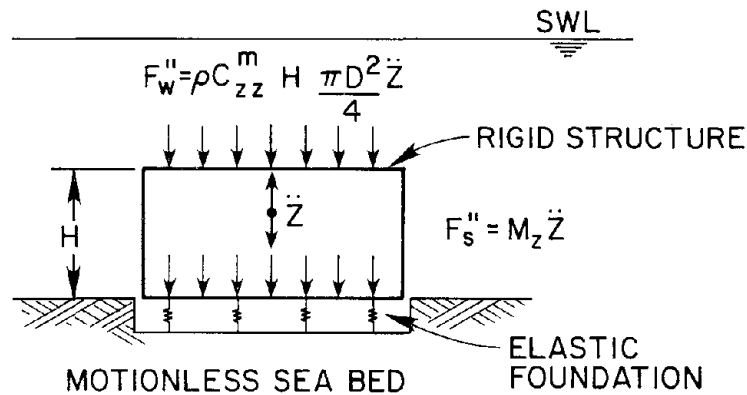


$$F'_z = (M_z + \rho \Delta H \frac{\pi D^2}{4}) \dot{V}_g =$$

FORCE DUE TO RIGID BODY MOTION

+

(2) RELATIVE MOTION ONLY



$$F''_z = (M_z + \rho C_{zz}^m H \frac{\pi D^2}{4}) \ddot{Z} =$$

FORCE DUE TO RELATIVE MOTION

=

$$F_z = M_z (\ddot{Z} + \dot{V}_g) + \rho C_{zz}^m H \frac{\pi D^2}{4} \ddot{Z} + \rho \Delta H \pi \frac{D^2}{4} \dot{V}_g$$

FIGURE 4.17: VERTICAL INERTIA FORCE REPRESENTATION

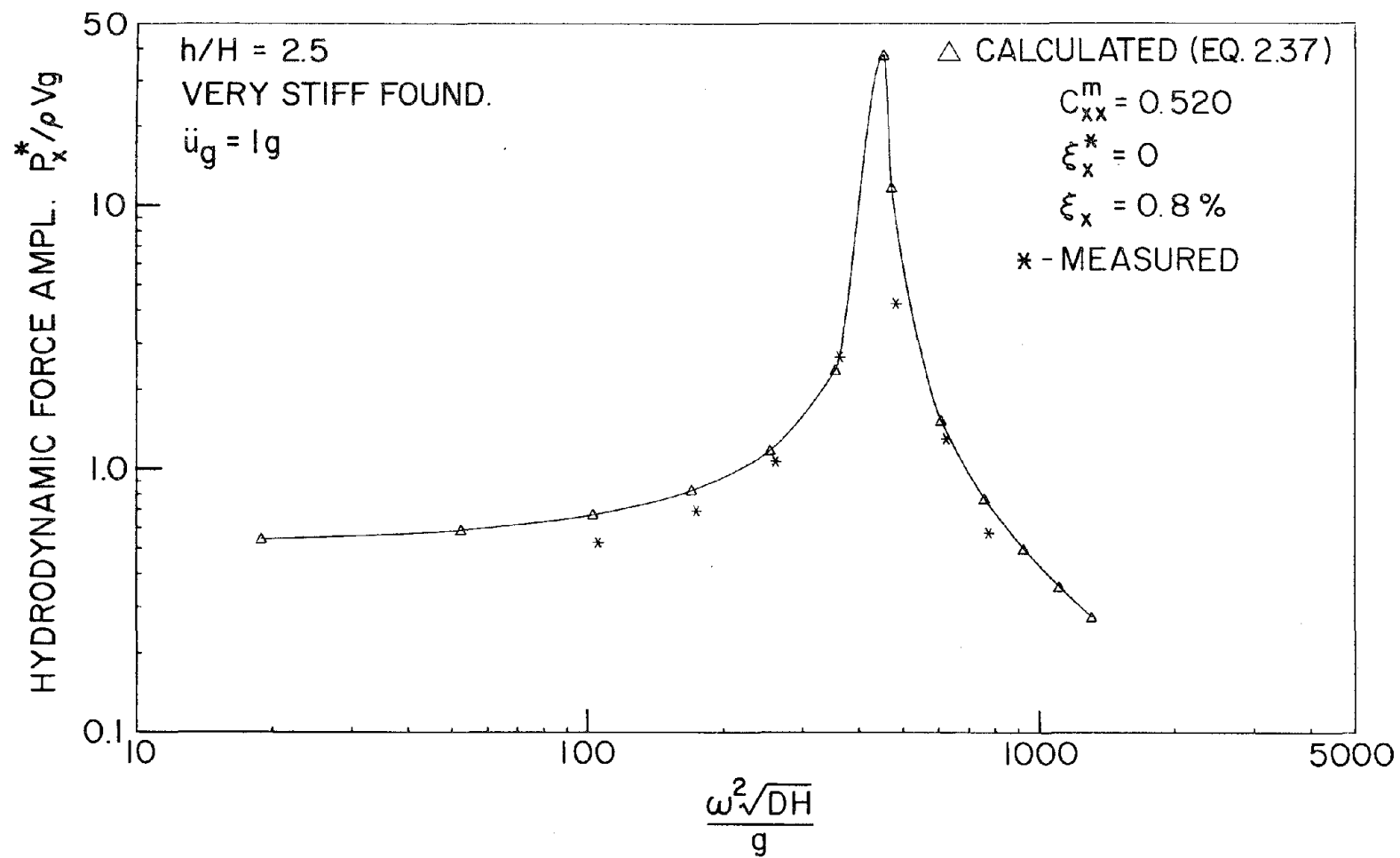


FIGURE 4.18: CALCULATED VERSUS MEASURED HORIZONTAL HYDRODYNAMIC FORCE AMPLITUDE, $h/H = 2.5$

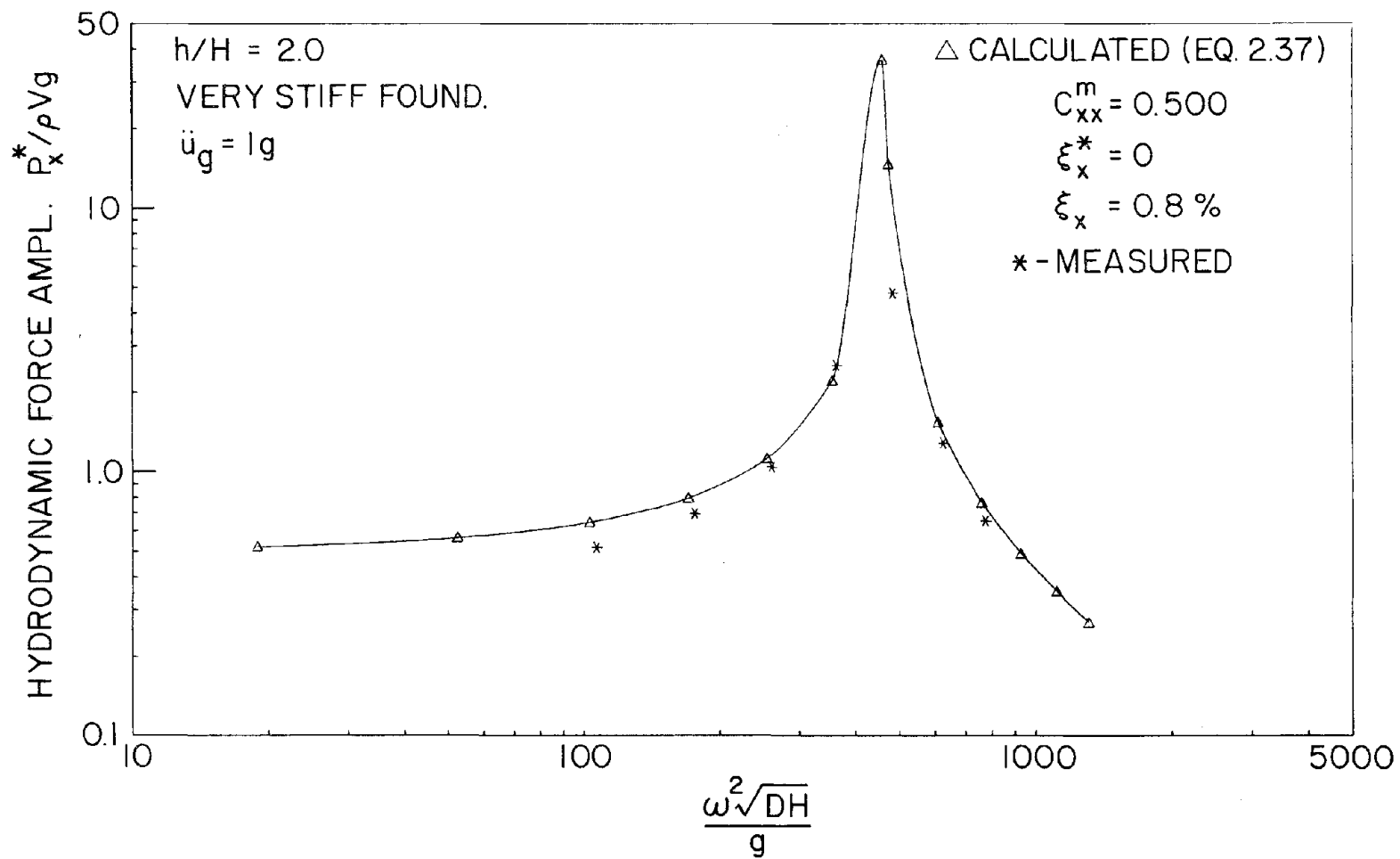


FIGURE 4.19: CALCULATED VERSUS MEASURED HORIZONTAL HYDRODYNAMIC FORCE AMPLITUDE, $h/H = 2.0$

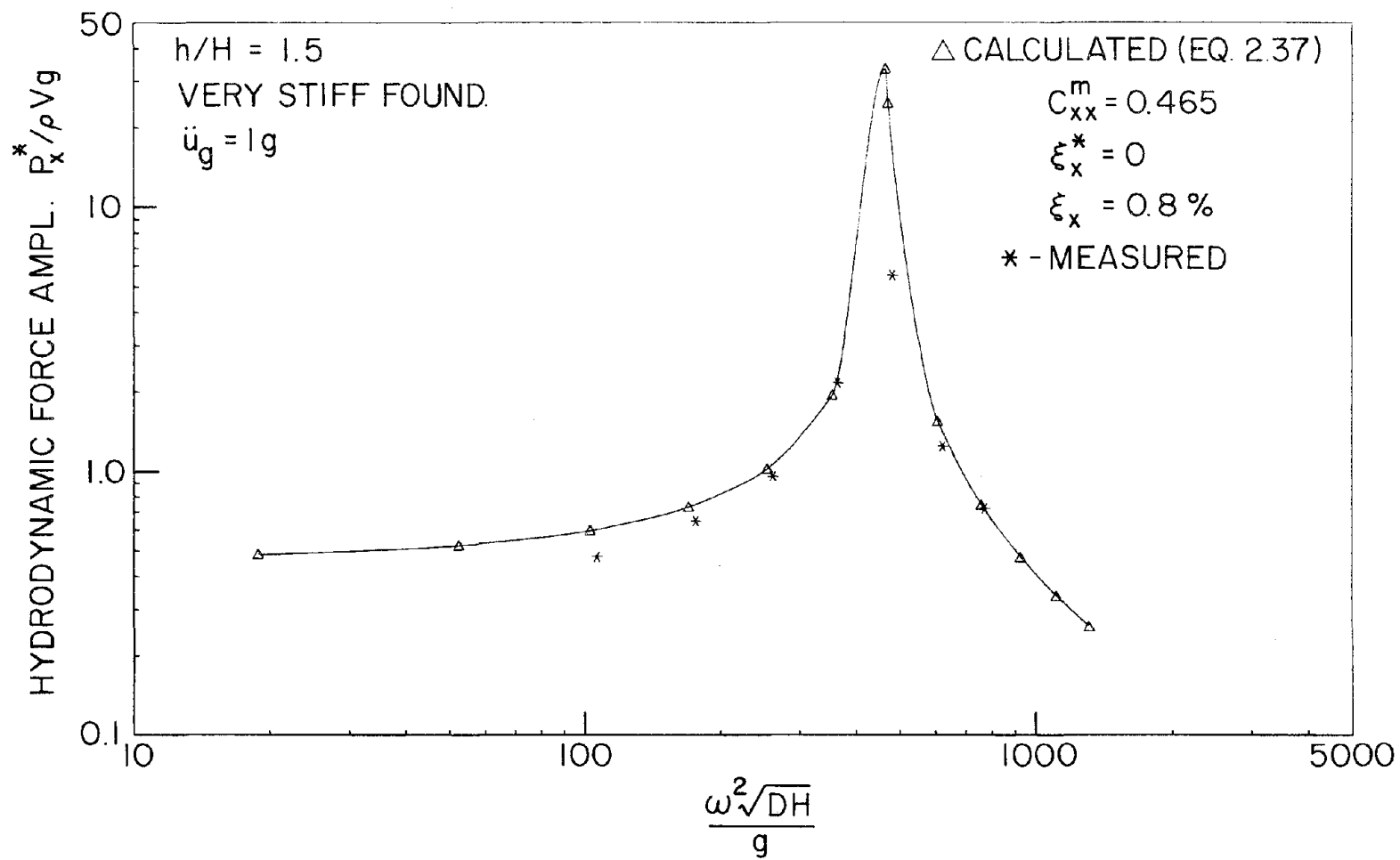


FIGURE 4.20: CALCULATED VERSUS MEASURED HORIZONTAL HYDRODYNAMIC FORCE AMPLITUDE, $h/H = 1.5$

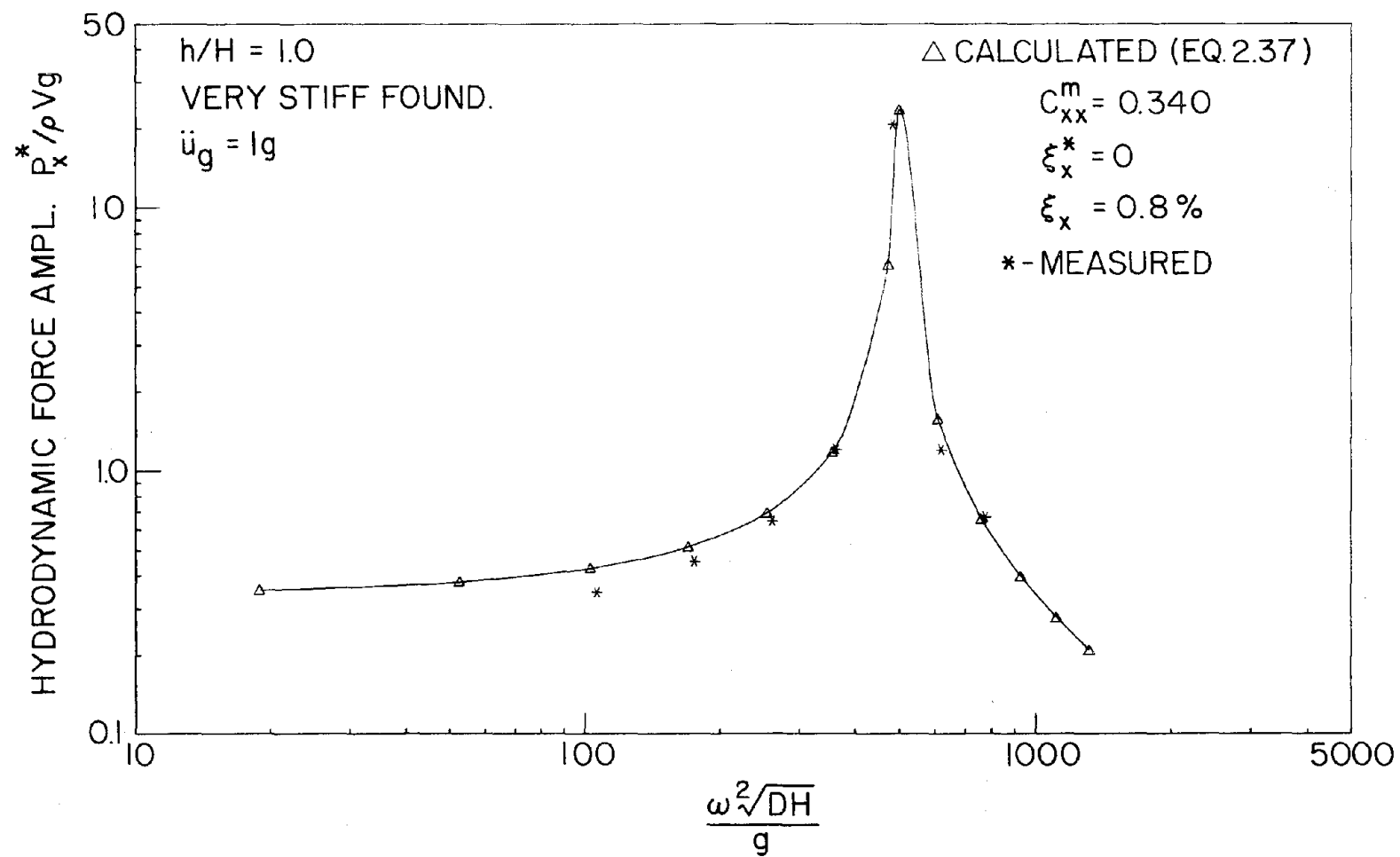


FIGURE 4.21: CALCULATED VERSUS MEASURED HORIZONTAL HYDRODYNAMIC FORCE AMPLITUDE, $h/H = 1.0$

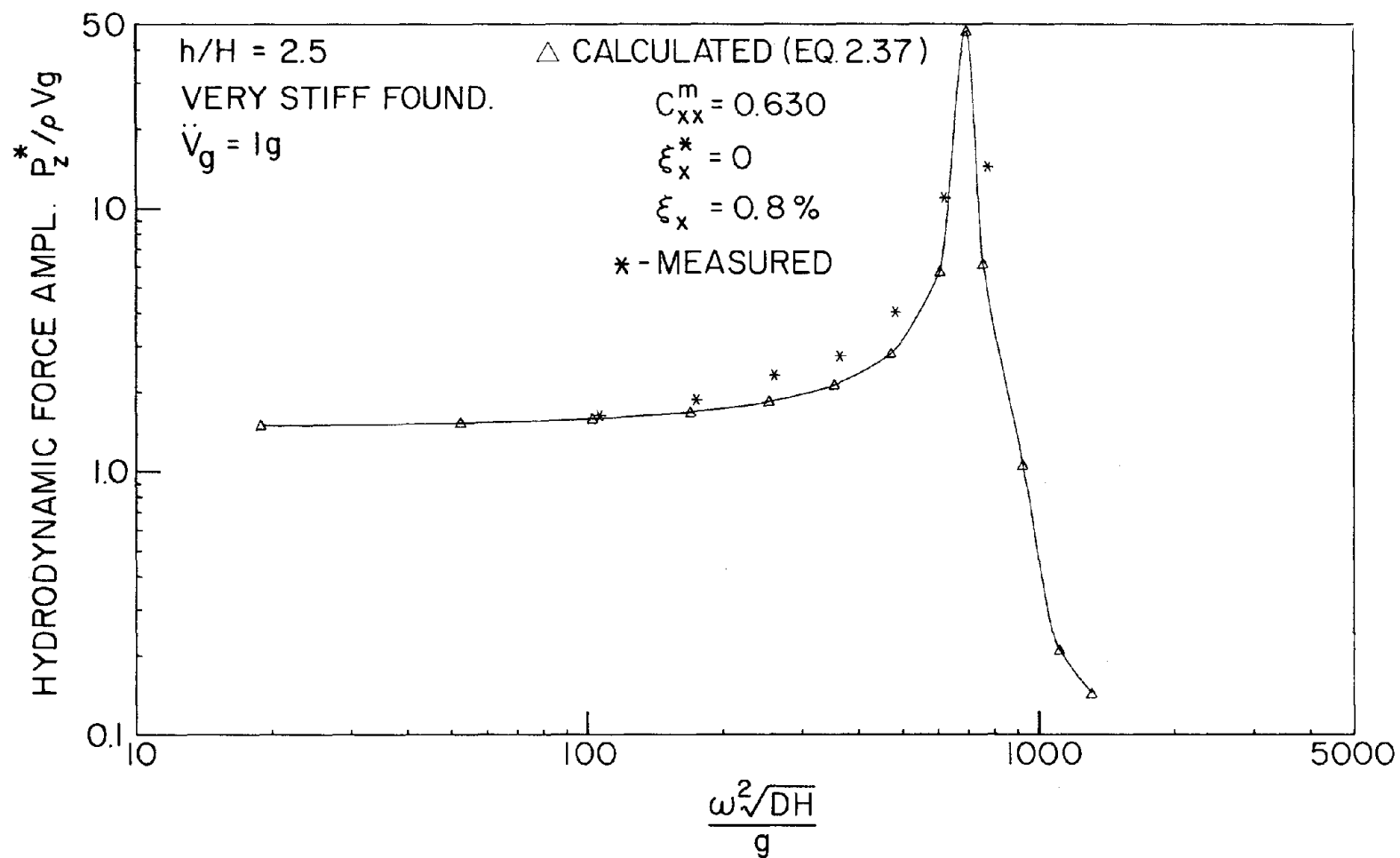


FIGURE 4.22: CALCULATED VERSUS MEASURED VERTICAL HYDRODYNAMIC FORCE AMPLITUDE, $h/H = 2.5$

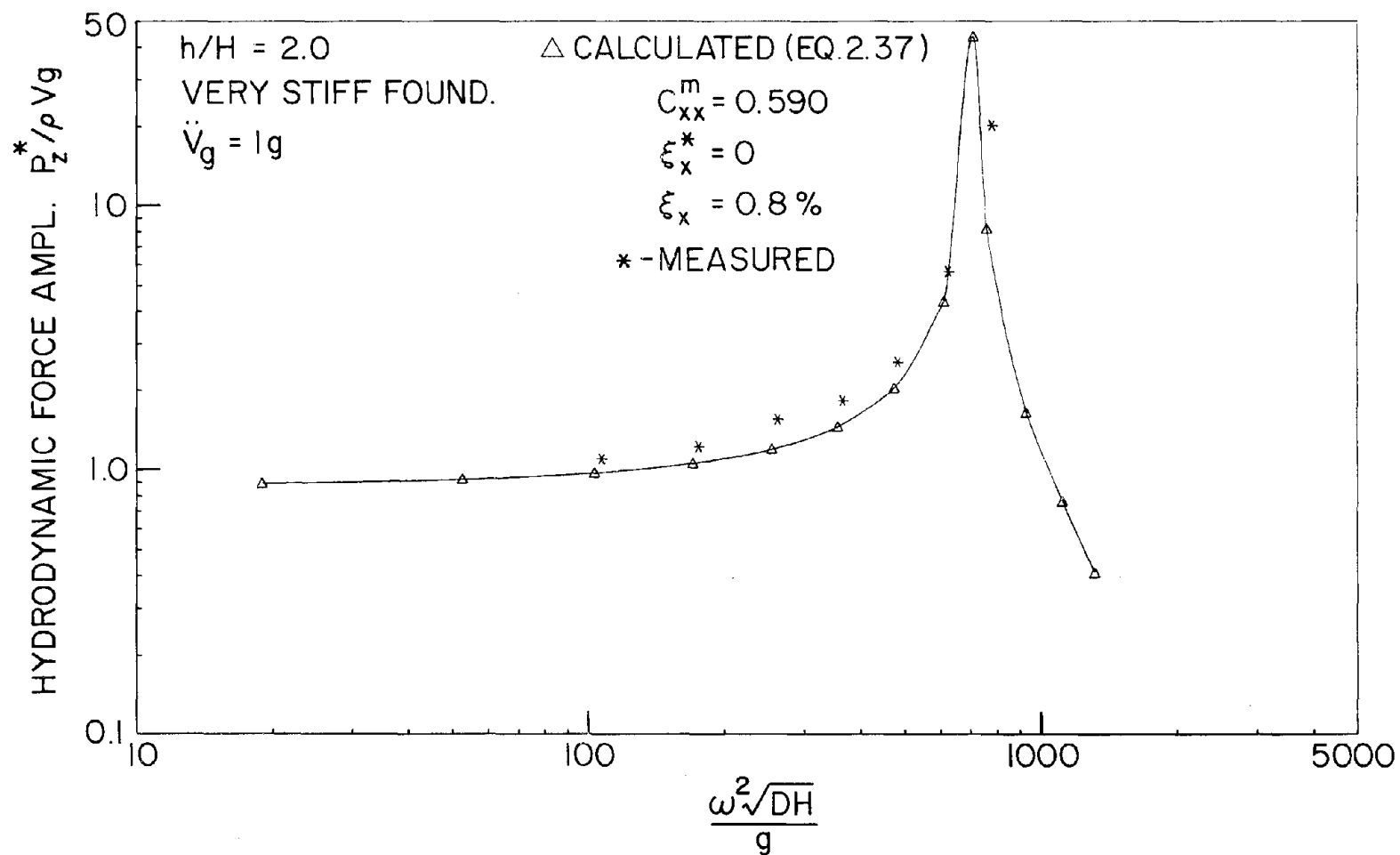


FIGURE 4.23: CALCULATED VERSUS MEASURED VERTICAL HYDRODYNAMIC FORCE AMPLITUDE, $h/H = 2.0$

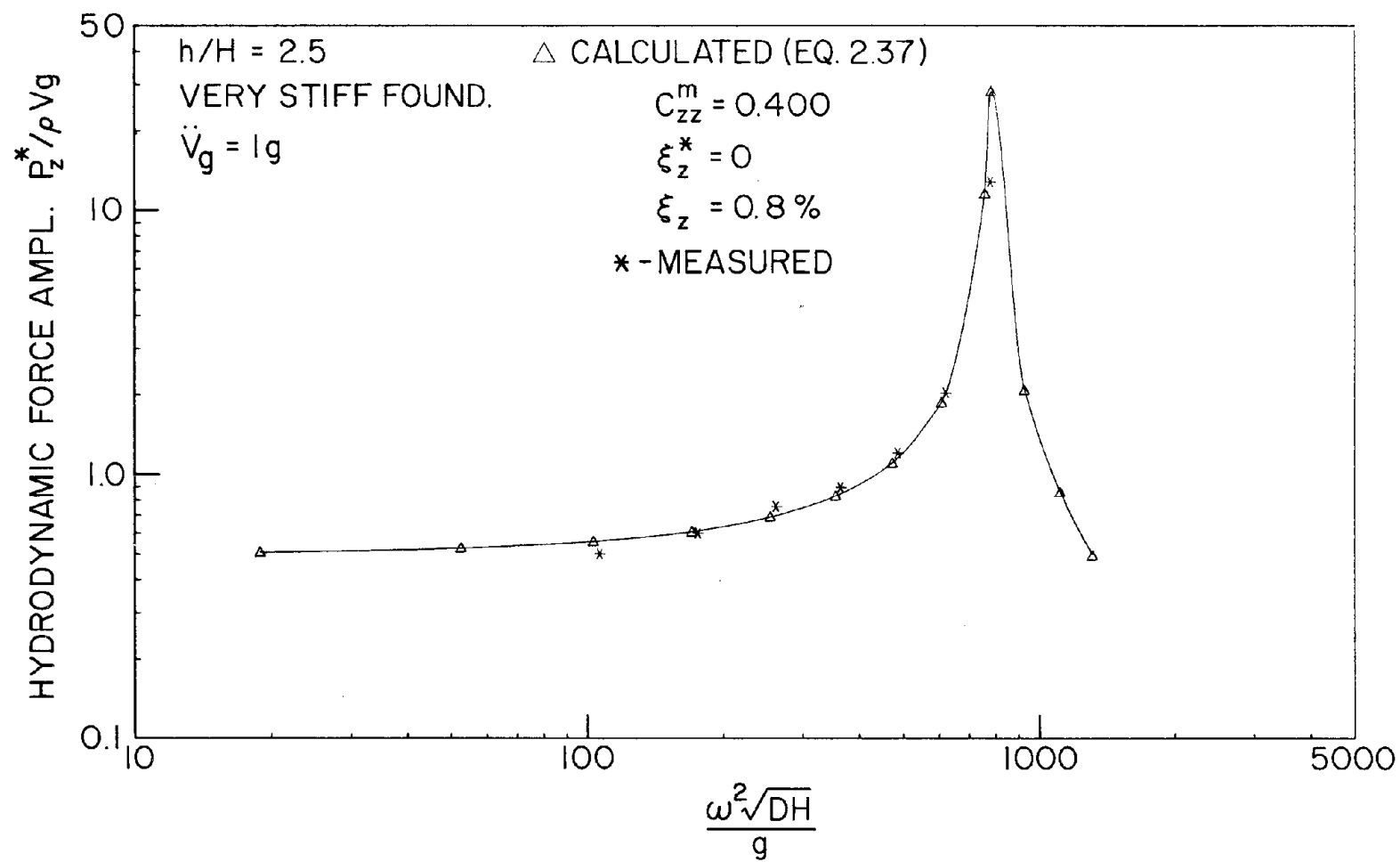


FIGURE 4.24: CALCULATED VERSUS MEASURED VERTICAL HYDRODYNAMIC FORCE AMPLITUDE, $h/H = 1.5$

5. SUMMARY AND DISCUSSION

5.1 Inertia Coefficients

Summaries of the inertia coefficients resulting from these experiments are shown in Figs. 5.1 - 5.4 as a function of relative water depth (h/H). The plotted values are the average of all data taken in each condition, as presented in Chapter 4.

5.1.1 Comparison with Theoretical Values

Table 5.1 shows a comparison of the data average values with those predicted by the two analytical techniques considered in this study. All averages have been taken over the range of the dimensionless frequency parameter (σ) from 20 to 1000.

It can be seen that the agreement between the measured and predicted values is quite good. In all cases, the differences are less than nine percent (9%).

These results are somewhat surprising in some cases, e.g., the rotational coefficients of Fig. 4.9, in light of the large standard deviation of data values. The scatter in these data is related to the fact that the rotational acceleration observed in the tests was very small. However, the numbers of samples observed was sufficiently large to give a good approximation of the mean value of quantities which are essentially constant. This is apparently the case with the rotational inertia terms. It is interesting to observe that both the horizontal and vertical inertia terms decrease rapidly for h/H less than about 2.0, and they appear to approach a constant value for relative water depths greater than 2.0.

5.1.2 Frequency Dependence

Examination of the experimental results and theoretical values shows that frequency dependence in the inertia coefficients is generally very small for σ greater than 20.

The only appreciable change with frequency occurs in horizontal motion for the case of the structure piercing the surface ($h/H = 1.0$), Fig. 4.5. In this case, the coefficient is essentially constant for values of σ greater than about 50. For smaller values of this parameter, the inertia term decreases rapidly with decreasing frequency. It should be noted that the theoretical solution in this case includes the effect of wave generation by the structure. The force dissipated in wave generation exceeds one percent (1%) of the inertia force at about σ equal 20 and increases rapidly for lower frequencies.

Ignoring frequency dependence in the surface piercing case would mean that the inertia coefficient would be overestimated by approximately thirteen percent (13%) at σ equal 20. This error would be expected to decrease rapidly with submergence of the structure.

5.1.3 Horizontal-Rotational Coupling

Coupling between the horizontal and rotational modes of motion in the inertia coefficients is predicted by the theory and can be measured, Fig. 4.13. However, the value of this coupling is very small.

Eigenvalue calculations with the largest value of hydrodynamic coupling observed in these tests show that the effect is seen in the

fifth digit of natural frequency and mode shape.

5.2 Hydrodynamic Pressure Force

Most of the considerations in this report have dealt with defining the hydrodynamic inertia coefficients. We would now like to consider the variation in hydrodynamic pressure force directly before we conclude our study.

5.2.1 Parameter Sensitivity

We have stated previously that the hydrodynamic pressure force can be related directly to structure response (and vice versa) through the inertia terms, e.g., Eqs. 2.37 and 2.39. We would now like to examine which of the system characteristics most affect the pressure force.

Fig. 5.5 shows the effect of a fifteen percent (15%) increase or decrease in the value of the horizontal inertia coefficient. These results show that the pressure force changes approximately in proportion to the change in the inertia coefficient (actually $\pm 17\%$). In addition, there is the resonant frequency shift that would be expected.

Fig. 5.6 shows the effect of a ten percent (10%) increase or decrease in foundation stiffness. It can be observed that foundation stiffness changes only shift the location of resonance and have no influence on the magnitude of the pressure force.

Fig. 5.7 shows the effect of change in foundation dampening from approximately eight tenths of one percent (0.8%) of critical, the value observed in the model, to fifteen percent (15%). We note that

the pressure force decreases by sixty-five percent (65%) as foundation dampening is increased from five percent (5%) to fifteen percent (15%) of critical.

5.2.2 Phase Angle

Fig. 5.8 shows the phase relationship between hydrodynamic pressure force and foundation acceleration for varying values of foundation dampening. The phase angle is seen to be highly dependent on foundation dampening at frequencies near resonance. It is also interesting to note that while the pressure force and foundation acceleration are in phase at frequencies far below resonance, they are out of phase by a fixed angle dependent on the damping at frequencies far above resonance.

5.3 Foundation forces in Random Excitation

We have examined fluid-structure interaction in harmonic motion in considerable detail and have demonstrated that hydrodynamic inertia forces can be measured or predicted accurately under these conditions.

However, earthquakes occur as random ground accelerations and structures must be designed to withstand this condition.

One common method of determining response to random excitation is step-by-step integration of the equations of motion using a discrete acceleration time series as the forcing function. A variety of methods are available to accomplish this calculation. Most of these methods rely on system coefficients which are constant in frequency and independent of the magnitude of structure response.

The hydrodynamic coefficients measured in these experiments meet the requirements for use in step-by-step integration. Therefore, we can use this technique to examine the differences between forces measured during actual random excitations and those that can be calculated using a digitized record of the same ground acceleration.

The above comparison has been performed using the program SUBTANK which is listed in APPENDIX F. This program is based on integration methods and subroutines developed by Professor E. L. Wilson of the Civil Engineering Department at the University of California, Berkeley. The ground acceleration used in testing was a reproduction of the N-S component of the 1940 El Centro earthquake, scaled to a maximum acceleration value of approximately 0.31 g (304 cm/sec^2). A version of this record was used as a control signal for the earthquake simulator table, and the resulting table and structure responses were recorded. A digitized record of the actual table acceleration was then used with the horizontal inertia coefficient determined by Garrison, as previously discussed, to calculate a foundation shear force time history.

Fig. 5.9(a) shows a plot of the horizontal foundation acceleration recorded (and used in the step-by-step integration) and Fig. 5.9(b) shows the measured horizontal shear force between the structure and foundation. Fig. 5.9(c) shows the calculated shear force time history assuming hydrodynamic dampening equals two tenths of one percent (0.2%) of critical and foundation dampening equals eight tenths of one percent (0.8%), the values determined from the resonant decay tests. Coupling between horizontal and rotational modes has been neglected in this calculation. The case considered is for horizontal ground acceleration only.

The maximum shear force measured in this test run was 3745 Newtons compared to a calculated force of 3740 Newtons, for a difference of approximately one tenth of one percent ($\sim 0.1\%$). The conclusion to be drawn is that the hydrodynamic effects are very linear and can be properly considered by use of constant coefficients.

Fig. 5.10 shows three additional calculated horizontal shear force time histories using the ground acceleration record of Fig. 5.9(a).

Fig. 5.10(a) shows the force record achieved when hydrodynamic dampening is ignored. The maximum shear force calculated was 3834 Newtons, an increase of approximately two and four tenths percent (2.4%) over the measured value. This would not be an important increase in most applications. However, one can see from the effect of this small amount of dampening that it would only need to be a little greater before the resulting force reduction would begin to be significant. This would occur as the depth of submergence was decreased.

Figs. 5.10(b) and 5.10(c) show horizontal shear force time histories calculated for foundation dampening of five percent (5%) and fifteen percent (15%) of critical, respectively. The maximum shear force is seen to increase by approximately fifty percent ($\sim 50\%$) for a decrease in foundation dampening over this range. It is apparent that foundation dampening will be a major consideration in properly predicting foundation forces induced by earthquakes.

TABLE 5.1 COMPARISON OF MEAN VALUES OF EXPERIMENTALLY AND THEORETICALLY
DETERMINED INERTIA COEFFICIENTS FOR THE RANGE OF FREQUENCIES
OF THE EXPERIMENT

COEFFICIENT	h/H	PREDICTED	MEASURED	DIFFERENCE
HORIZONTAL	2.5	0.54	0.52	4 %
HORIZONTAL	1.0	0.34	0.34	~ 1 %
VERTICAL	2.5	0.64	0.62	3 %
ROTATIONAL	2.5	0.26	0.24	8 %
COUPLED	2.5	0.037	0.036	3 %

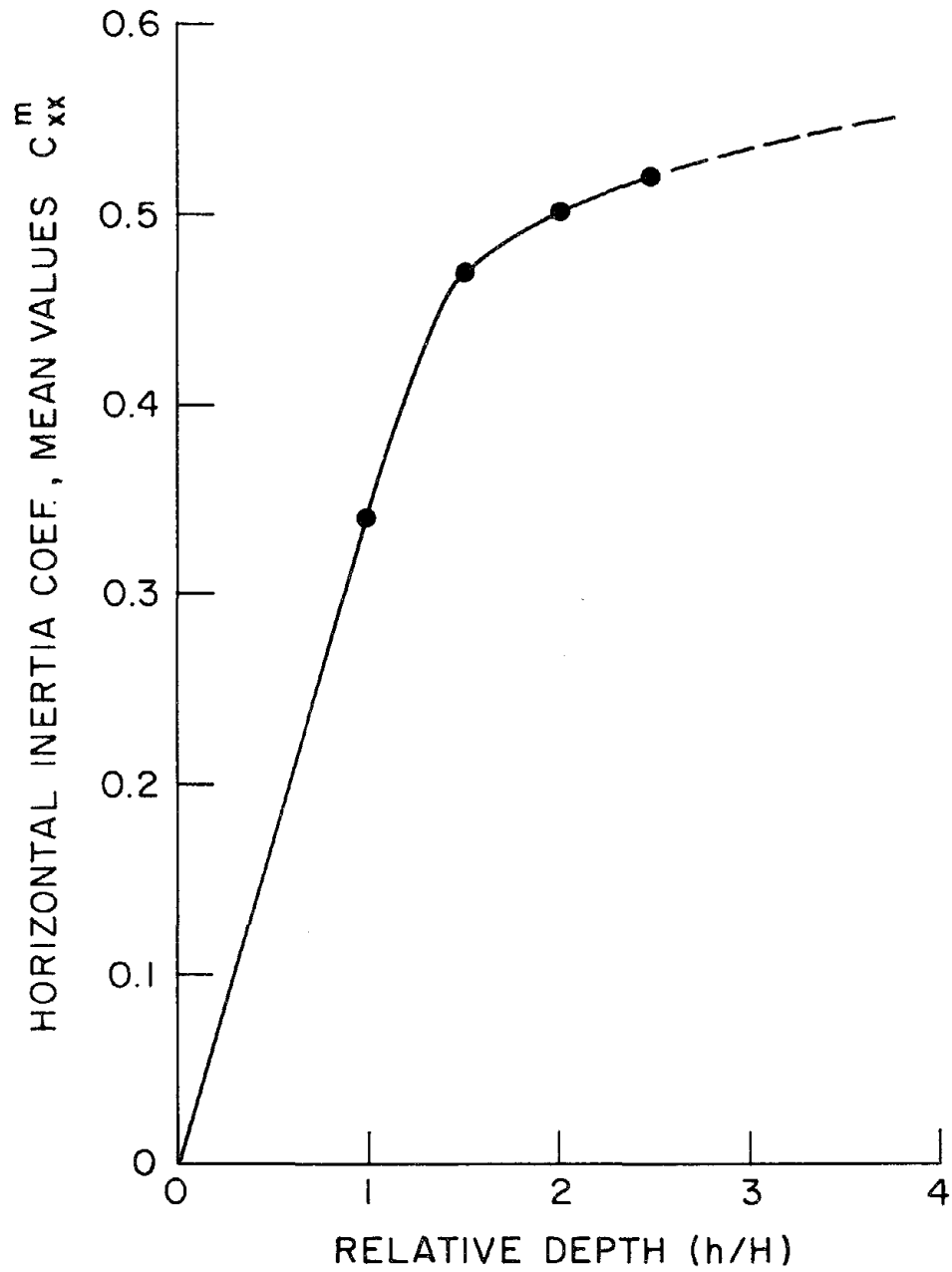


FIGURE 5.1: HORIZONTAL INERTIA COEFFICIENT (C_{xx}^m) MEAN VALUES VERSUS RELATIVE DEPTH (h/H)

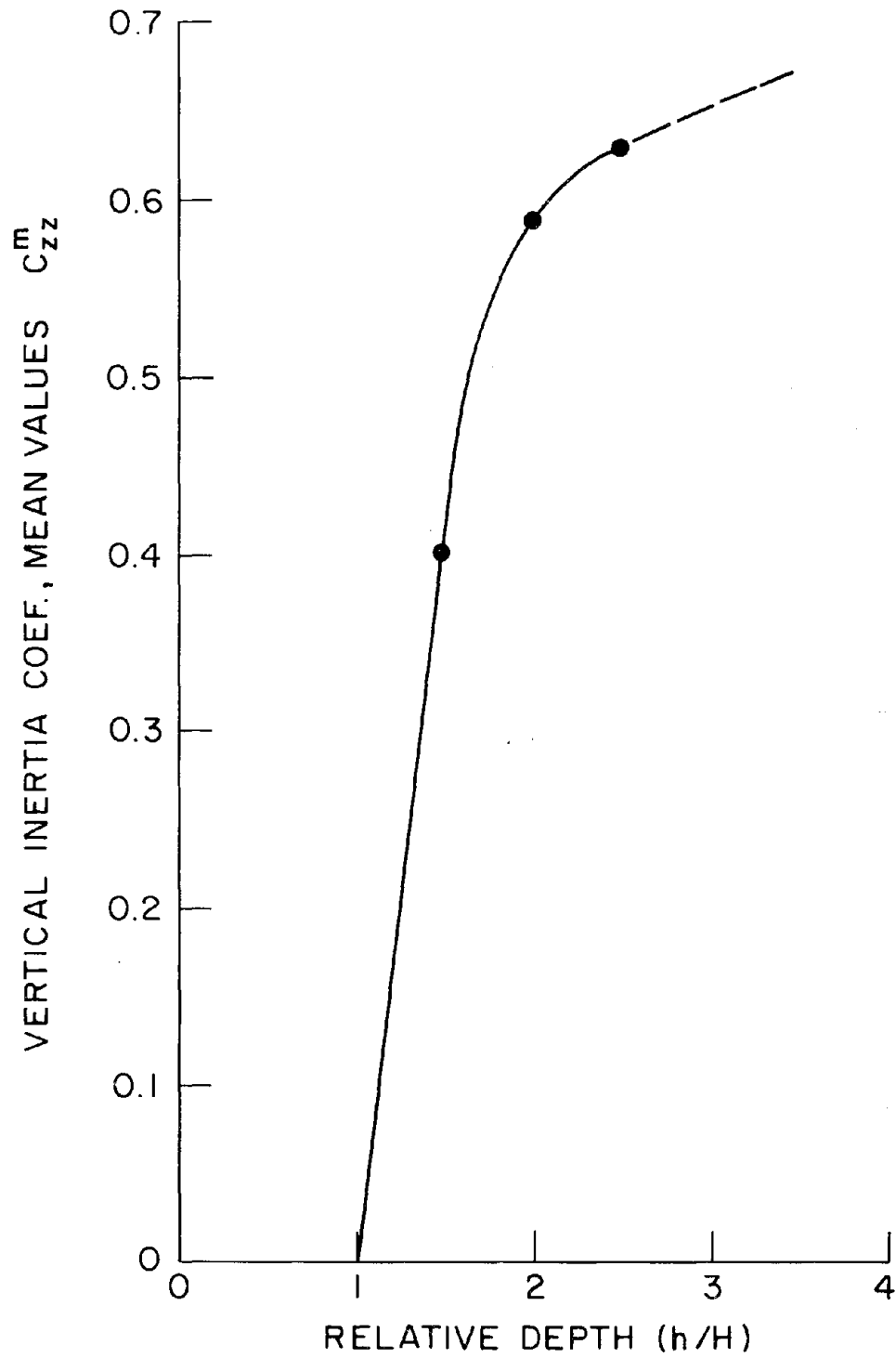


FIGURE 5.2: VERTICAL INERTIA COEFFICIENT (C_{zz}^m) MEAN VALUES VERSUS RELATIVE DEPTH (h/H)

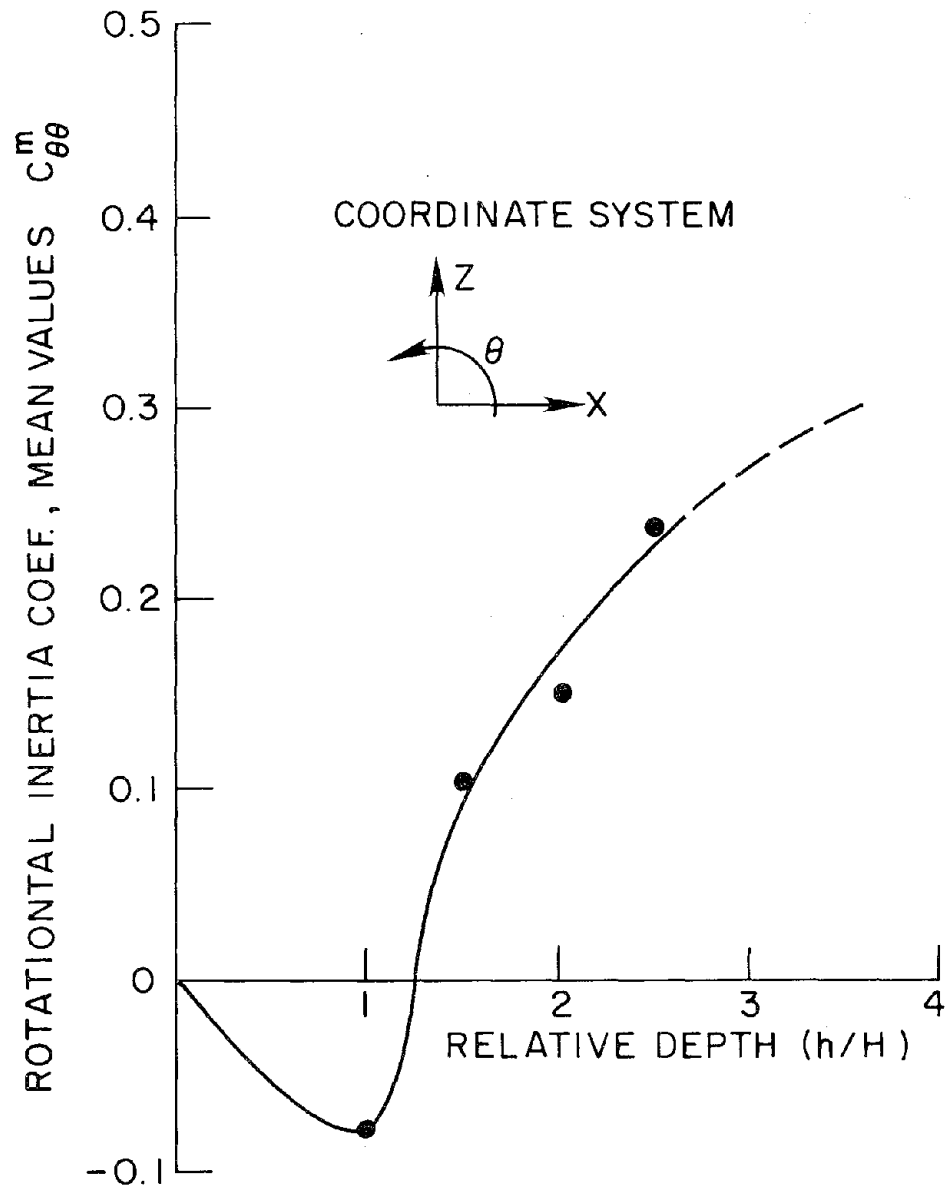


FIGURE 5.3: ROTATIONAL INERTIA COEFFICIENT ($C_{\theta\theta}^m$) MEAN VALUES VERSUS RELATIVE DEPTH (h/H)

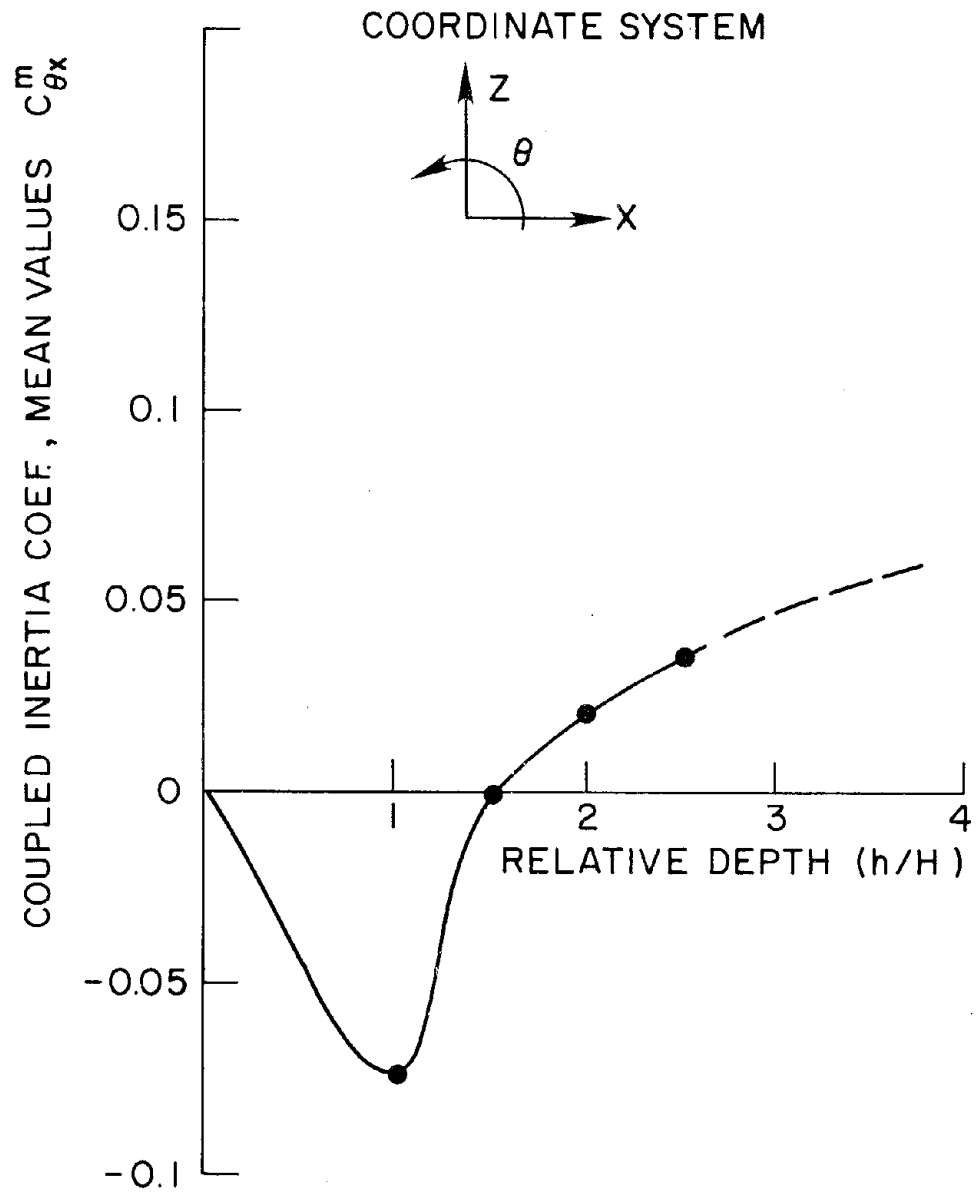


FIGURE 5.4: COUPLED INERTIA COEFFICIENT ($C_{\theta x}^m$) MEAN VALUES VERSUS RELATIVE DEPTH (h/H)

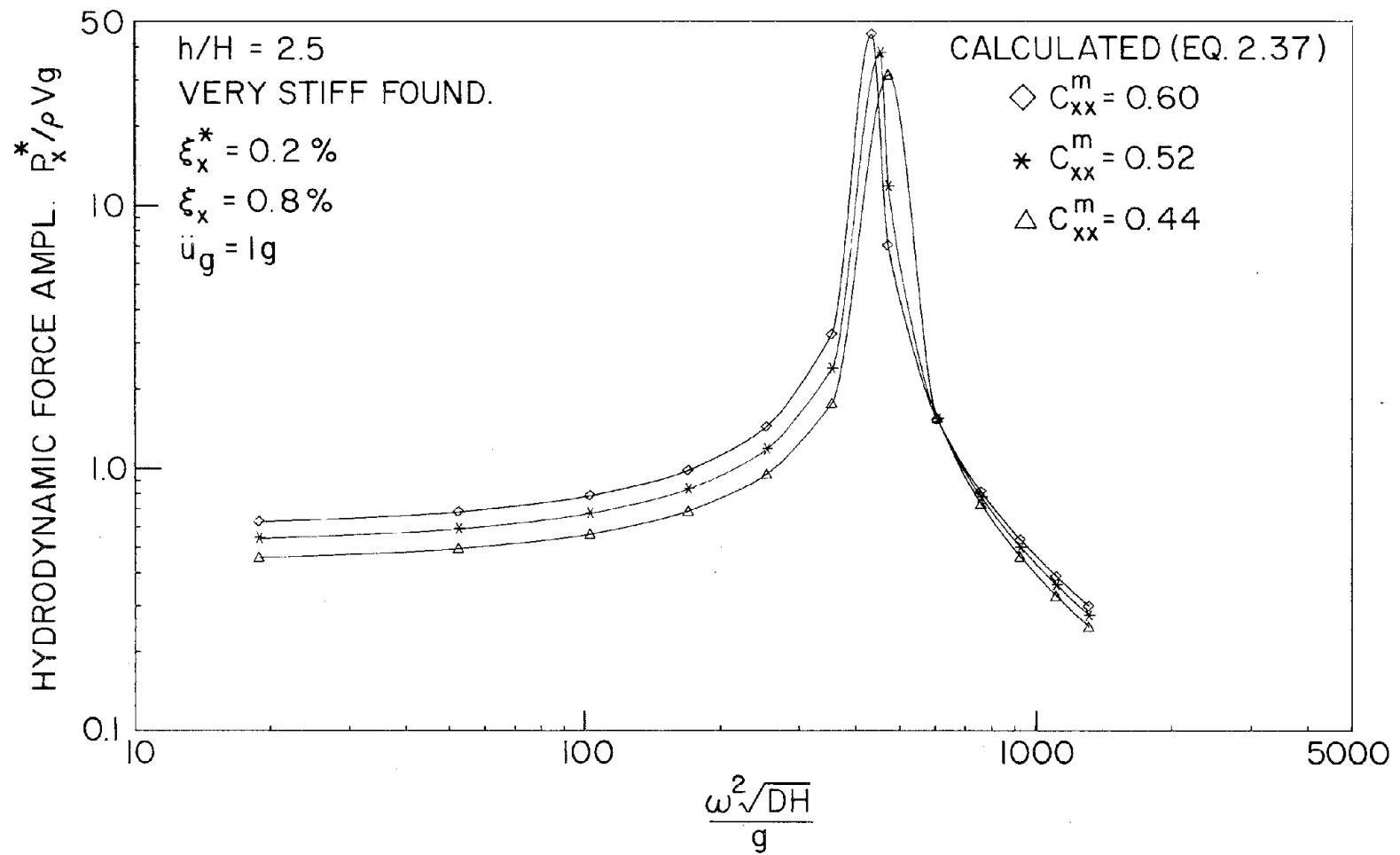


FIGURE 5.5: VARIATION IN HYDRODYNAMIC FORCE WITH CHANGES IN VIRTUAL MASS

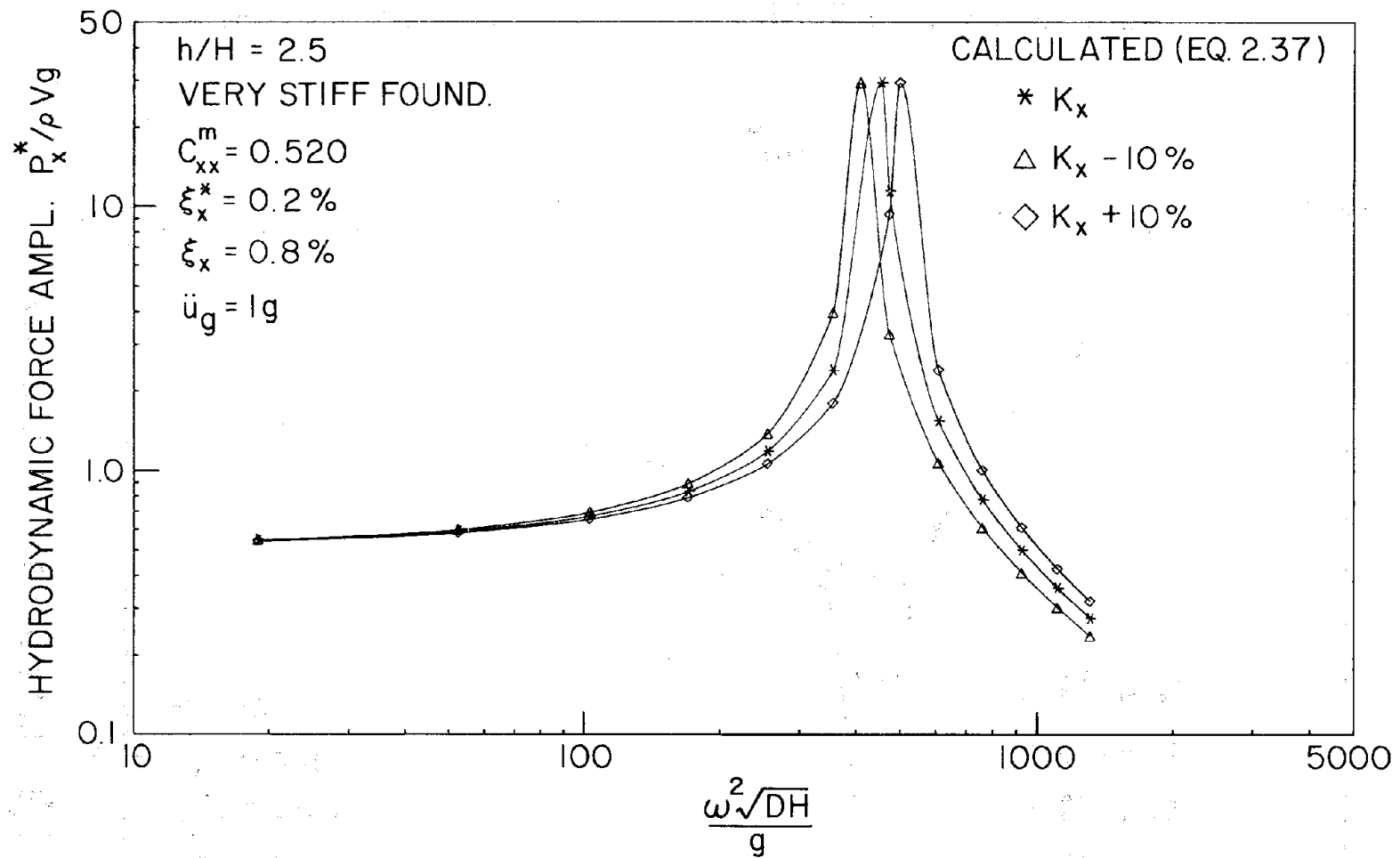


FIGURE 5.6: VARIATION IN HYDRODYNAMIC FORCE WITH CHANGES IN FOUNDATION STIFFNESS

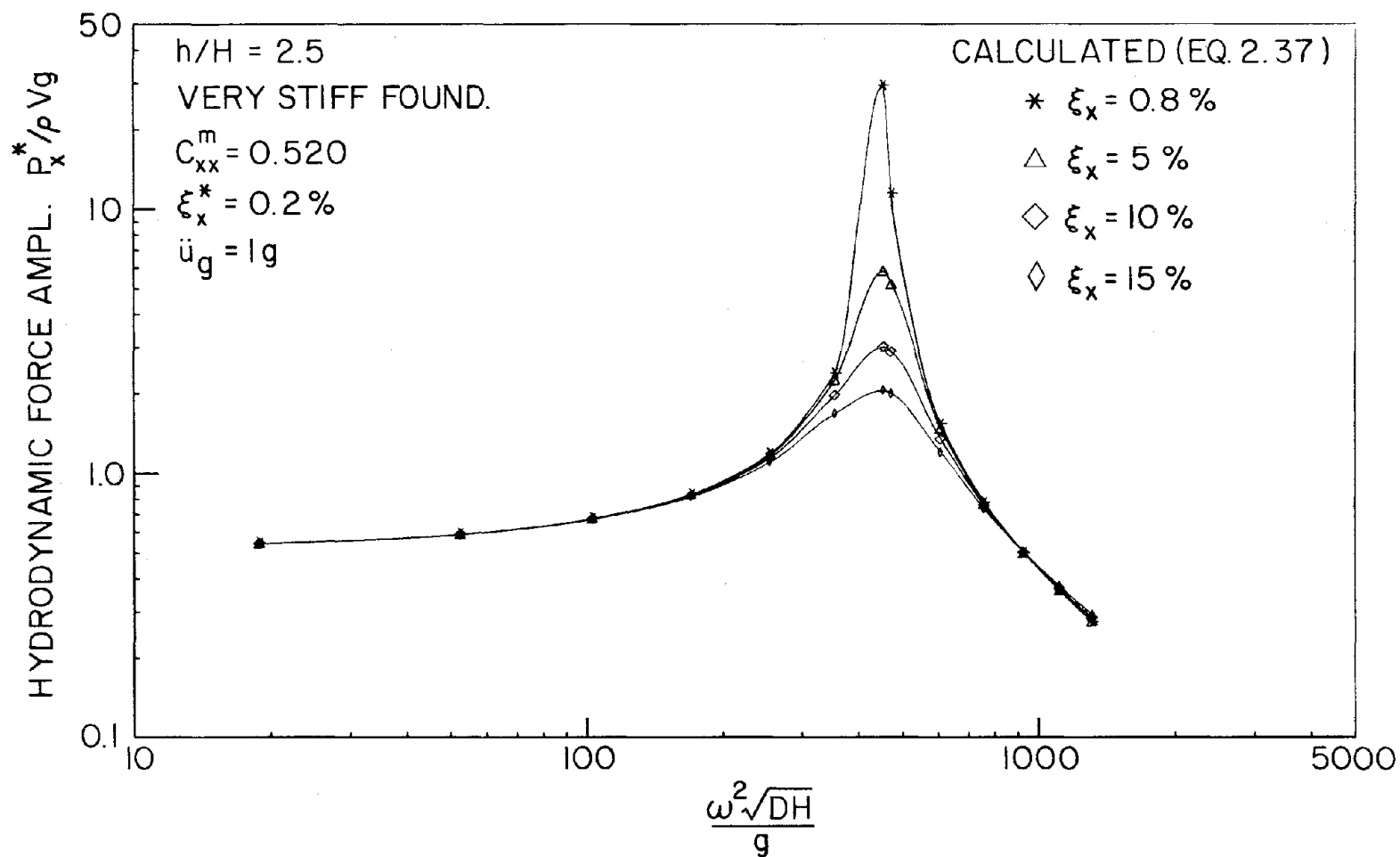


FIGURE 5.7: VARIATIONS IN HYDRODYNAMIC FORCE WITH CHANGES IN FOUNDATION DAMPENING

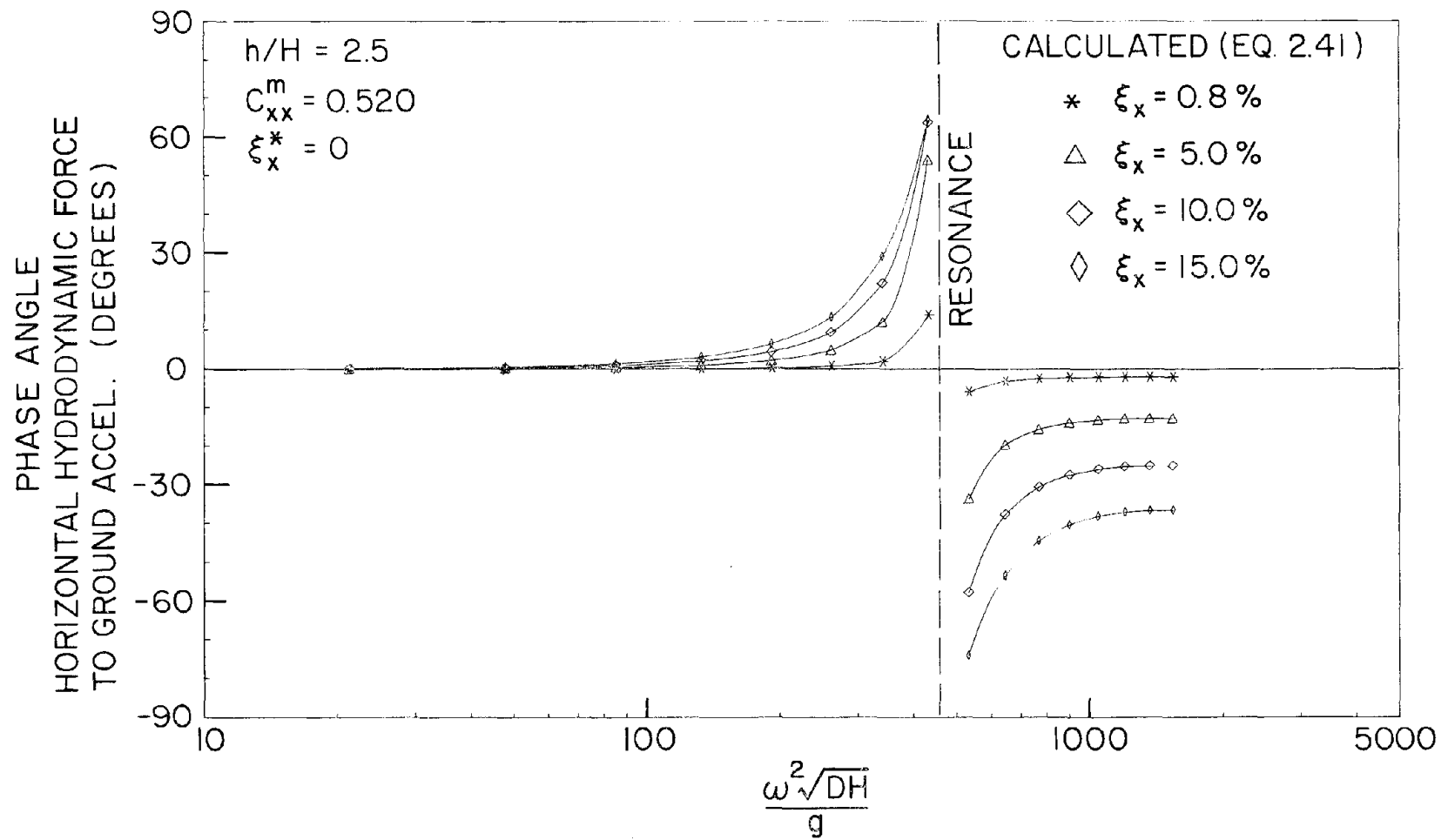


FIGURE 5.8: HYDRODYNAMIC FORCE PHASE ANGLE RELATIVE TO FOUNDATION ACCELERATION FOR VARIOUS VALUES OF FOUNDATION DAMPENING

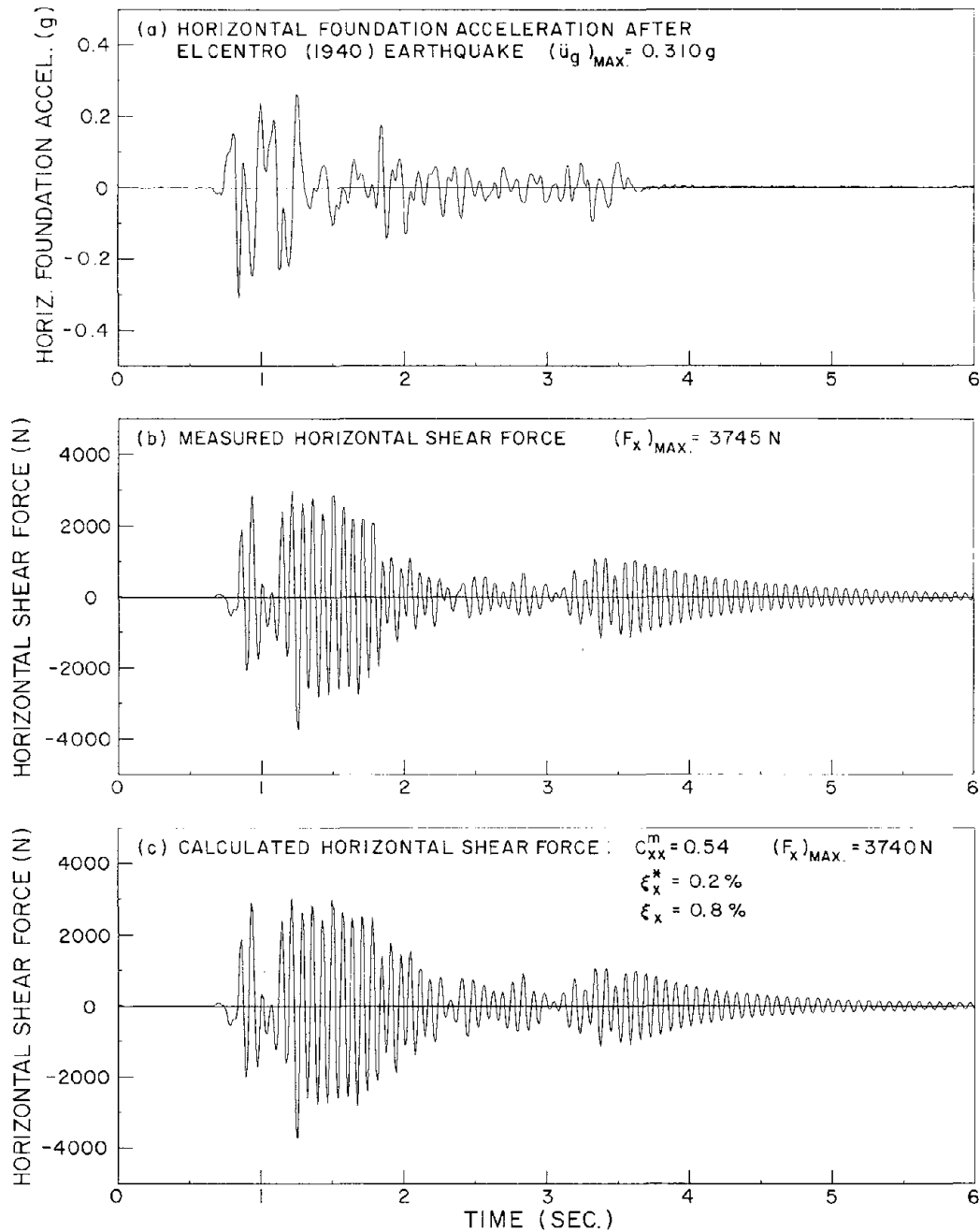


FIGURE 5.9: COMPARISON OF MEASURED AND CALCULATED HORIZONTAL SHEAR FORCE IN THE MODEL FOR THE EL CENTRO (1940) EARTHQUAKE, $h/H = 2.5$

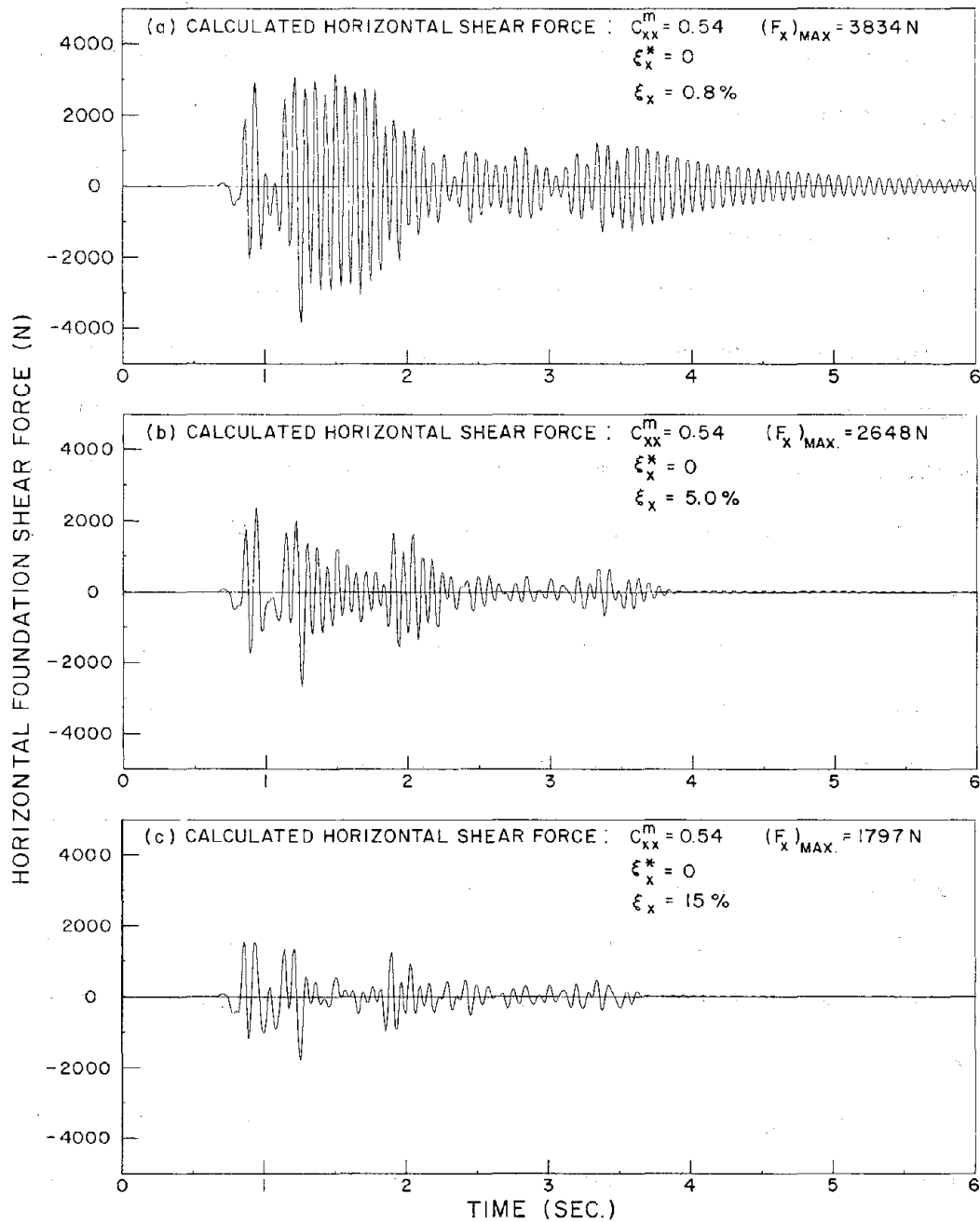


FIGURE 5.10: CALCULATED HORIZONTAL SHEAR FORCE IN THE MODEL FOR THE EL CENTRO (1940) EARTHQUAKE, (a) NEGLECTING HYDRODYNAMIC DAMPENING, (b) WITH FOUNDATION DAMPENING EQUAL TO 5% OF CRITICAL, (c) WITH FOUNDATION DAMPENING EQUAL TO 15% OF CRITICAL.

6. CONCLUSIONS

The findings of this study concerning the earthquake response of large gravity-type offshore structures are summarized as follows:

(a) Available analytical techniques provide good estimates of hydrodynamic inertia force coefficients in the range of frequencies of interest for the simple structure configuration considered.

(b) Foundation dampening is a major consideration in determining the magnitude of the hydrodynamic pressure force and the resulting foundation force. The sensitivity of foundation force to foundation dampening indicates that this site characteristic might dominate the design and placement of large offshore structures.

(c) Foundation stiffness only influences the hydrodynamic force by changing the resonant frequency. This characteristic does not influence the magnitude of this force directly.

(d) Frequency dependence in the inertia coefficients is not likely to be an important consideration.

(e) Coupling in the hydrodynamic inertia forces between the horizontal and rotational modes is not likely to be important at earthquake frequencies.

(f) Hydrodynamic dampening will not be an important factor in the earthquake response of deeply submerged structures, but may be significant in near surface and surface-piercing structures.

REFERENCES

1. Watt, B. J., Boaz, I. B., and Dowrick, D. J.: "Response of Concrete Gravity Platforms to Earthquake Excitation," Paper No. OTC2 2673, Proc. Offshore Tech. Conf., Houston, Texas (May 1976).
2. MacCamy, R. C. and Fuchs, R. A.: "Wave Forces on Piles: A Diffraction Theory," Beach Erosion Board, Technical Memorandum, No. 69 (1954).
3. Wehausen, J. V., and Laitone, E. V.: "Surface Waves" (in English), Handbuch der Physik, S. Flugge/Marburg, Ed., Springer-Verlag, Berlin (1960) IX, 445-778.
4. Garrison, C. J., and Chow, P. C.: "Wave Forces on Submerged Bodies," J. Waterways and Harbors Div., ASCE (1972) 98, 375-392.
5. Hogben, N., and Standing, R. G.: "Wave Loads on Large Bodies," Proc. Intl. Symp. on the Dynamics of Marine Vehicles and Structures in Waves, Institution of Mechanical Engineers, London (April 1974) 273-292.
6. Bai, K. J.: "A Variational Method in Potential Flows with a Free Surface," Naval Architecture Report No. NA 72-2, Univ. of California, Berkeley (September 1972).
7. Zienkiewicz, O. Z., and Newton, R. E.: "Coupled Vibration of a Structure Submerged in a Compressible Fluid," Proc. Intl. Symp. on Finite Element Techniques, Stuttgart (1969) 359-379.
8. Liaw, C-Y., and Chopra, A. K.: "Earthquake Response of Axisymmetric Tower Structures Surrounded by Water," Report No. EERC 73-25, Earthquake Engineering Research Center, Univ. of California, Berkeley (October 1973).
9. Petruskas, C: "Hydrodynamic Damping and 'Added Mass' for Flexible Offshore Platforms," Tech. Report No. HEL 9-23, Hydraulic Engineering Laboratory, Univ. of California, Berkeley (May 1973).
10. Garrison, C. J., Tørum, A., Iverson, C., Leivseth, S. and Ebbesmeyer, C. C.: "Wave Forces on Large Volume Structures--A Comparison Between Theory and Model Tests," Paper No. OTC 2137, Proc. Offshore Tech. Conf., Houston, Texas (May 1974).
11. Penzien, J.: "Structural Dynamics of Fixed Offshore Structures," Proc. First Intl. Conf. on Behavior of Off-Shore Structures, Trondheim, Norway (August 1976) 1, 581-592.
12. Wiegel, R. L.: Oceanographical Engineering, Prentice-Hall Inc., Englewood Cliffs, New Jersey (1964).

13. Veletsos, A. S., and Verbic, B.: "Basic Response Functions for Elastic Foundations," J. Eng. Mechanics Div., ASCE (April 1974) 100, No. EM2, 189-201.
14. Benjamin, J. R., and Cornell, C. A.: Probability, Statistics, and Decision for Civil Engineers, McGraw-Hill, Inc. (1970) 419-440.
15. Hald, A.: Statistical Theory with Engineering Applications, John Wiley and Sons, Inc., New York (1952).
16. Clough, R. W., and Penzien, J.: Dynamics of Structures, McGraw-Hill, Inc., New York (1975).
17. Whitman, R. V.: "Soil-Platform Interaction," Proc. First Intl. Conf. on Behavior of Off-Shore Structures, Trondheim, Norway (August 1976) 1, 817-829.
18. Luco, J. E. and Westman, R. A.: "Dynamic Response of Circular Footings," J. Eng. Mechanics Div., ASCE (October 1971) 97, No. EM5, 1381-1395.
19. Veletsos, A. S. and Wei, Y. T.: "Lateral and Racking Vibration of Footings," J. Soil Mechanics and Foundation Div., ASCE (September 1971) 97, No. SM9, 1249-1277.
20. Seed, H. B. and Idriss, I. M.: "Soil Moduli and Damping Factors for Dynamic Response Analyses," Report No. EERC 70-10, Earthquake Engineering Research Center, Univ. of California, Berkeley (December 1970).
21. Sower, G. B. and Sower, G. F.: Introductory Soil Mechanics and Foundations, MacMillan Publishing Co., Inc., New York (1970).

APPENDIX A

RESPONSE OF ELASTIC FOUNDATIONS

A1. Complex Foundation Impedance Representation

This study has concerned itself with the rigid body response of large gravity-type structures on elastic foundations. Figure A1 shows such a structure in an exaggerated displaced configuration. The foundation-structure interaction of such system has been described by a number of researchers.^{13,17-19} In the case of structures which essentially sit on the bottom, the force-displacement relations of the system can be equated to those of a rigid massless disk resting on a homogeneous foundation. These relationships are expressed in the form of complex frequency dependent functions, the real part of which represents foundation stiffness, and the imaginary part dampening. These functions relate a set of harmonic forces, see Fig. A3, applied to the rigid disk at frequency ω to the resulting displacements.

The three degree of freedom system subjected to the harmonic forces

$$\begin{Bmatrix} f_x^b(t) \\ f_z^b(t) \\ f_\theta^b(t) \end{Bmatrix} = \begin{Bmatrix} \bar{F}_x^b(\omega) \\ \bar{F}_z^b(\omega) \\ \bar{F}_\theta^b(\omega) \end{Bmatrix} e^{i\omega t} \dots \dots \dots \text{A1.1}$$

has the following force-displacement relations:

$$\begin{Bmatrix} \bar{F}_x^b(\omega) \\ \bar{F}_z^b(\omega) \\ \bar{F}_\theta^b(\omega) \end{Bmatrix} e^{i\omega t} = \begin{bmatrix} \bar{K}_{xx}^b & 0 & \bar{K}_{x\theta}^b \\ 0 & \bar{K}_{zz}^b & 0 \\ \bar{K}_{\theta x}^b & 0 & \bar{K}_{\theta\theta}^b \end{bmatrix} \begin{Bmatrix} \bar{x}^b(\omega) \\ \bar{z}^b(\omega) \\ \bar{\theta}^b(\omega) \end{Bmatrix} e^{i\omega t} \quad \text{A1.2}$$

where $\bar{F}_x^b(\omega)$, $\bar{F}_z^b(\omega)$, and $\bar{F}_\theta^b(\omega)$ are, respectively the harmonic exciting forces and moment at frequency ω acting on the rigid massless disk; $\bar{X}^b(\omega)$, $\bar{Z}^b(\omega)$, and $\bar{\Theta}^b(\omega)$ are, respectively, the corresponding harmonic horizontal, vertical, and angular displacements of the base. It should be noted that for a linear system response to a real excitation will also be real valued (see Section 2.3.2). Bars on the above quantities indicate complex values for the general case.

The foundation impedances may be written in the form

$$\begin{bmatrix} \bar{K}_{xx}^b & 0 & \bar{K}_{x\theta}^b \\ 0 & \bar{K}_{zz}^b & 0 \\ \bar{K}_{\theta x}^b & 0 & \bar{K}_{\theta\theta}^b \end{bmatrix} = \begin{bmatrix} K_{xx}^b & 0 & K_{x\theta}^b \\ 0 & K_{zz}^b & 0 \\ K_{\theta x}^b & 0 & K_{\theta\theta}^b \end{bmatrix} + i\omega \begin{bmatrix} C_{xx}^b & 0 & C_{x\theta}^b \\ 0 & C_{zz}^b & 0 \\ C_{\theta x}^b & 0 & C_{\theta\theta}^b \end{bmatrix} \quad \text{A1.3}$$

where K_{ij}^b and C_{ij}^b terms represent the magnitude of stiffness and dampening, respectively, in the various modes.

It has been noted that the coupling between horizontal and rotational motion of the rigid disk is negligible^{13,19} and will, therefore, be dropped from further consideration.

We would now like to relate the impedance functions of the base to the motions of the structure under consideration, Fig. A2. This can be accomplished by noting the following relationships:

$$\begin{Bmatrix} \bar{X}^b(\omega) \\ \bar{Z}^b(\omega) \\ \bar{\Theta}^b(\omega) \end{Bmatrix} = \begin{bmatrix} 1 & 0 & Z_{cg} \\ 0 & 1 & 0 \\ 0 & 0 & 1 \end{bmatrix} \begin{Bmatrix} \bar{X}(\omega) \\ \bar{Z}(\omega) \\ \bar{\Theta}(\omega) \end{Bmatrix} \dots \dots \dots \text{A1.4}$$

where $\bar{X}(\omega)$, $\bar{Z}(\omega)$ and $\bar{\Theta}(\omega)$ are displacements of the structure center of gravity and Z_{cg} is the height of the center of gravity above the foundation surface.

We may also write

$$\begin{Bmatrix} \bar{F}_x(\omega) \\ \bar{F}_z(\omega) \\ \bar{F}_\theta(\omega) \end{Bmatrix} = \begin{bmatrix} 1 & 0 & 0 \\ 0 & 1 & 0 \\ Z_{cg} & 0 & 1 \end{bmatrix} \begin{Bmatrix} \bar{F}_x^b(\omega) \\ \bar{F}_z^b(\omega) \\ \bar{F}_\theta^b(\omega) \end{Bmatrix} \dots \dots \dots \text{A1.5}$$

Applying Eq. A1.2 (ignoring coupling) and A1.4 to Eq. A1.5, we have

$$\begin{Bmatrix} \bar{F}_x(\omega) \\ \bar{F}_z(\omega) \\ \bar{F}_\theta(\omega) \end{Bmatrix} = \begin{bmatrix} \bar{K}_{xx}^b(\omega) & 0 & Z_{cg} \bar{K}_{xx}^b(\omega) \\ 0 & \bar{K}_{zz}^b(\omega) & 0 \\ Z_{cg} \bar{K}_{xx}^b(\omega) & 0 & \bar{K}_{\theta\theta}^b(\omega) \end{bmatrix} \begin{Bmatrix} \bar{X}(\omega) \\ \bar{Z}(\omega) \\ \bar{\Theta}(\omega) \end{Bmatrix} \dots \dots \dots \text{A1.6}$$

We are now able to describe the structure foundation impedances in terms of the appropriate impedances of the rigid disk.

A2. The Elastic Half-Space Impedance Approximation

Veletsos and Verbic¹³ have presented frequency dependent expressions for the foundation impedances of Eq. A1.6 as follows:

$$\bar{K}_{xx}^b(\omega) = 4.8 \text{ GR} \{1. + i 0.65 a_o(\omega)\} \quad \text{A2.1}$$

$$\begin{aligned} \bar{K}_{zz}^b(\omega) = 6.0 \text{ GR} \left\{ 1. - \frac{0.224 a_o^2(\omega)}{1. + 0.64 a_o^2(\omega)} \right. \\ \left. + i \left(0.75 a_o(\omega) + \frac{0.179 a_o^3(\omega)}{1. + 0.64 a_o^2(\omega)} \right) \right\} \\ \text{A2.2} \end{aligned}$$

$$\begin{aligned} \bar{K}_{\theta\theta}^b(\omega) = 4.0 \text{ GR}^3 \left\{ 1. - \frac{0.32 a_o^2(\omega)}{1 + 0.64 a_o^2(\omega)} + i \left(\frac{0.256 a_o^3(\omega)}{1. + 0.64 a_o^2(\omega)} \right) \right\} \\ \text{A2.3} \end{aligned}$$

where Poisson's ratio equal to one third (1/3) has been assumed and

G = soil shear modulus of elasticity in the half space.

R = radius of the foundation

$a_o(\omega) = \omega R / C_s$, where C_s is the shear wave velocity

A3. Evaluation of Foundation Stiffness for the Prototype Offshore Gravity Structure

It is necessary to make a number of assumptions in order to evaluate Eqs. A2.1 - A2.3, for the prototype system. We shall simplify these calculations by noting that we will not include additional foundation damping in our model system, therefore, we will not consider these coefficients further.

Shear wave velocity can be expressed as²¹

$$C_s = \sqrt{G/\rho_s} \quad \text{A3.1}$$

where, ρ_s = mass density of the soil, we can now write

$$a_o^2(\omega) = (\omega^2 R^2 \rho_s)/G \quad A3.2$$

We will assume that the foundation material in our system has a mean density of

$$\rho_s = 2000 \text{ kg/m}^3$$

and that we are interested in response in the near vicinity of

$$\omega_{\text{mean}} \doteq 7.5 \text{ radius/sec.}$$

or,

$$f_{\text{mean}} = 1.2 \text{ Hz.}$$

Finally, we will assume a prototype such that

$$R \doteq 40 \text{ meters}$$

Eq. A3.2 becomes

$$a_o^2(\omega) \doteq \frac{1.8 \times 10^5}{G}$$

where G is expressed in KN/m^2 ($1 \text{ KN} = 1000 \text{ Newton's}$; $1 \text{ KN/m}^2 \doteq 21 \text{ lb/ft}^2$).

With these assumptions, we can now write the stiffness portions of Eqs. A2.1 - A2.3 as

$$K_{xx}^b \doteq 192 G \quad A3.3$$

$$K_{zz}^b \doteq 240 G \left(1 - \frac{4.03 \times 10^4}{G + 1.152 \times 10^5} \right) \quad A3.4$$

$$K_{\theta\theta}^b \doteq 2.56 \times 10^5 G \left(1 - \frac{5.76 \times 10^4}{G + 1.152 \times 10^5} \right) \quad A3.5$$

where translational stiffness values are in KN/m and rotational stiffness is in (KN-m)/radian.

The stiffness relationships of Eqs. A3.3 - A3.5 are plotted in Figs. 3.1 - 3.3 and the equivalent prototype stiffnesses used in this study are indicated. An attempt was made to maintain a consistent relationship between horizontal and rotational stiffness but vertical stiffness was considered to be independent of the other two.

An attempt was made to model three stiffness values which would represent the range of shear modulus change experienced by a dense sand undergoing strong shaking such that shear strain varied from approximately 0.0001 percent to 0.1 percent, as reported by Seed and Idriss.²⁰ The stiffnesses actually achieved were in this range but somewhat short of the extremes on either end. The actual values were dictated by material availability and space limitations in the model.

The detail of the analysis of model foundation characteristics are contained in APPENDIX B.

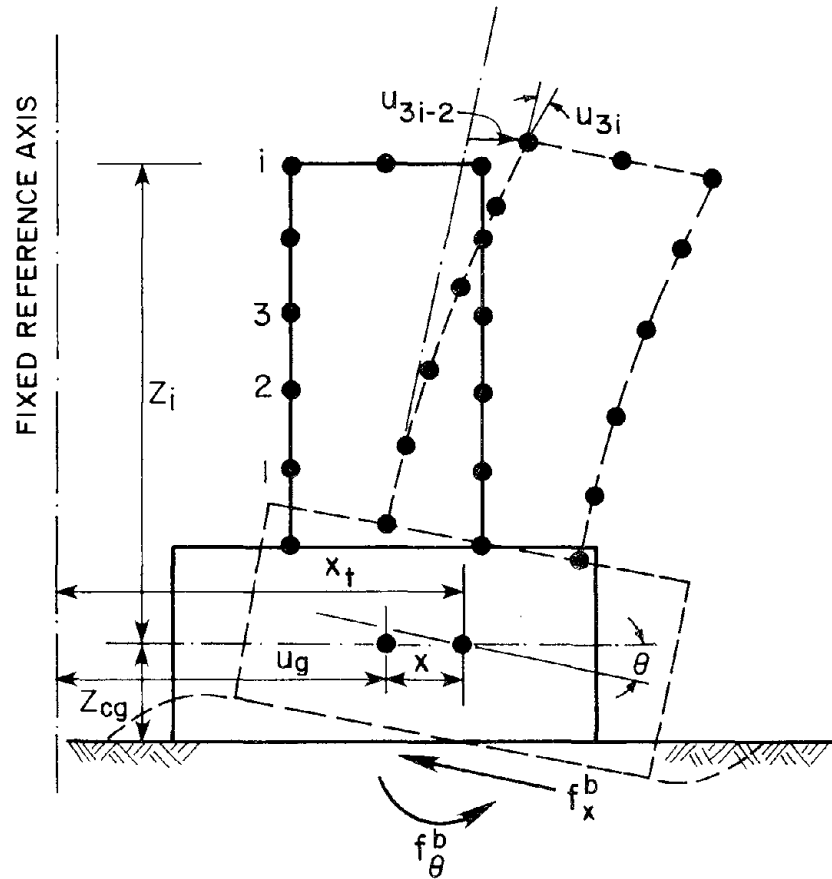


FIGURE A1: A GRAVITY STRUCTURE IN AN EXAGGERATED DISPLACED CONFIGURATION

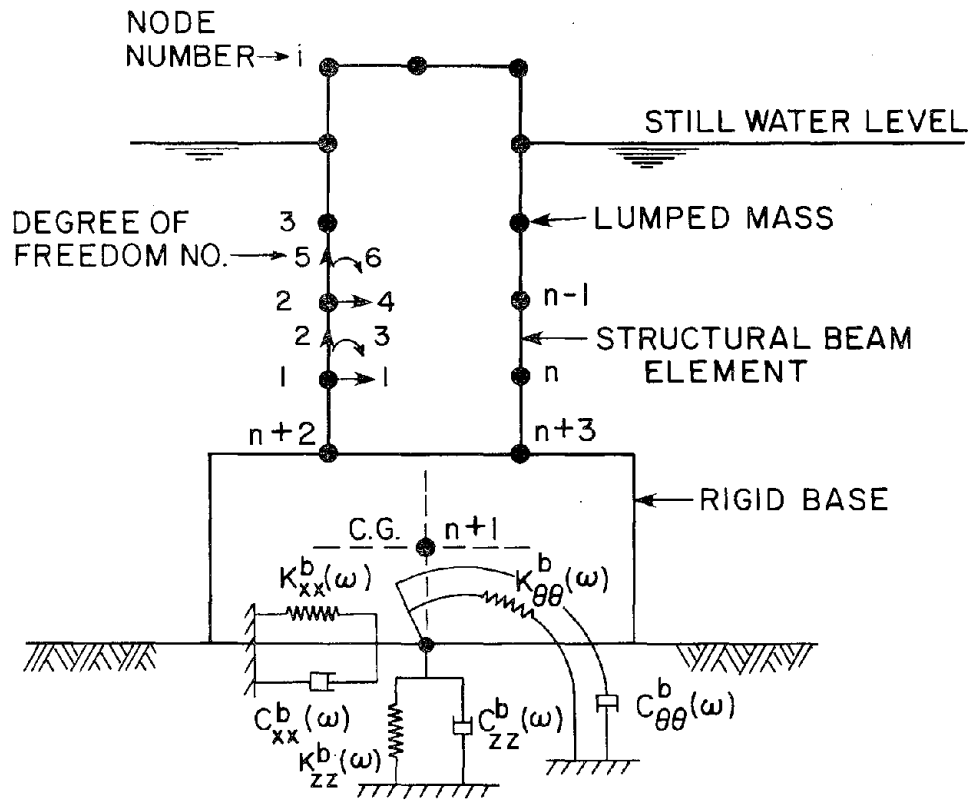


FIGURE A2: GRAVITY STRUCTURE-FOUNDATION SYSTEM IDEALIZATION

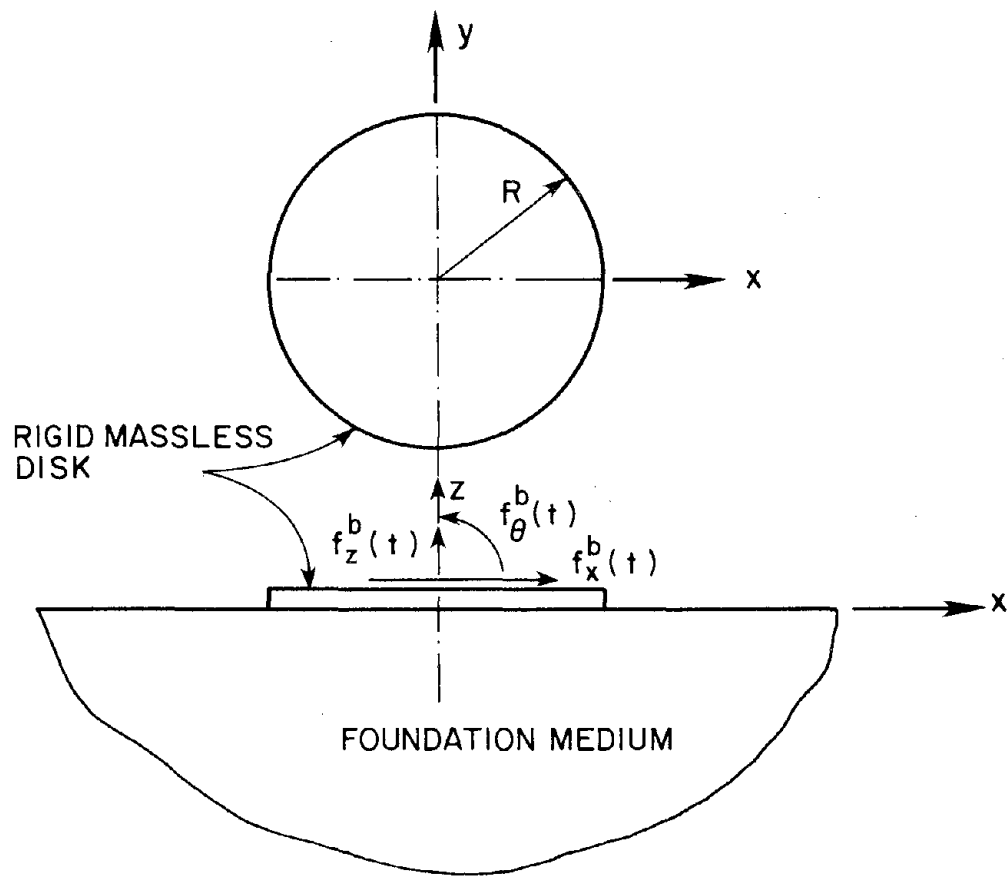


FIGURE A3: FOUNDATION FORCES ON A RIGID DISK

APPENDIX B

MODEL FOUNDATION DESIGN

B1. Analysis of Foundation Spring Characteristics

An example of a typical model foundation spring is shown in Fig.

B1. This particular configuration was chosen because it allowed for independent control of stiffness in axial compression and tension (vertical) and in lateral deflection (horizontal). These stiffnesses were controlled by varying the individual beam segment sizes and lengths. This spring design has the added advantage of allowing the model to be supported without friction surfaces (bearings) and retain freedom to move in three degrees.

Calculation of the individual spring stiffnesses in the axial (S_{zz}) and shear (S_{xx}) directions was performed by a standard two dimensional frame analysis program using a compound beam idealization with lumped masses as shown in Fig. B2. Axial and shear flexibility were calculated by determination of deflection for unit load in each direction with the upper and lower beam ends clamped against rotation.

The lumped mass idealization allowed the calculation of individual spring eigenvalues so that it could be determined that the spring resonant frequencies were well above the frequencies of interest for the model tests. The lowest natural frequency encountered was 660 radian/sec for the soft foundation condition springs. The highest excitation frequency encountered during testing was 120 rad/sec.

After the individual springs were manufactured their actual static stiffness was determined by testing on a dynamometer. An example of the results for the axial stiffness of one set of springs is shown

in Figs. B2. The static calibration indicated that the actual spring stiffness was within fifteen percent (15%) of the stiffness calculated from the compound beam analysis.

Each spring was instrumented with two full bridge strain gauge rosetts (see Fig. 3.5, Chapter 3) which were calibrated during the dynamometer tests to indicate spring force in axial and shear directions directly. An example of these calibration results are shown in Fig. B2. Table B1 shows the results of the calibration of all of the load cells used in the model tests.

It was necessary to calculate the individual spring flexure characteristics due to end rotation in order to determine the overall model rotational stiffness and foundation coupling.

The spring system of Fig. B1 can be viewed as a simple beam in terms of end deflections. It can be easily shown that if the translational stiffness (force per unit of deflection without rotation) is S_{xx} , then the lateral and rotational stiffness matrix for the beam end can be represented as

$$\begin{bmatrix} S_{xx} & S_{x\theta} \\ S_{\theta x} & S_{\theta\theta} \end{bmatrix} = S_{xx} \begin{bmatrix} 1 & -\frac{L}{2} \\ -\frac{L}{2} & \frac{L}{3} \end{bmatrix} \dots \dots \dots \text{B1.1}$$

In our case, the values of S_{xx} were determined for each spring system by testing as discussed previously.

B2. Analysis of Overall Model Foundation Stiffness

Fig. B3 shows an idealization of model foundation system, consisting of four springs located in pairs on either side of the model center of gravity in a two dimensional plane. The model stiffness

characteristics in the three degrees of freedom in the plane motion can be described completely by the two individual spring stiffness characteristics S_{xx} and S_{zz} and by the system dimensional characteristics X_s and Z_s . The spring stiffness characteristics are those of lateral and axial deflection, respectively, of the spring end as discussed in Section B1. The dimensions X_s and Z_s refer to the horizontal and vertical distances, respectively, that the moveable ends of the springs are located from the center of rotation, i.e., the model center of gravity.

It should be noted in interpretation of Fig. B4 that the upper ends of the springs are attached to the fixed foundation of the model and the lower ends are attached to the model. The connection of the springs to the model and foundation are considered to be rigid, thus the lower end of each spring deflects with the model motion.

The model stiffness in the horizontal and vertical degrees of freedom can easily be seen to be

$$K_{xx} = 4 S_{xx} \quad B2.1$$

$$K_{zz} = 4 S_{zz} \quad B2.2$$

The rotational and coupled foundation stiffness require somewhat more consideration. For the purposes of uniformity, all springs sets were designed with a height (L) of 20. centimeters. With this dimension and the sign convention of Fig. B4, the moment created due to a small horizontal deflection (Δx) can be written

$$\begin{aligned} F_{\theta x} &= (4 S_{xx} Z_s - 4 S_{\theta x}) \Delta x \\ &= 4 S_{xx} Z_s - \frac{4 S_{xx} L}{2} \\ &= K_{xx} (Z_s - 10.) \Delta x \end{aligned}$$

Therefore, the coupled stiffness is

$$K_{\theta x} = K_{xx} (Z_s - 10.) \quad B2.3$$

We are thus able to eliminate elastic coupling in the foundation by adjusting the center of gravity of the model such that the distance Z_s equals 10. centimeters. This was accomplished in the model and verified by dry resonant tests.

The moment created due to a small rotation ($\Delta\theta$) of the model about its center of gravity can be written

$$\begin{aligned} F_{\theta\theta} &= 4\{S_{xx} Z_s^2 + S_{zz} X_s^2 + S_{\theta x} Z_s + S_{\theta\theta}\} \Delta\theta \\ &= 4\{S_{xx} Z_s^2 + S_{zz} X_s^2 - \frac{S_{xx} L Z_s}{2} + \frac{S_{xx} L^2}{3}\} \Delta\theta \end{aligned}$$

Rotational stiffness is, therefore

$$\begin{aligned} K_{\theta\theta} &= K_{xx} (Z_s^2 - \frac{L Z_s}{2} + \frac{L^2}{3}) + K_{zz} X_s^2 \\ &= 133. K_{xx} + K_{zz} X_s^2 \quad B2.4 \end{aligned}$$

where L and Z_s have been taken as 20. and 10. centimeters, respectively.

We can summarize by saying that for a given set of foundation springs with characteristics S_{xx} and S_{zz} , the translational stiffnesses are fixed (Eqs. B2.1 and B2.2) and the rotational and coupled stiffnesses can be varied by proper selection of the dimension Z_s and X_s (Eqs. B2.3 and B2.4). As mentioned before, Z_s has been chosen to eliminate the coupled foundation stiffness.

TABLE B1: FOUNDATION LOAD CELL
 CALIBRATION INFORMATION
 (English units, see note
 below)

CONDITION	CELL	STIFFNESS (lb/in)		FORCE (lb/ μ e)	
		HORIZ.	VERT.	HORIZ.	VERT.
1	A	3976.8	6619.1	0.12661	0.10202
	B	4040.3	6786.2	0.12618	0.10122
	C	4005.8	6467.2	0.12500	0.10134
	D	3926.0	6795.7	0.12697	0.10455
2	A	2787.1	6591.8	0.05310	0.09850
	B	2697.0	6611.3	0.05247	0.09752
	C	2742.9	6430.4	0.05280	0.09360
	D	2767.1	6452.3	0.05332	0.10017
3	A	648.2	1642.1	0.01888	0.03774
	B	697.1	1555.1	0.01887	0.03760
	C	679.1	1535.7	0.01888	0.03677
	D	717.8	1582.5	0.01895	0.03865

NOTE: English units were used for load cell calibration because current EERC Earthquake Simulator Laboratory procedures and support software required their use.

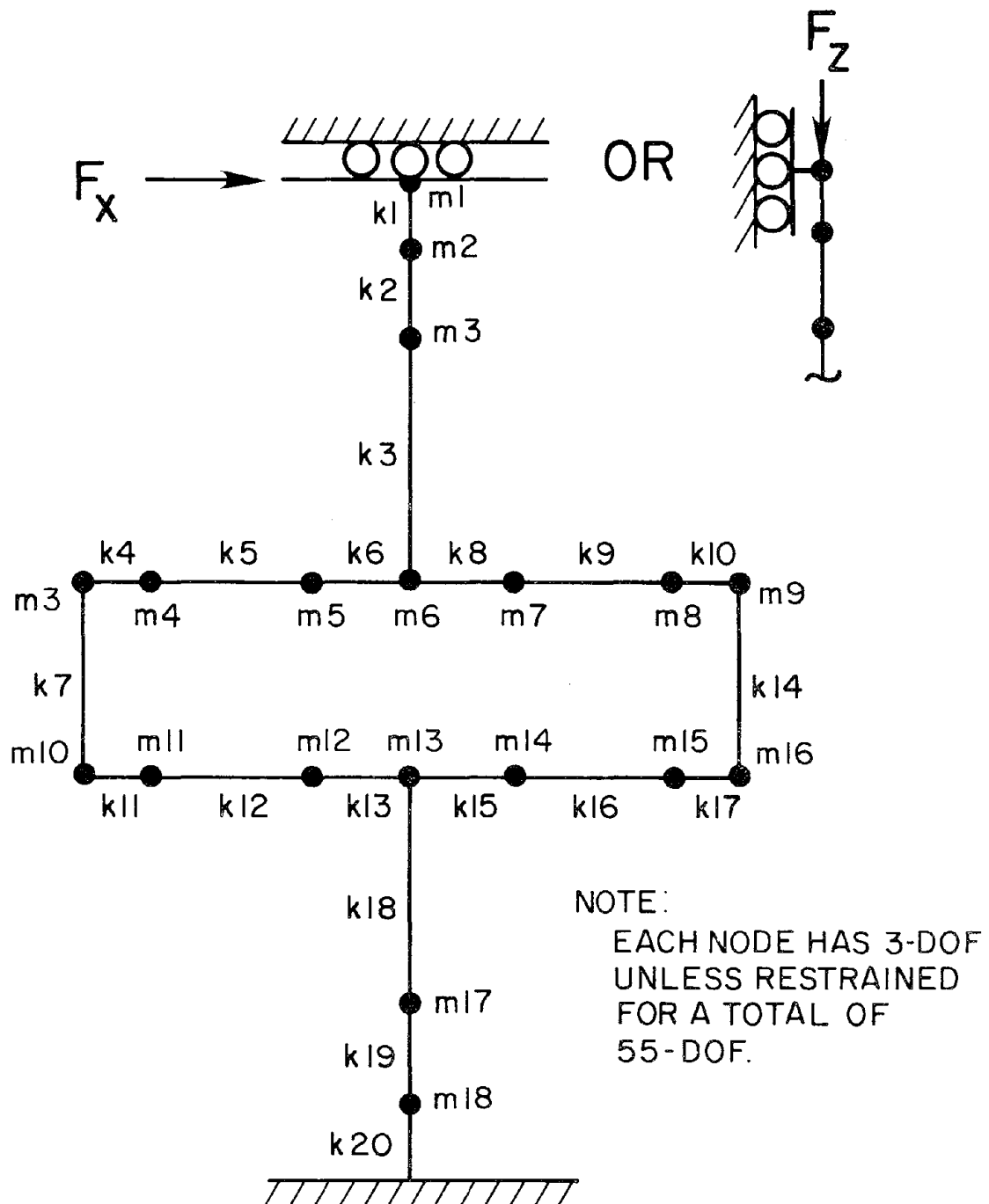


FIGURE B1: TYPICAL LUMPED MASS IDEALIZATION OF A FOUNDATION SPRING,
55-DOF

CELL # 1B HORIZONTAL

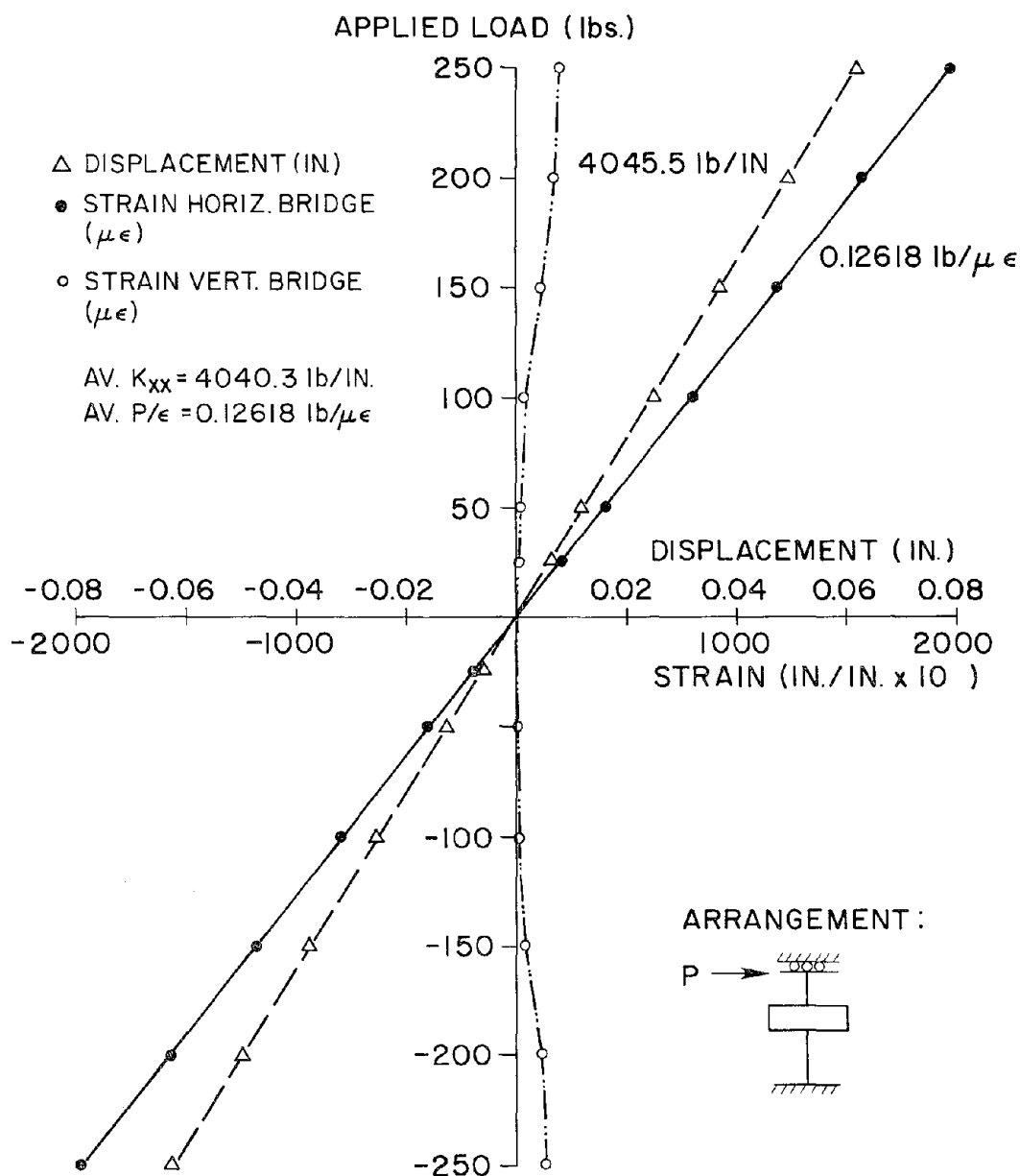


FIGURE B2: A TYPICAL CALIBRATION CURVE FOR A VERY STIFF FOUNDATION SPRING/LOAD CELL, HORIZONTAL DIRECTION (IN ENGLISH UNITS)

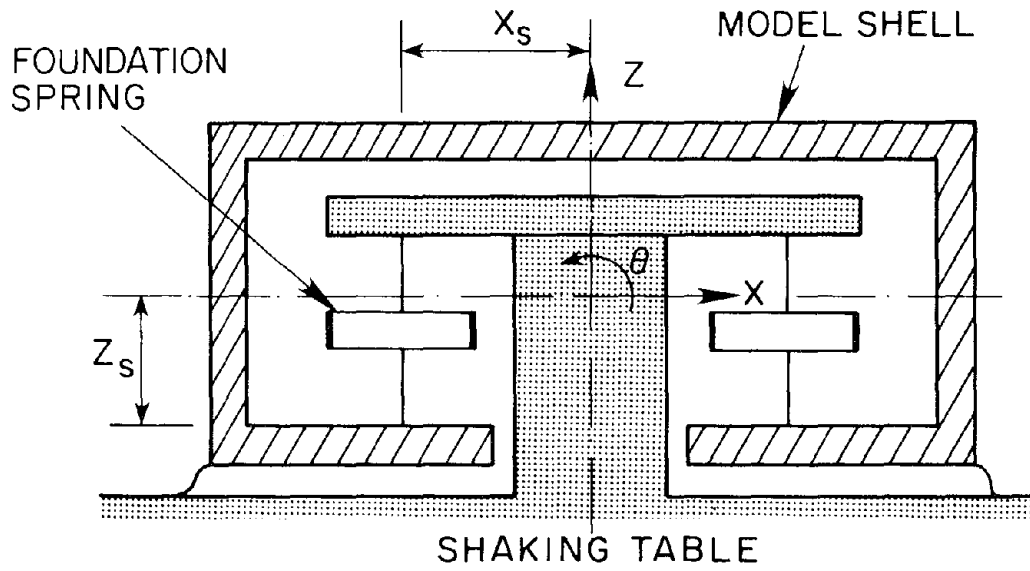


FIGURE B3: MODEL IDEALIZATION FOR FOUNDATION STIFFNESS EVALUATION

APPENDIX C

DISCRETE DYNAMIC TIME SERIES ANALYSIS

C1. Processing of the Raw Data Time Series

Sixty-seven (67) channels of discrete data were recorded in each run of the submerged tank tests, as shown in TABLE C1. Of these, only thirty-five (35) channels were of interest in determining model response, the rest pertaining to shaking table functions. The original data were collected as a continuous stream of data points such that each channel was sampled at a constant interval of ΔT and the time between sampling of one channel and the next channel was $\Delta T/67$. For this particular experiment ΔT equaled 0.01005 seconds, or a sampling rate of 99.5 samples per second per channel.

This technique is convenient from the standpoint of recording efficiency but very awkward in analysing the time series data. For a given channel, data point $n + 1$ occurs 67 data points after point n in the recorded data stream. In addition, there is a constant phase shift (or skew) between any individual data channel and any other channel, depending on their relative locations. The importance of this can be quickly seen when one considers the maximum harmonic frequency considered in these tests, 20 Hz, and notes that there was a phase shift of

$$\phi = \frac{20}{99.5} \cdot 360 = 72 \text{ degrees}$$

between the first and last data channels at this frequency.

The original data were recorded on a nine-track magnetic tape which became the property of the Earthquake Engineering Research Center

and is held in secure storage as a permanent record. A working copy of the pertinent data channels, as shown in TABLE C1, was transferred to seven-track magnetic tape for further conversion using the CDC-6400 computer.

The working tape data was "unpacked", corrected for phase shift between channels, combined into the fifteen (15) model system parameters needed for further analysis, and finally restored on a third tape in individual time series form. The fifteen time series resulting from this conversion are shown in TABLE C2.

The program CONTAPE which performed this conversion is listed in APPENDIX D. The algorithms used at each step in the conversion process are indicated by comment statements.

There are several important points concerning the conversion which should be noted:

a. A second order phase shift (skew) correction was applied since a linear correction filtered the high frequency response data excessively.

b. A base-line correction was applied by averaging all of the data points and then subtracting the average value from the individual data point values. This simple average correction results in a maximum error of less than 5% of the amplitude for harmonics of approximately 3 Hz. The error decreases rapidly for higher frequencies, based on a minimum of 300 data points. The error results when a non-integer number of cycles is averaged.

c. Conversion from English units to S.I. units (Newton, Centimeter, Second) was included in the response time series conversion.

d. Hydrodynamic pressure force was calculated based on a two

dimensional gaussian quadrature arrangement of the pressure sensors. This allowed the maximum possible efficiency in the use of available pressure gauges. Fig. C1 shows the gauge locations for the horizontal pressure and Fig. C2 shows vertical pressure force gauge locations.

e. All other response quantities were calculated based on the kinematic conditions of the model in three degrees of freedom motion about the center of gravity and individual instrument locations.

C2. Calculation of the Virtual Masses

The forms of the equations of motion as arranged for solution were stated in Chapter 3 and are repeated here,

$$M_{xx}^* \ddot{x}_t = -M_x \ddot{x}_t - C_x \dot{x} - K_x x - C_x^* \dot{x}_t \quad C2.1$$

$$M_{zz}^* \ddot{z}_t = -M_z \ddot{z}_t - C_z \dot{z} - K_z z - C_z^* \dot{z}_t \quad C2.2$$

$$M_{\theta\theta}^* \ddot{\theta}_t + M_{\theta x}^* \ddot{x}_t = -M_\theta \ddot{\theta}_t - C_\theta \dot{\theta} - K_\theta \theta - C_\theta^* \dot{\theta}_t \quad C2.3$$

where,

$$\begin{Bmatrix} x_t \\ z_t \\ \theta_t \end{Bmatrix} = \begin{Bmatrix} x \\ z \\ \theta \end{Bmatrix} + \begin{Bmatrix} u_g \\ v_g \\ \theta_g \end{Bmatrix}$$

= sum of relative motion and ground displacement vectors.

And,

C_i = foundation dampening,

C_i^* = hydrodynamic dampening due to wave generation,

K_i = foundation stiffness,

M_i = dry mass or moment of inertia,

M_{ij}^* = virtual mass of mode i due to motion in mode j.

The dots above the displacement quantities indicate first or second derivatives with respect to time.

TABLE C2 lists the kinematic quantities which are derived as a direct result of recorded data. These include all of the total accelerations and relative displacement of Eqs. C1 - C3. The structure dry mass and foundation stiffnesses resulted from design considerations as discussed previously. Foundation and hydrodynamic dampening were measured in the shock tests, the results of which are shown in Chapter 4, Table 4.2.

The only remaining quantities needed were relative and total velocities. These were calculated using a fourth order differentiation and a second order integration scheme, respectively. The algorithms used are shown in the subroutine VELCAL listed in the program MASSCAL of APPENDIX E.

The virtual mass quantities of Eqs. C1 and C2 were calculated using a linear regression technique in one variable (least squares fit) as described in Benjamin and Cornell.¹⁴ This technique is a special case of the multiple regression technique used to solve for the rotational and coupled virtual mass in Eq. C3 and, therefore, only the latter will be discussed in detail.

Eq. C3 represents balance of forces in the dynamic systems which is, in principle, satisfied at each of the N data points recorded in the testing. If the masses are assumed to be constant for all time, then Eq. C3 can be seen to describe a plane in three dimensional space and can be rewritten as

$$B_1 X_1 + B_2 X_2 = Y \quad C4$$

where the X_i values (rotational and horizontal acceleration) represent two orthogonal horizontal axes and Y (right-hand side of Eq. C3) represents the vertical axis. The coefficients B_1 and B_2 represent the slope of the plane in the X_1 and X_2 directions, respectively. An additional term could be included in Eq. C4 to describe the point where the plane crosses the Y axis ($X_1 = X_2 = 0$) but this is assumed to be zero in our case.

We can summarize our data reduction problem in the following way: For each test run we have obtained N sample points, each described by a set of coordinates (X_{1i}, X_{2i}, Y_i) . We wish to find the best possible fit of a plane through these sample points. The slopes of this plane are the coupled and rotational masses.

The solution of Eqs. C1 and C2 for horizontal and vertical virtual mass is essentially the same except that the slope of the plane in one coordinate is known (or assumed) to be zero. Therefore, we are solving for the best fit of a straight line through the data points in this case.

It can be shown^{14,15} that the solution for the slope coefficients of Eq. C4 can be achieved by solving a system of simultaneous equations,

$$\begin{aligned} a_{11} B_1 + a_{12} B_2 &= b_{1y} \\ a_{21} B_1 + a_{22} B_2 &= b_{2y} \end{aligned} \quad C5$$

where

$$\begin{aligned}
 a_{ii} &= \sum_{n=1}^N x_{in}^2 - \left(\frac{\sum_{n=1}^N x_{in}}{N} \right)^2 \\
 a_{ji} &= a_{ij} = \sum_{n=1}^N (x_{in} x_{jn}) - \frac{\sum_{n=1}^N x_{in} \cdot \sum_{n=1}^N x_{jn}}{N} \\
 b_{iy} &= \sum_{n=1}^N (x_{in} y_n) - \frac{\sum_{n=1}^N x_{in} \cdot \sum_{n=1}^N y_n}{N}
 \end{aligned}$$

The slope coefficients are then

$$\{B\} = [a]^{-1} \{b\} \quad \dots \dots \dots C6$$

It can be noted that Eqs. C5 and C6 can easily be generalized to systems of any number of variables. For our case, Eq. C6 becomes

$$\begin{aligned}
 B_1 &= a'_{11} b_{1y} + a'_{12} b_{2y} \\
 B_2 &= a'_{21} b_{1y} + a'_{22} b_{2y}
 \end{aligned}
 \quad \dots \dots \dots C7$$

where the a'_{ij} are the respective values of the inverted coefficient matrix of C5.

This solution process has been implemented in the Program MASSCAL of APPENDIX E. The regression calculation is performed in Subroutine SOLMASS and REGRESS.

The accuracy of the regression calculation is directly related to two factors associated with the characteristics of the variables X_i and Y of Eq. C4. These factors are:

a. The relative size of the variance of each X_i compared to Y , i.e., the larger the variance of X_i relative to Y , the greater will be the accuracy of B_i .

b. The statistical independence of the x_i , i.e., if x_1 and x_2 are highly correlated it would be difficult to find the individual coefficients B_i . This could occur in dynamics when two variables are in phase at the same frequency.

TABLE C1: DATA CHANNEL LISTS FOR THE MASTER AND WORKING TAPES

CHANNEL NR.		DATA IDENTIFICATION	RECORDED UNITS *
MASTER	WORKING TP.		
0	-	BLANK	-
1	-	BLANK	-
2	1	Command horiz. displacement	inches
3	2	Command vert. displacement	inches
4	3	Av. horiz. table displacement	inches
5	4	Av. vert. table displacement	g's
6	5	Av. horiz. table acceleration	g's
7	6	Av. vert. table acceleration	g's
8	7	Table pitch	rad/sec ²
9	8	Table roll	rad/sec ²
10	9	Table twist	rad/sec ²
11	-	Table actuator force H1	kips
12	-	Table actuator force H2	kips
13	-	Table actuator force H3	kips
14	-	Table acceleration H1	g's
15	-	Table acceleration H2	g's
16	-	Table acceleration V1	g's
17	-	Table acceleration V2	g's
18	-	Table acceleration V3	g's
19	-	Table acceleration V4	g's
20	-	Table actuator force V1	kips
21	-	Table actuator force V2	kips
22	-	Table actuator force V3	kips
23	-	Table actuator force V4	kips
24	-	Table displacement V1	inches

CHANNEL NR.		DATA	RECORDED
MASTER	WORKING TP.	IDENTIFICATION	UNITS *
25	-	Table displacement V2	inches
26	-	Table displacement V3	inches
27	-	Table displacement V4	inches
28	-	Table displacement H1	inches
29	-	Table displacement H2	inches
30	-	Table displacement H3	inches
31	-	BLANK	-
32	-	Table support force 1	kips
33	-	Table support force 2	kips
34	-	Table support force 3	kips
35	-	Table support force 4	kips
36	10	Model foundation force AV	kips
37	11	Model foundation force AH	kips
38	12	Model foundation force BV	kips
39	13	Model foundation force BH	kips
40	14	Model foundation force CV	kips
41	15	Model foundation force CH	kips
42	16	Model foundation force DV	kips
43	17	Model foundation force DH	kips
44	18	Model displacement V1	inches
45	19	Model displacement H1	inches
46	20	Model displacement V2	inches
47	21	Model displacement H2	inches
48	22	Model acceleration V1	g's
49	23	Model acceleration H1	g's
50	24	Model acceleration V2	g's

CHANNEL NR.		DATA	RECORDED
MASTER	WORKING TP.	IDENTIFICATION	UNITS *
51	25	Model acceleration H2	g's
52	26	Hydrodynamic pressure 1	lb/in ²
53	27	Hydrodynamic pressure 2	lb/in ²
54	28	Hydrodynamic pressure 3	lb/in ²
55	29	Hydrodynamic pressure 4	lb/in ²
56	30	Hydrodynamic pressure 5	lb/in ²
57	31	Hydrodynamic pressure 6	lb/in ²
58	32	Hydrodynamic pressure 7	lb/in ²
59	33	Hydrodynamic pressure 8	lb/in ²
60	-	BLANK	-
61	-	BLANK	-
62	-	BLANK	-
63	-	BLANK	-
64	34	Model foundation accel. V1	g's
65	-	BLANK	-
66	35	Model foundation accel. H1	g's

*NOTE: Current EERC Earthquake Simulator Laboratory procedures and support software require use of English units.

TABLE C2: TIME SERIES RECORDED ON MODEL RESPONSE TAPES

RESPONSE TAPE CHANNEL NR.	CHANNEL IDENTIFICATION	WORKING TAPE DATA CHANNELS USED
1	Horizontal foundation acceleration recorded on the shaking table	5
2	Vertical foundation acceleration recorded on the shaking table	6
3	Angular foundation acceleration recorded on the shaking table	7
4	Relative horizontal displacement of the model	19,21
5	Relative vertical displacement of the model	18,20
6	Relative angular displacement of the model	18,20
7	Horizontal foundation force on the model	11,13,15,17
8	Vertical foundation force on the model	10,12,14,16
9	Rotational moment on the model	18-20
10	Total horizontal acceleration of the model	23,25
11	Total vertical acceleration of the model	22,24
12	Total angular acceleration of the model	22,24
13	Horizontal or vertical force due to integrated hydrodynamic pressure	26-33
14	Horizontal foundation acceleration recorded on the model foundation	35
15	Vertical foundation acceleration recorded on the model foundation	34

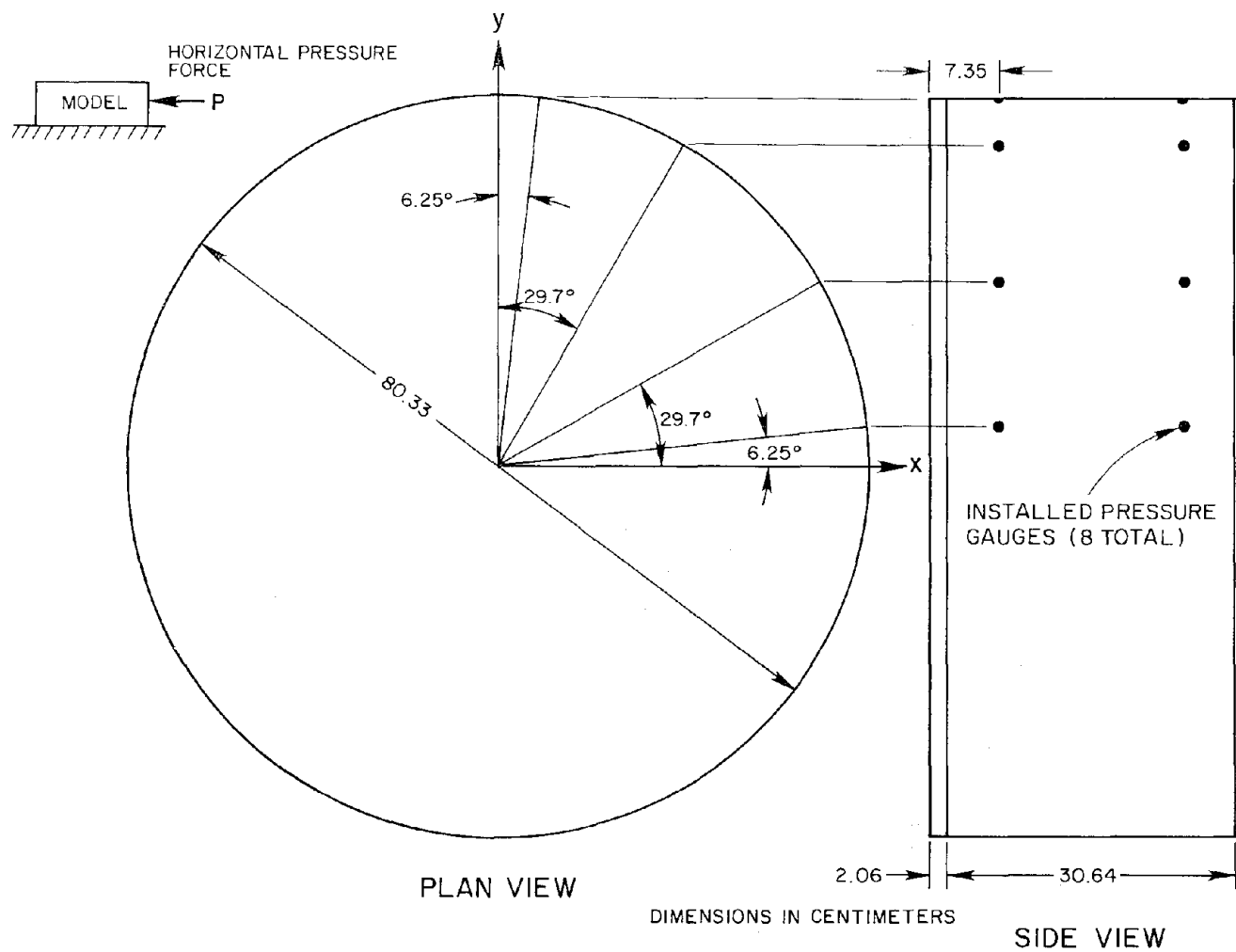


FIGURE C1: PRESSURE GAUGE LOCATIONS FOR HORIZONTAL FORCE DETERMINATION

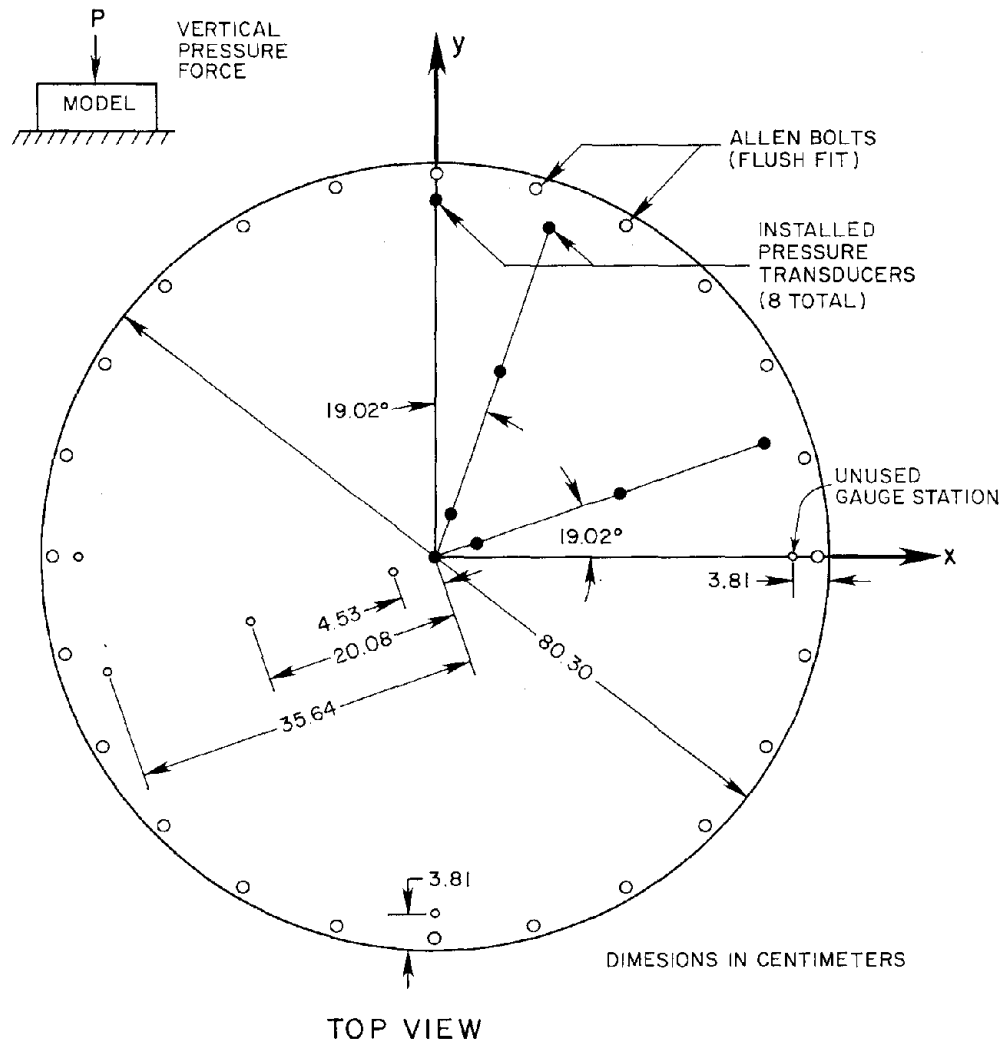


FIGURE C2: PRESSURE GAUGE LOCATIONS FOR VERTICAL FORCE DETERMINATION

APPENDIX D. CONTAPE--PROGRAM LISTING

FORTRAN COMPILATION

RUN 2.3C0-75274

26 APR 78 19:12:33 PAGE NO. 1

```

      PROGRAM CONTAPE(TAPE1,TAPE2,INPUT,OUTPUT)
      COMMON INAME,IDRLN,NLCH,TINTV,NRUN,CHANID(128),STRID,DATE,
+ CCAL(128),ITYPE(067),NCH(35),EDATA(35),EDT(35,307),
+ SDATA(35),TEMP(2,35),ZERO(35)
      DIMENSION CHLABEL(15),CONDATA(15,305),DMAX(15),DMIN(15)
      DATA CHLABEL/6HT XACC,6HT ZACC,8HT ANGACC,1HX,1HZ,SHANG-Y,2HFX,2HF
+ Z,2HMY, 4HXACC,4HZACC,6HANGACC,3HFXP,6HF ZACC,6HF XACC/
      DATA TMASS,RMASS,ZCG/249.827,152427.5,5.28509/
      COMMON /PLT/CONDATA,DMAX,DMIN
      LFET1=LFN(5LTAPE1)
C INPUT DATA ENTERED IN LB-INCH UNITS
      5 READ 1000,NPRINT,NFILS,SX,SY,XS
      1000 FORMAT(12,I3,15X,3F10.0)
      IF(SX.LE.0.) GO TO 900
      IF(NFILS.LE.0) NFILS=1
C INITIALIZE TAPE FILES FOR READING BLOCK BINARY
      DO 500 NF=1,NFILS
      CALL FETZERO(LFET1,5LTAPE1)
      CALL BLDK(1)
C READ HEADING AND CAL. DATA FROM ROUGH DATA TAPE
      READ(1)INAME,NDRLN,NLCH,TINTV,NRUN
      IF(EOF,1)900,100
      100 READ(1)CHANID,STRID,DATE
      READ(1)CCAL,ITYPE
      NLC=NLCH+1
C FORM A LIST OF DATA CHANNEL NUMBERS
      N=1
      DO 120 I=1,NLC
      IF(ITYPE(I).LT.0) GO TO 120
      NCH(N)=I-1
      N=N+1
      120 CONTINUE
C READ ROUGH DATA AND FORM ZERO VECTOR
      NRT=0
      DO 130 I=1,NDRLN
      130 ZERO(I)=0.
      DO 134 J=1,1000
      READ(1) (EDATA(I), I=1,NDRLN)
      IF (EOF,1) 135,131
      131 DO 133 I=1,NDRLN
      ZERO(I)=ZERO(I)+EDATA(I)
C FORM ROUGH DATA MATRIX FOR 307 POINTS
      IF (NRT-307) 132,132,133
      132 EDT(I,J)=EDATA(I)
      133 CONTINUE
      NRT=NRT+1
      134 CONTINUE
      135 CONTINUE
      FNRT=FLOAT(NRT)
      DO 140 I=1,NDRLN
C COMPUTE ZEROES
      ZERO(I)=ZERO(I)/FNRT
C ESTABLISH INITIAL VALUES FOR SWEEP POSITION CORRECTION
      TEMP(1,I)=EDT(1,I)
      TEMP(2,I)=EDT(1,2)
      140 CONTINUE
      DO 150 I=1,15
      DMAX(I)=DMIN(I)=0.
      150 CONTINUE
      NPOINTS=305
      IF(NRT.LT.307) NPOINTS=NRT-2
C

```

FORTRAN COMPILATION

RUN 2.300-75274

26 APR 78 19:12:33 PAGE NO. 2

C START PROCESSING DATA

C

FLCH=FLOAT(NLCH)+1.

FLCH2=FLCH*FLCH

NREC=0

DO 200 K=1,NPOINTS

C INTERPOLATE FOR SWEEP POSITION CORRECTION

DO 200 I=1,NDRLN

KK=K+2

EDATA(I)=EDT(I,KK)

FCH=FLOAT(NCH(I))+1.

FCH2=FCH*FCH

$$SDATA(I) = TEMP(1,I) * ((-FLCH * FCH + FCH2) / (2. * FLCH2)) - TEMP(2,I) * (FCH2 + (-2. * FLCH * FCH) / FLCH2 + EDATA(I) * (2. * FLCH2 - 3. * FLCH * FCH + FCH2) / (2. * FLCH2))$$

SDATA(I)=SDATA(I)-ZERO(I)

TEMP(1,I)=TEMP(2,I)

TEMP(2,I)=EDATA(I)

200 CONTINUE

205 CONTINUE

C

C FORM THE CONVERTED RESPONSE DATA VECTORS

C

C

C EXCITATION (NORMALIZED TO G)

C

C HORIZONTAL TABLE ACC.

CONDATA(1,K)=SDATA(5)

C VERTICAL TABLE ACC.

CONDATA(2,K)=SDATA(6)

C ANGULAR TABLE ACC.

CONDATA(3,K)=-SDATA(7)

C MODEL FOUNDATION VERT. ACC.

CONDATA(14,K)=SDATA(34)

C MODEL FOUNDATION HORIZ. ACC.

CONDATA(15,K)=SDATA(35)

C

C MODEL DISPLACEMENTS (SI UNITS - CENTIMETERS, RADIANS)

C

C HORIZONTAL

CONDATA(4,K)=(SDATA(21)+(SDATA(19)-SDATA(21))*0.418916)*2.54001

C VERTICAL

CONDATA(5,K)=-((SDATA(18)+SDATA(20))/2.)*2.54001

C ANGULAR

CONDATA(6,K)=(SDATA(20)-SDATA(18))/25.3125

C

C ACCELERATIONS (NORMALIZED TO G=980.665)

C

C ANGULAR

CONDATA(12,K)=(SDATA(24)-SDATA(22))/0.0734936

C HORIZONTAL

CONDATA(10,K)=((-SDATA(25)+SDATA(23))/2.)+0.0026689*CONDATA(12,K)

C VERTICAL

CONDATA(11,K)=-((SDATA(22)+SDATA(24))/2.

C

C FORCE AND MOMENT (SI UNITS - NEWTONS, NEWTON-CENTIMETERS)

C

C HORIZONTAL

$$CONDATA(7,K) = (SDATA(11) + SDATA(13) + SDATA(15) + SDATA(17) - CONDATA(6,K) + 0.00403509 * SX) * 4448.22$$

C VERTICAL

CONDATA(8,K)=(SDATA(10)+SDATA(12)+SDATA(14)+SDATA(16))*4448.22

FORTRAN COMPILATION

RUN 2.3C0-75274

26 APR 78 19:12:33 PAGE NO. 3

```

C   ANGULAR
      CONDATA(9,K)=CONDATA(6,K)*(SX*21.4753+SY*XS*XS)*11.2985
C   HORIZONTAL FORCE DUE TO PRESSURE ON THE POSITIVE HALF-CYLINDER
      CONDATA(13,K)=-261.4634*(SDATA(26)+SDATA(27))-255.5173*(SDATA(28)+
      + SDATA(29))-244.3226*(SDATA(30)+SDATA(31))-28.6297*(SDATA(32)+
      + SDATA(33))
C
C   THE FOLLOWING ALGORITHM IS USED WHEN THE VERTICAL PRESSURE FORCE IS
C   BEING CALCULATED:
C
C   TOTAL VERTICAL FORCE ON CYLINDER TOP, FROM PRESSURE GAUGES (NEWTONS)
      CONDATA(13,K)=-109.377*(SDATA(26)+SDATA(29))-776.423*(SDATA(27)+
      + SDATA(30))-861.141*(SDATA(28)+SDATA(31))
C
C   NOTE THAT THIS EXPRESSION COMPUTES THE TOTAL VERTICAL FORCE WHILE
C   THE EXPRESSION ABOVE FOR HORIZONTAL PRESSURE FORCE YIELDS ONLY THE
C   FORCE ON HALF THE CYLINDER, I.E., 1/2 OF THE TOTAL FORCE.
C
C
      NREC=NREC+1
C   FIND THE MAXIMA AND MINIMA FOR THESE FILES
      DO 210 I=1,15
        IF(DMAX(I).LT.CONDATA(I,K)) DMAX(I)=CONDATA(I,K)
      210 IF(DMIN(I).GT.CONDATA(I,K)) DMIN(I)=CONDATA(I,K)
C
      220 CONTINUE
C
C   WRITE STRING DATA TO THE OUTPUT FILE
      PRINT 2004,NF,NRT
      2004 FORMAT(//////I5,5X,*TOTAL NR. DATA PTS.=#,I5/)
      WRITE(2) INAME,STRID,NREC,IMASS,RMASS,ZCG,SX,SY,XS
      DO 240 I=1,15
        PRINT 2001, I, INAME,STRID,DATE,NRUN,CHLABEL(I),TINTV,NREC,DMAX(I),
        + DMIN(I)
      2001 FORMAT( * NO.*,I3,10X,* DATA FILE NAME: *,A10,10X,*STRUCTURE: *
      + ,A10,10X,*DATE: *,A6,10X,*RUN NO.*,I3/* DATA: *,A10,10X,*SAMPLE I
      +NIVL:*,F8.5,*SEC.*,10X,*DATA POINTS:*,I5/* DATA MAX:*,1P,E12.3,
      + 10X,*DATA MIN:*,E12.3/)
      WRITE(2) I, INAME,STRID,DATE,NRUN,CHLABEL(I),TINTV,NREC,DMAX(I),
      + DMIN(I),(CONDATA(I,K),K=1,NREC)
      IF(NPRNT) 240,240,235
      235 PRINT 2002,(CONDATA(I,K),K=1,NREC)
      2002 FORMAT(1P,10E12.3)
      240 CONTINUE
      ENDFILE 2
      490 PRINT 2003
      2003 FORMAT(//* END-OF-FILE*)
      500 CONTINUE
      GO TO 5
      900 STOP
      END

```

APPENDIX E. MASSCAL--PROGRAM LISTING

FORTRAN COMPILATION

RUN 2.3C0-75274

26 APR 78 19:12:33 PAGE NO. 1

```

      PROGRAM MASSCAL(TAPE2,TAPE3,INPUT,OUTPUT,PUNCH)
C
C   THIS PROGRAM:
C       (A) DETERMINES THE CHARACTERISTICS OF THE INDIVIDUAL
C   MODEL HARMONIC RESPONSE TIME SERIES WITH RESPECT TO AMPLITUDE AND
C   FREQUENCY,
C       (B) CALCULATES A RELATIVE VELOCITY TIME SERIES FOR
C   EACH DEGREE OF FREEDOM,
C       (C) CALCULATES THE INERTIA COEFFICIENTS IN
C   THREE DEGREES OF FREEDOM AND HORIZ.-ROT. COUPLING BASED ON A
C   STATISTICAL BEST FIT.
C
C   PROGRAMED BY R.C. BYRD (1978)
C
      COMMON D(15,305),DM(6),FM(6),CHLABEL(15),ZR(6,102),TINTV,NREC,
+   NZR(6),INAME,PHI,RF(3),DEPTH,CD(3),KK
      COMMON /REG/ A(2,2),BY1,BY2,SSDX,SSDY,SSDYD,FNP,VM(4),R1,R2,SX1,
+   SX2,SSDXD
      COMMON /DAMP/K(3),DP(3),MASS(3),C(3),ZCG,SX,SY,XS,G(3)
      COMMON /LD/ DMAX(15)
      REAL MASS,K
      DATA MASS,G/249.827,249.827,172094.8,980.665,980.665,1./
      DATA VM/173.785,257.454,87116.77,3890.962/
      NFT=0
      5 READ 1000,KK,NFILS,CD,DEPTH
1000 FORMAT(I1,I4,4F10.0)
      IF(NFILS.LE.0) GO TO 900
      IF(CD(2).EQ.0.) CD(2)=CD(1)
      IF(CD(3).EQ.0.) CD(3)=CD(1)
      VM(2)=5.0681*DEPTH
      PHI=2.*ASIN(1.)
C   LOAD TIME SERIES DATA FROM TAPE FOR EACH TEST RUN
      DO 500 NF=1,NFILS
C   READ FILE HEADING RECORD
      READ(2) INAME,STRID,NREC,TMASS,RMASS,ZCG,SX,SY,XS
      IF(EOF,2) 900,10
      10 NFT=NFT+1
C   LOAD INDIVIDUAL TIME SERIES
      12 CONTINUE
      READ(2) I,INAME,STRID,DATE,NRUN,CHLABEL(I),TINTV,NREC,DMAX(I),
+   DMIN,(D(I,L),L=1,NREC)
      IF(EOF,2) 20,15
      15 GO TO 12
      20 CONTINUE
      IF(DMAX(2).LT..035.OR.DEPTH.LE.0.) GO TO 25
      PRINT 1001,NFT,INAME,DEPTH
1001 FORMAT(1H1,* FILE NO.*,I4,4X,*TEST NO. *,A10,4X,*DEPTH=*,F5.1/)
      25 CONTINUE
      CALL DAMPING
      IF(DMAX(2).LT..035.OR.VM(2).LE.0.) GO TO 500
      CALL TMSER
      CALL VELCAL
      WRITE(3) INAME,STRID,NREC,MASS,VM,K,FM,TINTV,DM,DP,CD,DEPTH
      CALL SOLMASS
      ENDFILE 3
      500 CONTINUE
      KK=0
      GO TO 5
      900 STOP
      END

```

FORTRAN COMPILATION

RUN 2.3C0-75274

26 APR 78 19:12:33 PAGE NO. 1

```

      SUBROUTINE TMSER
C
C  COMPUTE HARMONIC TIME SERIES CHARACTERISTICS
C
      COMMON D(15,305),DM(6),FM(6),CHLABEL(15),ZR(6,102),TINTV,NREC,
+ NZR(5),INAME,PHI,RF(3),DEPTH,CD(3),KK
      NTS=6
      DT=TINTV
      DT2=DT/2.
C  FIND AMPLITUDES AND ZERO CROSSING TIMES FOR EXCITATION AND RESPONSE
      DO 60 I=1,NTS
      NA=NZ=0
      T=SA=SAA=ST=STT=ADM=0.
      TEMP=ADMIN=1000000000.
C
      NI=1
      N2=NREC-3
      DO 40 J=NI,N2
C  INSERT A 3RD ORDER EST. POINT INTO DATA TIME SERIES
      T=T+DT
      TEMPLST=TEMP
      PA=D(I,J)
      PB=D(I,J+1)
      PC=D(I,J+2)
      PD=D(I,J+3)
      TEMP=(-PA+9.*PB+9.*PC-PD)/15.
C  CHECK FOR ZERO CROSSING
      IF(PB*TEMP) 21,24,22
21  ZT=(ABS(PB)/(ABS(PB)+ABS(TEMP)))*DT2
      GO TO 25
22  IF(TEMP*PC) 23,24,26
23  ZT=DT2+(ABS(TEMP)/(ABS(TEMP)+ABS(PC)))*DT2
      GO TO 25
24  IF(PB.EQ.0.) ZT=0.
      IF(TEMP.EQ.0.) ZT=DT2
      IF(PC.EQ.0.) GO TO 40
C  RECORD ZERO CROSSING TIME
25  CONTINUE
      IF(NZ.GE.102) GO TO 40
      NZ=NZ+1
      ZR(I,NZ)=T+ZT
      GO TO 40
C  CHECK FOR MAXIMA OR MINIMA
26  PB=ABS(PB)
      TEMP=ABS(TEMP)
      IF(PB.GT.EMPLST.AND.PB.GT.TEMP) GO TO 27
      IF(TEMP.GT.PB.AND.TEMP.GT.ABS(PC)) GO TO 28
      GO TO 40
27  NA=NA+1
      AM=PB
      GO TO 29
28  NA=NA+1
      AM=TEMP
C  SUM AMPL. AND AMPL. SQUARE FOR STATISTICAL ANALYSIS
29  SA=SA+AM
      SAA=SAA+AM*AM
      IF(AM.GT.ADMAX) ADMAX=AM
      IF(AM.LT.ADMIN) ADMIN=AM
40  CONTINUE
      NZR(I)=NZ

```

FORTRAN COMPILATION

RUN 2.3C0-75274

26 APR 78 19:12:33 PAGE NO. 2

```

C  CALCULATE HALF-PERIODS AND SUMS FOR STAT. ANAL.
    NHP=NZ-1
    DO 50 K=1,NHP
      HP=ZR(I,K+1)-ZR(I,K)
      ST=ST+HP
      STT=STT+HP*HP
    50 CONTINUE
C  CALCULATE PERIOD AND AMPL STATISTICS
    FNHP=FLOAT(NHP)
    FNA=FLOAT(NA)
    HPM=ST/FNHP
    DM(I)=SA/FNA
    PM=2.*HPM
    FM(I)=1./PM
    IF(I.LE.3) RF(I)=2.*PHI*FM(I)
    HPV=(ST-FNHP*HPM*HPM)/(FNHP-1.)
    PSD=2.*SQRT(HPV)
    DV=(SAA-FNA*DM(I)*DM(I))/(FNA-1.)
    DSD=SQRT(DV)
C  NORMALIZE STANDARD DEVIATION AS A PERCENTAGE OF THE MEAN VALUE
    DSD=(DSD/DM(I))*100.
    PSD=(PSD/PM)*100.
    PRINT 1002,I,CHLABEL(I),FM(I),PSD,DM(I),DSD,ADMAX,ADMIN,NHP,NA
1002 FORMAT(15,4X,A10,4X,*FM=*,F6.2,* HZ*,4X,*PSD=*,F6.1,5X,
+ *DM=*,E12.3,4X,*DSD=*,F6.1,4X,*MAXMIN=*,E10.3,E11.3,
+ * NHPNA=*,15,15)
    60 CONTINUE
    RETURN
    END

```

FORTRAN COMPILATION

RUN 2.3C0-75274

26 APR 78 19:12:33 PAGE NO. 1

```

    SUBROUTINE VELCAL
C
C  CALCULATE RELATIVE VELOCITY TIME SERIES FOR EACH DOF
C
    COMMON D(15,305),DM(6),FM(6),CHLABEL(15),ZR(6,102),TINTV,NREC,
+ NZR(6),INAME,PHI,RF(3),DEPTH,CD(3),KK
    COMMON /DAMP/K(3),DP(3),MASS(3),C(3),ZCG,SX,SY,XS,G(3)
    DT=TINTV
C
    N2=NREC-2
    DO 200 I=1,3
      DO 100 J=3,N2
C  RESTORE FOUNDATION ACCELERATIONS IN POSITIONS 13-15
        D(13,J)=D(15,J)
        D(15,J)=D(3,J)
C
C  CALCULATE THE RELATIVE VEL. BY DIFFERENTIATION OF THE RELATIVE DISPL.
C  USING A 4TH ORDER SCHEME
        D(I,J)=(D(I+3,J-2)-8.*D(I+3,J-1)+8.*D(I+3,J)-D(I+3,J+2))/(12.*
+ DT)
C
    100 CONTINUE
    200 CONTINUE
    RETURN
    END

```


FORTRAN COMPILATION

RUN 2.3C0-75274

26 APR 78 19:12:33 PAGE NO. 1

```

      SUBROUTINE SOLMASS
C
C  SOLVE FOR THE VIRTUAL MASS BY LINEAR OR MULTIPLE REGRESSION AND
C  RECORD IN COEFFICIENT FORM
C
      COMMON D(15,305),DM(6),FM(6),CHLABEL(15),ZR(6,102),TINTV,NREC,
+   NZR(6),INAME,PHI,RF(3),DEPTH,CD(3),KK
      COMMON /DAMP/K(3),DP(3),MASS(3),C(3),ZCG,SX,SY,XS,G(3)
      COMMON /REG/ A(2,2),BY1,BY2,SSDX,SSDY,SSDYD,FNP,VM(4),R1,R2,SX1,
+   SX2,SSDXD
      REAL MASS,K
      NLAST=NREC-2
C  INITIALIZE THE SUMS
      SHA=SVA=SRA=0.
      SYH=SYV=SYR=0.
      SSHA=SSHA=SSVA=0.
      SSYH=SSYV=SSYR=0.
      SPHARA=SPHAYH=SPHAYR=0.
      SPRAYR=SPVAYV=0.
      SYHD=SYVD=0.
      SSYHD=SSYVD=0.
      SPHAYHD=SPVAYVD=0.
      SVGA=SSVGA=0.
C  FORM THE SUMS OF INDEP. VARIABLES, SQUARES, AND CROSS-PRODUCTS
C
      NP=0
      DO 50 J=3,NLAST
      NP=NP+1
C
C  ACCELERATION SUMS AND SUMS OF SQUARES
      D(10,J)=D(10,J)*G(1)
      D(11,J)=D(11,J)*G(1)
      D(14,J)=D(14,J)*G(1)
      ZA=D(11,J)-D(14,J)
      SHA=SHA+D(10,J)
      SVA=SVA+D(11,J)
      SVGA=SVGA+ZA
      SRA=SRA+D(12,J)
      SSHA=SSHA+D(10,J)*D(10,J)
      SSVA=SSVA+D(11,J)*D(11,J)
      SSVGA=SSVGA+ZA*ZA
      SSRA=SSRA+D(12,J)*D(12,J)
C
C  DEPENDENT VARIABLES AND SQUARE SUMS
C
      YH=-MASS(1)*D(10,J)-C(1)*D(1,J)-K(1)*D(4,J)
      YV=-MASS(2)*D(11,J)-C(2)*D(2,J)-K(2)*D(5,J)
      YR=-MASS(3)*D(12,J)-C(3)*D(3,J)-K(3)*D(6,J)
C  CALCULATE THE UNDAMPED VARIABLE
      YHD=YH+C(1)*D(1,J)
C  CALCULATE THE DEPEND. VAR. FOR ADDED MASS (CORRECTED FOR CONST. LOAD)
      YVD=YV-VM(2)*D(14,J)
C
      SYH=SYH+YH
      SYV=SYV+YV
      SYR=SYR+YR
      SYHD=SYHD+YHD
      SYVD=SYVD+YVD
      SSYH=SSYH+YH*YH
      SSYV=SSYV+YV*YV
      SSYR=SSYR+YR*YR
      SSYHD=SSYHD+YHD*YHD
      SSYVD=SSYVD+YVD*YVD

```

FORTRAN COMPILATION

RUN 2.3C0-75274

26 APR 78 19:12:33 PAGE NO. 2

```

C
C  CROSS-PRODUCTS WITH HORIZ ACC.
      SPHARA=SPHARA+D(10,J)*D(12,J)
      SPHAYH=SPHAYH+D(10,J)*YH
      SPHAYR=SPHAYR+D(10,J)*YR
      SPHAYHD=SPHAYHD+D(10,J)*YHD
C
C  CROSS-PRODUCTS WITH VERT ACC.
      SPVAYV=SPVAYV+YV*D(11,J)
      SPVAYVD=SPVAYVD+YVD*ZA
C
C  CROSS-PRODUCTS WITH ROT. ACC.
      SPRAYR=SPRAYR+D(12,J)*YR
C
      50 CONTINUE
      FNP=FLOAT(NP)
      PRINT 901,FNP
901  FORMAT(/// * NR. OF DATA PTS. USED IN ANALYSIS =*,F5.0//)
C
C  HORIZONTAL MODE
      IF(DM(1).LT..02) GO TO 55
      N=1
C  FORM REGRESSION COEF. MATRIX
      SSDX=SSHA-SHA*SHA/FNP
      SSDXD=SSDX
      BY1=SPHAYH-SHA*SYH/FNP
      BY2=SPHAYHD-SHA*SYHD/FNP
      SSDY=SSYH-SYH*SYH/FNP
      SSDYD=SSYHD-SYHD*SYHD/FNP
      R1=SYH/FNP
      R2=SYHD/FNP
      SX1=SHA/FNP
      SX2=SX1
      PRINT 1000,N
1000 FORMAT(/// * COEFFICIENTS FOR MODE *,I1/)
      CALL REGRESS(N)
C
      55 CONTINUE
C  VERTICAL MODE
      IF(DM(2).LT..02) GO TO 60
      N=2
C  FORM REGRESSION COEF. MATRIX
      SSDX=SSVA-SVA*SVA/FNP
      SSDXD=SSVGA-SVGA*SVGA/FNP
      BY1=SPVAYV-SVA*SYV/FNP
      BY2=SPVAYVD-SVGA*SYVD/FNP
      SSDY=SSYV-SYV*SYV/FNP
      SSDYD=SSYVD-SYVD*SYVD/FNP
      R1=SYV/FNP
      R2=SYVD/FNP
      SX1=SVA/FNP
      SX2=SVGA/FNP
      PRINT 1000,N
      CALL REGRESS(N)
C
      60 CONTINUE
C  ROTATIONAL MODE
      IF(FM(6).GE.20.5.OR.DM(1).LT..02) GO TO 65
      N=3
C  FORM REGRESSION COEF. MATRIX
      A(1,1)=SSRA-SRA*SRA/FNP
      A(1,2)=A(2,1)=SPHARA-SHA*SRA/FNP
      A(2,2)=SSHA-SHA*SHA/FNP

```

FORTRAN COMPILATION

RUN 2.3C0-75274

26 APR 78 19:12:33 PAGE NO. 3

```

BY1=SPRAYR-SRA*SYR/FNP
RY2=SPHAYR-SHA*SYR/FNP
SSDY=SSYR-SYR*SYR/FNP
R1=SYR/FNP
SX1=SRA/FNP
SX2=SHA/FNP
PRINT 1000,N
CALL REGRESS(N)

```

C

```

65 CONTINUE
RETURN
END

```

FORTRAN COMPILATION

RUN 2.3C0-75274

26 APR 78 19:12:33 PAGE NO. 1

SUBROUTINE DAMPING

C

```

C CALCULATE DAMPING FOR EACH DEGREE OF FREEDOM USING DATA FROM SHOCK
C TESTS

```

C

```

COMMON D(15,305),DM(6),FM(6),CHLABEL(15),ZR(6,102),TINTV,NREC,
+ NZR(6),INAME,PHI,RF(3),DEPTH,CD(3),KK
COMMON /DAMP/K(3),DP(3),MASS(3), C(3),ZCG,SX,SY,XS,G(3)
COMMON /LD/ DMAX(15)
REAL MASS,K
IF(KK-1) 10,5,15

```

C STIFFNESS INPUT IN KG, CM, SEC UNITS

5 READ 1000,K

1000 FORMAT(3F20.0)

KK=KK+1

GO TO 15

10 CONTINUE

C CONVERT STIFFNESSES TO SI UNITS (KG, CM, SEC)

K(1)=SX*175.126

K(2)=SY*175.126

YS=ZCG-1.250

CYSS=YS*YS-21.333*(.1875*YS-1.)

K(3)=(SX*CYSS+SY*XS*XS)*1129.85

15 CONTINUE

IF(DMAX(2).LT..035.OR.DEPTH.LE.0.) RETURN

PRINT 1001,K

PRINT 1002,CD

1001 FORMAT(/3X,*K1=*,F9.0,5X,*K2=*,F9.0,5X,*K3=*,F12.0)

1002 FORMAT(3X,*CD=*,3F6.3/)

DO 20 I=1,3

C CALCULATE DRY CRITICAL DAMPING

DP(I)=2.*SQRT(MASS(I)*K(I))

C ESTIMATE MATERIAL DAMPING TO BE A PERCENT OF DRY DAMPING

C(I)=C(I)*DP(I)

20 CONTINUE

RETURN

END

FORTRAN COMPILATION

RUN 2.3C0-75274

26 APR 78 19:12:33 PAGE NO. 1

```

      SUBROUTINE REGRESS(N)
C
C   PERFORM THE REGRESSION OPERATION, COMPUTE STATISTICS, AND OUTPUT
C   TO CARDS AND TAPE
C
      COMMON D(15,305),DM(6),FM(6),CHLABEL(15),ZR(6,102),TINTV,NREC,
+   NZR(6),INAME,PHI,RF(3),DEPTH,CD(3),KK
      COMMON /DAMP/K(3),DP(3),MASS(3), C(3),ZCG,SX,SY,XS,G(3)
      COMMON /REG/ A(2,2),BY1,BY2,SSDX,SSDY,SSDYD,FNP,VM(4),R1,R2,SX1,
+   SX2,SSDXD
      REAL MASS,K
      IF(N.EQ.3) GO TO 100
C   CALCULATE THE MASS COEFFICIENTS WITH AND WITHOUT HYDRODYNAMIC DAMPING
      B1=BY1/SSDX
      B2=BY2/SSDXD
C   CALC. STANDARD DEV.
      V1=(SSDY-B1*BY1)/(FNP-2.)
      V2=(SSDYD-B2*BY2)/(FNP-2.)
      SD1=SQRT(ABS(V1/SSDX))/B1
      SD2=SQRT(ABS(V2/SSDXD))/B2
      R1=R1-R1*SX1
      R2=R2-B2*SX2
      SDR1=SQRT(ABS(V1/FNP))/R1
      SDR2=SQRT(ABS(V2/FNP))/R2
      IF(N.EQ.2.AND.VM(2).LE.0.) GO TO 50
      CAM1=B1/VM(N)
      CAM2=B2/VM(N)
      GO TO 60
50   CAM1=CAM2=0.
60   CONTINUE
      PRINT 1000,B1,SD1,R1,SDR1
      PRINT 1001,B2,SD2,R2,SDR2
      PRINT 1002,CAM1,CAM2
      PUNCH 1003,INAME,FM(N+3),N,FNP,CAM1,CAM2,SD1,SD2,DEPTH
      WRITE(3) N,FNP,B1,B2,SD1,SD2,CAM1,CAM2
      RETURN
1000  FORMAT(3X,*MA1=*,F12.2,T25,*SD=*,F12.2,T45,*RES=*,E10.4,5X,*SDR=*,
+   F10.2)
1001  FORMAT(3X,*MA2=*,F12.2,T25,*SD=*,F12.2,T45,*RES=*,E10.4,5X,*SDR=*,
+   F10.2)
1002  FORMAT(3X,*CAM1=*,F10.4,T25,*CAM2=*,F10.4//)
1003  FORMAT(A10,F4.1,I1,F5.0,4E10.4,F5.1)
C   CALC. MODE 3 COEF.
100  CONTINUE
C   FORM THE INVERSE OF MATRIX A
      DETA=A(1,1)*A(2,2)-A(2,1)*A(1,2)
      B1=A(2,2)/DETA
      B2=A(1,1)/DETA
      B3=-A(1,2)/DETA
C   CALC. REGRESSION COEF. FOR MASSES
      RM1=B1*BY1+B3*BY2
      RM2=B3*BY1+B2*BY2
C   CALC VARIANCE AND STANDARD DEV.
      VY=(SSDY-RM1*BY1-RM2*BY2)/(FNP-3.)
      SD1=SQRT(ABS(B1*VY))
      SD2=SQRT(ABS(B2*VY))
      SD1=SD1*100./RM1
      SD2=SD2*100./RM2
      R1=R1-RM1*SX1-RM2*SX2
      R2=SDR2=0.
      CAM1=RM1/VM(3)
      CAM2=RM2/VM(4)
      SDR1=SQRT(ABS(VY))

```

FORTRAN COMPILATION

RUN 2.3C0-75274

26 APR 78 19:12:33 PAGE NO. 2

```
PRINT 1000, RM1, SD1, R1, SDR1
PRINT 1001, RM2, SD2, R2, SDR2
PRINT 1002, CAM1, CAM2
PUNCH 1003, I NAME, FM(6), N, FNP, CAM1, CAM2, SD1, SD2, DEPTH
WRITE(3) N, FNP, RM1, RM1, SD1, SD2, CAM1, CAM2
RETURN
END
```

APPENDIX F. SUBTANK--PROGRAM LISTING

FORTRAN COMPILATION

RUN 2.3C0-75274

26 APR 78 19:12:33 PAGE NO. 1

```

      PROGRAM SUBTANK(INPUT,OUTPUT,PUNCH)
C   A PROGRAM FOR STEP-BY-STEP INTEGRATION OF A MULTI-DEGREE-OF-FREEDOM
C   SYSTEM, BASED ON THE METHODS OF E.L. WILSON, CODED BY R.C. BYRD
      DIMENSION A(4000)
      COMMON FOR,SK(3),DMAX(6),DMIN(6),NAME
      PRINT 990
990  FORMAT(1H1,1X, ***** SUBTANK *****
+*** /2X, #A PROGRAM FOR CALCULATING THE RESPONSE OF A RIGID#
+ /2X, #SUBMERGED TANK ON A FLEXIBLE FOUNDATION TO RANDOM#
+ /2X, #EXCITATION -- CODED BY R.C. BYRD (1978)#
+ /# *****
+*****#//)
C   READ THE SYSTEM DIMENSIONS AND OUTPUT FORMAT
      READ 1000,NE,NDOF,NIN,NOUT,FOR
      IF(NOUT.LE.NIN) NOUT=NIN+1
      PRINT 1001,NDOF,NIN,NOUT
1000 FORMAT(11,I4,2I5/A10)
1001 FORMAT( /# NO. OF DOF=#,I5/2X,*NO. OF INPUT TIME STEPS=#,I5/
+ 2X,*NO. OF OUTPUT TIME STEPS=#,I5/)
      MAX=4000
      NM=1
      NN=NDOF*NDOF
      NC=1+NN
      NS=NC+NN
      NXT=NS+NN
      NU=NXT+2*NDOF
      NUI=NU+NDOF*NOUT
      NDT=NUI+NDOF*3-1
      IF(NDT.GT.MAX) GO TO 900
C   READ THE INTEGRATION COEFFICIENTS AND TIME STEP
      READ 1002,DEL,ALF,THE,DTT
1002 FORMAT(4F10.0)
      PRINT 1003,DEL,ALF,THE,DTT
1003 FORMAT(/2X,*INTEGRATION COEFFICIENTS-*,2X,*DEL=#,F10.6,
+ 5X,*ALF=#,F10.6, 5X,*THE=#,F10.6/T30*DTT=#,F10.6,* SEC.#/)
      CALL HYDRO3 (A(NM),A(NC),A(NS),A(NU),NIN,NOUT,DTT,NE)
      CALL STEPS(A(NS),A(NM),A(NC),A(NUI),A(NU),NDOF,NOUT,DTT,DEL,ALF,
+ THE)
      CALL OUTPUT(A(NU),A(NXT),NDOF,NOUT,NE)
      GO TO 950
900  PRINT 1004
1004 FORMAT(//# ***** THE PROBLEM EXCEEDS THE CURRENT STORAGE LIMITS
+TS -- ADJUSTMENTS MUST BE MADE *****#)
950  CONTINUE
      STOP
      END

```

FORTRAN COMPILATION

RUN 2.3C0-75274

26 APR 78 19:12:33 PAGE NO. 1

```

      SUBROUTINE HYDRO3 (XM,C,S,R,NP,NOUT,DT,NE)
C   THIS ROUTINE READS THE HYDRODYNAMIC COEFFICIENTS, SYSTEM CONSTANTS,
C   AND GROUND ACCELERATION AND ESTABLISHES THE MASS, DAMPING, STIFFNESS,
C   AND LOAD MATRICES FOR A SYSTEM WITH 3 RIGID BODY DOF.
C   CODED BY R. C. BYRD (1978).
      DIMENSION XM(3,3),C(3,3),S(3,3),R(3,1),
+       V(3),PB(3),PC(3),PD(3),D(3),RM(3)
      COMMON FOR,SK(3),DMAX(6),DMIN(6),NAME
      READ 1000,DMASS,RMASS,HS,RAD
C   NOTE: ALL UNITS ARE ( KG, CM )
      PRINT 903,RAD,HS,DMASS,RMASS
903 FORMAT(///2X,*TANK CHARACTERISTICS:*/)
+       16X,*RADIUS=*,F10.1/
+       16X,*HEIGHT=*,F10.1/
+       14X,*DRY MASS=*,F10.1/
+       2X,*MASS MCMNT. OF INERT.=*,F10.1/)
      READ 1000,CMXX,CMZZ,CMRR,CMRX,DEPTH
1000 FORMAT(5F10.0)
      PRINT 900,DEPTH,CMXX,CMZZ,CMRR,CMRX
900 FORMAT(12X,*WATER DEPTH=*,F5.1/
+       T19,*CMXX=*,F6.3/T19,*CMZZ=*,F6.3/
+       T19,*CMRR=*,F6.3/T19,*CMRX=*,F6.3/)
      READ 1000,CDMAT,CDHX,CDHZ,CDHR
      PRINT 901,CDMAT,CDHX,CDHZ,CDHR
901 FORMAT(/2X,*FOUNDATION DAMPING (ALL MODES)=*,F6.3/
+       T28,*CDHX=*,F6.3/T28,*CDHZ=*,F6.3/T28,*CDHR=*,F6.3/)
      N=3
C   NOTE: STIFFNESSES ARE IN ( KG, CM, SEC ) UNITS
      READ 1002,SX,SZ,SR
1002 FORMAT(3E10.4)
C
      SK(1)=SX/100.
      SK(2)=SZ/100.
      SK(3)=SR/100.
C
C   ESTABLISH THE MASS, DAMPING AND STIFFNESS MATRICES
C
C   INITIALIZE THE MATRICES
      DO 10 I=1,3
      DO 10 J=1,3
10 XM(I,J)=C(I,J)=S(I,J)=0.
C
C   MASS (COUPLED)
      DTH=DEPTH-HS
      PHI=2.*ASIN(1.)
      AR=PHI*RAD*RAD
      VMWC=AR*DTH/1000.
      VMT=AR*HS/1000.
      RG2=(RAD*RAD/4.)+(HS*HS/12.)
      VMR=VMT*RG2
      VMC=SQRT(RG2)*VMT
C
      XM(1,1)=XMXX=DMASS+CMXX*VMT
      XM(2,2)=XMZZ=DMASS+CMZZ*VMT
      XM(3,3)=XMRR=RMASS+CMRR*VMR
      XM(1,3)=XM(3,1)=XMRX=CMRX*VMC
C
C   STIFFNESS (UNCOUPLED)
      S(1,1)=SX
      S(2,2)=SZ
      S(3,3)=SR
C

```


FORTRAN COMPILATION

RUN 2.3C0-75274

26 APR 78 19:12:33 PAGE NO. 2

```

      IF(NE.EQ.0).OR.NE.EQ.3) GO TO 15
C   CALCULATE CHARACTERISTIC VALUES AND VECTORS (NAT. FREQS. AND MODES)
      CALL JACOBI(S,XM,C,PC,3,4,10)
      PRINT 1009
      PRINT FDP,PC
      PRINT 1010
      PRINT FOR,((C(I,J),J=1,N),I=1,N)
1009 FORMAT(/2X,*SYSTEM EIGENVALUES:*)
1010 FORMAT(/2X,*SYSTEM EIGENVECTORS:*)
C   REINITIALIZE THE MATRICES
      DO 12 I=1,3
      DO 12 J=1,3
12  XM(I,J)=C(I,J)=S(I,J)=0.
C   RESET STIFFNESS AND MASS MATRICES
      XM(1,1)=XMXX
      XM(2,2)=XMZZ
      XM(3,3)=XMRR
      XM(1,3)=XM(3,1)=XMRX
      S(1,1)=SX
      S(2,2)=SZ
      S(3,3)=SR
15  CONTINUE
C
C   DAMPING (UNCOUPLED)
C   COMPUTE CRITICAL DAMPING FOR EACH MODE
      DCX=2.*SQRT(XM(1,1)*SX)
      DCZ=2.*SQRT(XM(2,2)*SZ)
      DCR=2.*SQRT(XM(3,3)*SR)
C   ESTABLISH THE DAMPING MATRIX
      C(1,1)=(CDMAT+CDHX)*DCX
      C(2,2)=(CDMAT+CDHZ)*DCZ
      C(3,3)=(CDMAT+CDHR)*DCR
C
      PRINT 1003
1003 FORMAT(/2X,*MASS MATRIX-*)
      PRINT FOR,((XM(I,J),J=1,N),I=1,N)
      PRINT 1004
1004 FORMAT(/2X,*DAMPING MATRIX-*)
      PRINT FOR,((C(I,J),J=1,N),I=1,N)
      PRINT 1005
1005 FORMAT(/2X,*STIFFNESS MATRIX-*)
      PRINT FOR,((S(I,J),J=1,N),I=1,N)
C
C   ESTABLISH THE LOAD MATRIX, INCLUDING THE EFFECT OF HYDRODYNAMIC
C   DAMPING. ASSUME THAT THE SYSTEM IS AT REST FOR T LESS THAN ZERO.
C
C   READ EXCITATION FILE NAME AND MAX-MINS
      READ 1011,NAME,((DMAX(I),DMIN(I)),I=1,6)
1011 FORMAT(A10/6E12.5/6E12.5)
C
C   READ GROUND ACCELERATIONS
      READ 1006,((R(I,J),I=1,N),J=1,NR)
      PRINT 1008
      PRINT 1007,((R(I,J),I=1,N),J=1,NR)
1006 FORMAT(6E12.5)
1007 FORMAT(4(3X,3F3.4))
1008 FORMAT(/2X,*GROUND ACCELERATION:*)
C
C   INITIALIZE THE COEFFICIENTS FOR A 2ND ORDER INTEGRATION OF THE
C   GROUND ACCELERATION.
      DO 20 I=1,3
      PB(I)=R(I,1)
      PC(I)=R(I,2)
      PD(I)=R(I,3)

```

FORTRAN COMPILATION

RUN 2.3C0-75274

26 APR 78 19:12:33 PAGE NO. 3

```

20 CONTINUE
  D(1)=DCX*CDHX*980.665
  D(2)=0.
  D(3)=DCR*CDHR
  RM(1)=XM(1,1)*980.665
  RM(2)=(VMWC+DMASS)*980.665
  RM(3)=XM(3,3)
C
C  INITIALIZE THE LOAD MATRIX AT T=0 AND 0+DT
  DO 30 I=1,3
    R(I,1)=-R(I,1)*RM(1)
    TEMP=(9.*PB(I)+9.*PC(I)-PD(I))/16.
    V(I)=DT*(PB(I)+2.*TEMP+PC(I))/4.
    R(I,2)=-R(I,2)*RM(1)-D(I)*V(I)
  30 CONTINUE
C
C  SET ALL VALUES IN RESPONSE MATRIX FOR T GREATER THAN NIN*DT EQUAL 0.
  NSTART=NR+1
  DO 40 J=NSTART,NOUT
    40 R(1,J)=R(2,J)=R(3,J)=0.
C
C  CALCULATE THE REMAINDER OF THE LOAD MATRIX.
  DO 50 J=3,NR
    DO 50 I=1,3
C  CALCULATE VELOCITIES
    PA=PB(I)
    PB(I)=PC(I)
    PC(I)=PD(I)
    PD(I)=R(I,J+1)
    TEMP=(-PA+9.*PB(I)+9.*PC(I)-PD(I))/16.
    V(I)=V(I)+DT*(PB(I)+2.*TEMP+PC(I))/4.
    R(I,J)=-R(I,J)*RM(1)-D(I)*V(I)

50 CONTINUE
  V(1)=V(1)*980.665
  PRINT 902,V(1)
902 FORMAT(/2X,#HORIZ.GROUND VELOCITY AT DT*NIN=#,F10.1/)
  RETURN
  END

```

FORTRAN COMPILATION

RUN 2.3C0-75274

26 APR 78 19:12:33 PAGE NO. 1

```

      SUBROUTINE STEPS(S,XM,C, UI,U,N,NOUT,DTT,DEL,ALF,THE)
      DIMENSION S(N,N),XM(N,N),C(N,N),UI(N,3),U(N,NOUT)
C   SET THE INITIAL CONDITIONS TO ZERO
      DO 10 I=1,N
      DO 10 J=1,3
      10 UI(I,J)=0.
C   COMPUTE THE INTEGRATION CONSTANTS
      IF(THE.EQ.0.)THE=1.0
      DT=THE*DTT
      A0=1./(ALF*DT*DT)
      A1=DEL/(ALF*DT)
      A2=1./(ALF*DT)
      A3=0.5/ALF-1.
      A4=DEL/ALF-1.
      A5=0.5*DT*(DEL/ALF-2.)
      A6=DTT*(1.-DEL)
      A7=DTT*DEL
      A8=(.5-ALF)*DTT*DTT
      A9=ALF*DTT*DTT
C   FORM THE TRIANGULARIZED EFFECTIVE STIFFNESS MATRIX
      DO 100 I=1,N
      DO 100 J=1,N
      100 S(I,J)=S(I,J)+A0*XM(I,J)+A1*C(I,J)
      CALL SYMSOL(S,UI,N,1,1)
C
C   FOR EACH TIME STEP
C
      DO 400 I=1,NOUT
C   1. CALCULATE THE EFFECTIVE LOAD AT TIME T+DT
C
      DO 250 L=1,N
      X=A0*UI(L,1)+A2*UI(L,2)+A3*UI(L,3)
      Y=A1*UI(L,1)+A4*UI(L,2)+A5*UI(L,3)
      DO 250 M=1,N
      250 U(M,I)=U(M,I)+XM(M,L)*X+C(M,L)*Y
C   2. SOLVE FOR THE DISPLACEMENT AT T+DT
C
      CALL SYMSOL(S,U(I,I),N,1,2)
C
C   3. CALCULATE ACCELERATIONS AND VELOCITIES AT TIME T+DT
      DO 300 L=1,N
      A=A0*(U(L,I)-UI(L,1))-A2*UI(L,2)-A3*UI(L,3)
      DA=(A-UI(L,3))/THE
      A=UI(L,3)+DA
      V=UI(L,2)+A6*UI(L,3)+A7*A
      U(L,I)=UI(L,1)+DTT*UI(L,2)+A8*UI(L,3)+A9*A
      UI(L,3)=A
      UI(L,2)=V
      300 UI(L,1)=U(L,I)
      400 CONTINUE
C
      RETURN
      END

```

FORTRAN COMPILATION

RUN 2.3C0-75274

26 APR 78 19:12:33 PAGE NO. 1

```

      SUBROUTINE SYMSOL(A,B,NN,LL,M)
C   SYMMETRIC EQUATION SOLVER-AFTER E.L.WILSON (1976)
C   M=0 TRIANGULARIZE AND SOLVE
C   M=1 TRIANGULARIZE ONLY
C   M=2 FORWARD REDUCTION AND BACKSUBSTITUTION ONLY
      DIMENSION A(NN,NN),B(NN,LL)
C
      IF(M.EQ.2) GO TO 500
      DO 400 N=1,NN
      IF(N.EQ.NN) GO TO 500
      D=A(N,N)
      IF(D.EQ.0.0) PRINT 2000,N
      N1=N+1
      DO 300 J=N1,NN
      IF(A(N,J).EQ.0.0) GO TO 300
      A(N,J)=A(N,J)/D
      DO 200 I=J,NN
      A(I,J)=A(I,J)-A(I,N)*A(N,J)
200  A(J,I)=A(I,J)
300  CONTINUE
400  CONTINUE
C   FORWARD REDUCTION AND BACKSUBSTITUTION
500  IF(M.EQ.1) RETURN
      DO 700 N=1,NN
      DO 600 L=1,LL
600  B(N,L)=B(N,L)/A(N,N)
      IF(N.EQ.NN) GO TO 800
      N1=N+1
      DO 700 L=1,LL
      DO 700 I=N1,NN
700  B(I,L)=B(I,L)-A(I,N)*B(N,L)
C
800  N1=N
      N=N-1
      IF(N.EQ.0) RETURN
      DO 900 L=1,LL
      DO 900 J=N1,NN
900  B(N,L)=B(N,L)-A(N,J)*B(J,L)
      GO TO 800
C
2000 FORMAT(39H0***ZERO DIAGONAL TERM EQUATION NUMBER I4)
      END

```

```

      SUBROUTINE JACOBI (A,B,X,E,N,NFIG,NSMAX)
C-----
C  AN EIGENVALUE SOLUTION AFTER E.L. WILSON (1977)
C  SUBROUTINE SOLVES EIGENVALUE PROBLEM  $AX = BXE$  WHERE
C  A AND B ARE N X N SYMMETRIC MATRICES
C  E IS A DIAGONAL MATRIX OF EIGENVALUES STORED AS A ROW ARRAY
C  X IS A N X N MATRIX OF EIGENVECTORS
C  NSMAX IS THE MAXIMUM NUMBER OF SWEEPS TO BE PERFORMED
C  NFIG IS THE NUMBER OF SIGNIFICANT FIGURES TO BE OBTAINED
C-----
      DIMENSION A(N,N),B(N,N),X(N,N),E(N)
C-----INITIALIZATION-----
      NT=0
      NN=N-1
      RTOL=0.1**(2*NFIG)
      EPS=0.01
      DO 30 I=1,N
      DO 20 J=1,N
20  X(I,J)=0.
30  X(I,I)=1.
      IF(N.EQ.1) GO TO 820
C-----SWEEP OFF-DIAGONAL TERMS FOR POSSIBLE REDUCTION---
      DO 800 M=1,NSMAX
      YMAX=0.0
      DO 700 J=1,NN
      JJ=J+1
      DO 700 K=JJ,N
C-----COMPARE WITH THRESHOLD VALUE-----
      EA=ABS((A(J,K)*A(J,K))/(A(J,J)*A(K,K)))
      EB=ABS((B(J,K)*B(J,K))/(B(J,J)*B(K,K)))
      Y=EA+EB
      IF(Y.GT.YMAX) YMAX=Y
      IF(Y.LT.EPS) GO TO 700
C-----CALCULATE TRANSFORMATIONS TERMS-----
      Y=A(J,J)*B(K,K)-A(K,K)*B(J,J)
      AK=A(K,K)*B(J,K)-B(K,K)*A(J,K)
      AJ=A(J,J)*B(J,K)-B(J,J)*A(J,K)
      D1=Y/2.
      D2=Y**2+4.*AK*AJ
      IF(D2.LT.0.0) PRINT 4000,J,K
4000  FORMAT(20H OFF DIAGONAL TERM 2IS)
      IF(D2.LT.0.0) GO TO 700
      D2=SQRT(D2)/2.
      Z=D1+D2
      IF(D1.LT.0.0) Z=D1-D2
      IF(Z) 80,70,80
70  CA=0.0
      CG=-A(J,K)/A(K,K)
      GO TO 90
80  CA=AK/Z
      CG=-AJ/Z
C-----ZERO TERMS A(J,K) AND B(J,K)-----
90  DO 100 I=1,N
      IF(I.EQ.J.OR.I.EQ.K) GO TO 100
      A(J,I)=A(I,J)+CG*A(I,K)
      A(K,I)=A(I,K)+CA*A(I,J)
      A(I,J)=A(J,I)
      A(I,K)=A(K,I)
      B(J,I)=B(I,J)+CG*B(I,K)
      B(K,I)=B(I,K)+CA*B(I,J)
      B(I,J)=B(J,I)
      B(I,K)=B(K,I)
100  CONTINUE

```

FORTRAN COMPILATION

RUN 2.3C0-75274

26 APR 78 19:12:33 PAGE NO. 2

```

      AK=A(K,K)
      BK=B(K,K)
      A(K,K)=AK+CA*(A(J,K)+A(J,K)+CA*A(J,J))
      B(K,K)=BK+CA*(B(J,K)+B(J,K)+CA*B(J,J))
      A(J,J)=A(J,J)+CG*(A(J,K)+A(J,K)+CG*AK)
      B(J,J)=B(J,J)+CG*(B(J,K)+B(J,K)+CG*BK)
      A(J,K)=0.
      B(J,K)=0.
      A(K,J)=0.0
      B(K,J)=0.0
C-----TRANSFORM EIGENVECTORS-----
      DO 200 I=1,N
      XJ=X(I,J)
      XK=X(I,K)
      X(I,J)=XJ+CG*XK
200   X(I,K)=XK+CA*XJ
      NT=NT+1
      700 CONTINUE
      IF(YMAX.LT. RTOL) GO TO 820
      EPS=.01*(YMAX)**2
      IF(YMAX.GT.1.0) EPS=0.01
      900 CONTINUE
C-----SCALE EIGEN VECTORS
      820 DO 840 J=1,N
      E(J)=A(J,J)/B(J,J)
      BB=SQRT(B(J,J))
      DO 840 K=1,N
      840 X(K,J)=X(K,J)/BB
      IF(NN.EQ.0) RETURN
C-----ORDER EIGENVALUES AND EIGENVECTORS -----
      DO 900 I=1,NN
      JL=I+1
      HT=E(I)
      IM=I
      DO 850 J=JL,N
      IF(HT.LT.E(J)) GO TO 850
      HT=E(J)
      IM=J
      850 CONTINUE
      E(IM)=E(I)
      E(I)=HT
      DO 900 J=1,N
      HT=X(J,I)
      X(J,I)=X(J,IM)
      900 X(J,IM)=HT
      RETURN
C-----
      END

```

FORTRAN COMPILATION

RUN 2.3C0-75274

26 APR 78 19:12:33 PAGE NO. 1

```

      SUBROUTINE OUTPUT(U,XT,N,NOUT,NE)
      DIMENSION U(N,NOUT),XT(N,2)
      COMMON FOR,SK(3),DMAX(6),DMIN(6),NAME
C   FIND THE EXTREME VALUES
      DO 50 I=1,N
      50 XT(I,1)=XT(I,2)=0.
      DO 100 J=1,NOUT
      DO 90 I=1,N
      IF(XT(I,1).LT.U(I,J)) XT(I,1)=U(I,J)
      IF(XT(I,2).GT.U(I,J)) XT(I,2)=U(I,J)
      90 CONTINUE
      100 CONTINUE
      IF(NE.LT.2) GO TO 105
      PUNCH FOR,((U(K,J),K=1,N),J=1,NOUT)
      105 CONTINUE
      DO 110 I=1,N
      XT(I,1)=XT(I,1)*SK(I)
      XT(I,2)=XT(I,2)*SK(I)
      DMAX(I+3)=DMAX(I+3)*SK(I)
      DMIN(I+3)=DMIN(I+3)*SK(I)
      110 CONTINUE
      PRINT 980,((I,DMAX(I),DMIN(I)),I=1,3)
      PRINT 990
      PRINT 1000,((I,DMAX(I+3),DMIN(I+3),XT(I,1),XT(I,2)),I=1,N)
      980 FORMAT(///2X,*MEASURED MAX-MIN FOUNDATION ACCELERATIONS:*
      +      /( 2X,*DOF: *,I2,3X,*MAX=*,E10.4,3X,*MIN=*,E10.4))
      990 FORMAT( //2X,*FOUNDATION FORCES AND MOMENT ABOUT THE C.G. (N AND
      +CM UNITS)*//T25,*MEASURED*,T59,*CALCULATED* )
      1000 FORMAT(/2X,*DOF: *,I2,3X,*MAX=*,E10.4,3X,*MIN=*,E10.4,
      +      5X,*MAX=*,E10.4,3X,*MIN=*,E10.4)
      RETURN
      END

```

EARTHQUAKE ENGINEERING RESEARCH CENTER REPORTS

NOTE: Numbers in parenthesis are Accession Numbers assigned by the National Technical Information Service; these are followed by a price code. Copies of the reports may be ordered from the National Technical Information Service, 5285 Port Royal Road, Springfield, Virginia, 22161. Accession Numbers should be quoted on orders for reports (PB --- ---) and remittance must accompany each order. Reports without this information were not available at time of printing. Upon request, EERC will mail inquirers this information when it becomes available.

- EERC 67-1 "Feasibility Study Large-Scale Earthquake Simulator Facility," by J. Penzien, J.G. Bouwkamp, R.W. Clough and D. Rea - 1967 (PB 187 905)A07
- EERC 68-1 Unassigned
- EERC 68-2 "Inelastic Behavior of Beam-to-Column Subassemblages Under Repeated Loading," by V.V. Bertero - 1968 (PB 184 888)A05
- EERC 68-3 "A Graphical Method for Solving the Wave Reflection-Refraction Problem," by H.D. McNiven and Y. Menqi - 1968 (PB 187 943)A03
- EERC 68-4 "Dynamic Properties of McKinley School Buildings," by D. Rea, J.G. Bouwkamp and R.W. Clough - 1968 (PB 187 902)A07
- EERC 68-5 "Characteristics of Rock Motions During Earthquakes," by H.B. Seed, I.M. Idriss and F.W. Kiefer - 1968 (PB 188 338)A03
- EERC 69-1 "Earthquake Engineering Research at Berkeley," - 1969 (PB 187 906)A11
- EERC 69-2 "Nonlinear Seismic Response of Earth Structures," by M. Diba and J. Penzien - 1969 (PB 187 904)A08
- EERC 69-3 "Probabilistic Study of the Behavior of Structures During Earthquakes," by R. Ruiz and J. Penzien - 1969 (PB 187 886)A06
- EERC 69-4 "Numerical Solution of Boundary Value Problems in Structural Mechanics by Reduction to an Initial Value Formulation," by N. Distefano and J. Schujman - 1969 (PB 187 942)A02
- EERC 69-5 "Dynamic Programming and the Solution of the Biharmonic Equation," by N. Distefano - 1969 (PB 187 941)A03
- EERC 69-6 "Stochastic Analysis of Offshore Tower Structures," by A.K. Malhotra and J. Penzien - 1969 (PB 187 903)A06
- EERC 69-7 "Rock Motion Accelerograms for High Magnitude Earthquakes," by H.B. Seed and I.M. Idriss - 1969 (PB 187 940)A02
- EERC 69-8 "Structural Dynamics Testing Facilities at the University of California, Berkeley," by R.M. Stephen, J.G. Bouwkamp, R.W. Clough and J. Penzien - 1969 (PB 189 111)A04
- EERC 69-9 "Seismic Response of Soil Deposits Underlain by Sloping Rock Boundaries," by H. Dezfulian and H.B. Seed - 1969 (PB 189 114)A03
- EERC 69-10 "Dynamic Stress Analysis of Axisymmetric Structures Under Arbitrary Loading," by S. Ghosh and E.L. Wilson - 1969 (PB 189 026)A10
- EERC 69-11 "Seismic Behavior of Multistory Frames Designed by Different Philosophies," by J.C. Anderson and V. V. Bertero - 1969 (PB 190 662)A10
- EERC 69-12 "Stiffness Degradation of Reinforcing Concrete Members Subjected to Cyclic Flexural Moments," by V.V. Bertero, B. Bresler and H. Ming Liao - 1969 (PB 202 942)A07
- EERC 69-13 "Response of Non-Uniform Soil Deposits to Travelling Seismic Waves," by H. Dezfulian and H.B. Seed - 1969 (PB 191 023)A03
- EERC 69-14 "Damping Capacity of a Model Steel Structure," by D. Rea, R.W. Clough and J.G. Bouwkamp - 1969 (PB 190 663)A06
- EERC 69-15 "Influence of Local Soil Conditions on Building Damage Potential during Earthquakes," by H.B. Seed and I.M. Idriss - 1969 (PB 191 036)A03
- EERC 69-16 "The Behavior of Sands Under Seismic Loading Conditions," by M.L. Silver and H.B. Seed - 1969 (AD 714 982)A07
- EERC 70-1 "Earthquake Response of Gravity Dams," by A.K. Chopra - 1970 (AD 709 640)A03
- EERC 70-2 "Relationships between Soil Conditions and Building Damage in the Caracas Earthquake of July 29, 1967," by H.B. Seed, I.M. Idriss and H. Dezfulian - 1970 (PB 195 762)A05
- EERC 70-3 "Cyclic Loading of Full Size Steel Connections," by E.P. Popov and R.M. Stephen - 1970 (PB 213 545)A04
- EERC 70-4 "Seismic Analysis of the Charaima Building, Caraballeda, Venezuela," by Subcommittee of the SEAONC Research Committee: V.V. Bertero, P.F. Fratessa, S.A. Mahin, J.H. Sexton, A.C. Scordelis, E.L. Wilson, L.A. Wyllie, H.B. Seed and J. Penzien, Chairman - 1970 (PB 201 455)A06

- EERC 70-5 "A Computer Program for Earthquake Analysis of Dams," by A.K. Chopra and P. Chakrabarti - 1970 (AD 723 994)A05
- EERC 70-6 "The Propagation of Love Waves Across Non-Horizontally Layered Structures," by J. Lysmer and L.A. Drake 1970 (PB 197 896)A03
- EERC 70-7 "Influence of Base Rock Characteristics on Ground Response," by J. Lysmer, H.B. Seed and P.B. Schnabel 1970 (PB 197 897)A03
- EERC 70-8 "Applicability of Laboratory Test Procedures for Measuring Soil Liquefaction Characteristics under Cyclic Loading," by H.B. Seed and W.H. Peacock - 1970 (PB 198 016)A03
- EERC 70-9 "A Simplified Procedure for Evaluating Soil Liquefaction Potential," by H.B. Seed and I.M. Idriss - 1970 (PB 198 009)A03
- EERC 70-10 "Soil Moduli and Damping Factors for Dynamic Response Analysis," by H.B. Seed and I.M. Idriss - 1970 (PB 197 869)A03
- EERC 71-1 "Koyna Earthquake of December 11, 1967 and the Performance of Koyna Dam," by A.K. Chopra and P. Chakrabarti 1971 (AD 731 496)A06
- EERC 71-2 "Preliminary In-Situ Measurements of Anelastic Absorption in Soils Using a Prototype Earthquake Simulator," by R.D. Borcherdt and P.W. Rodgers - 1971 (PB 201 454)A03
- EERC 71-3 "Static and Dynamic Analysis of Inelastic Frame Structures," by F.L. Porter and G.H. Powell - 1971 (PB 210 135)A06
- EERC 71-4 "Research Needs in Limit Design of Reinforced Concrete Structures," by V.V. Bertero - 1971 (PB 202 943)A04
- EERC 71-5 "Dynamic Behavior of a High-Rise Diagonally Braced Steel Building," by D. Rea, A.A. Shah and G.G. Bowknap 1971 (PB 203 584)A06
- EERC 71-6 "Dynamic Stress Analysis of Porous Elastic Solids Saturated with Compressible Fluids," by J. Ghaboussi and E. L. Wilson - 1971 (PB 211 396)A06
- EERC 71-7 "Inelastic Behavior of Steel Beam-to-Column Subassemblages," by H. Krawinkler, V.V. Bertero and E.P. Popov 1971 (PB 211 335)A14
- EERC 71-8 "Modification of Seismograph Records for Effects of Local Soil Conditions," by P. Schnabel, H.B. Seed and J. Lysmer - 1971 (PB 214 450)A03
- EERC 72-1 "Static and Earthquake Analysis of Three Dimensional Frame and Shear Wall Buildings," by E.L. Wilson and H.H. Dovey - 1972 (PB 212 904)A05
- EERC 72-2 "Accelerations in Rock for Earthquakes in the Western United States," by P.B. Schnabel and H.B. Seed - 1972 (PB 213 100)A03
- EERC 72-3 "Elastic-Plastic Earthquake Response of Soil-Building Systems," by T. Minami - 1972 (PB 214 868)A08
- EERC 72-4 "Stochastic Inelastic Response of Offshore Towers to Strong Motion Earthquakes," by M.K. Kaul - 1972 (PB 215 713)A05
- EERC 72-5 "Cyclic Behavior of Three Reinforced Concrete Flexural Members with High Shear," by E.P. Popov, V.V. Bertero and H. Krawinkler - 1972 (PB 214 555)A05
- EERC 72-6 "Earthquake Response of Gravity Dams Including Reservoir Interaction Effects," by P. Chakrabarti and A.K. Chopra - 1972 (AD 762 330)A08
- EERC 72-7 "Dynamic Properties of Pine Flat Dam," by D. Rea, C.Y. Liaw and A.K. Chopra - 1972 (AD 763 928)A05
- EERC 72-8 "Three Dimensional Analysis of Building Systems," by E.L. Wilson and H.H. Dovey - 1972 (PB 222 438)A06
- EERC 72-9 "Rate of Loading Effects on Uncracked and Repaired Reinforced Concrete Members," by S. Mahin, V.V. Bertero, D. Rea and M. Atalay - 1972 (PB 224 520)A08
- EERC 72-10 "Computer Program for Static and Dynamic Analysis of Linear Structural Systems," by E.L. Wilson, K.-J. Bathe, J.E. Peterson and H.H. Dovey - 1972 (PB 220 437)A04
- EERC 72-11 "Literature Survey - Seismic Effects on Highway Bridges," by T. Iwasaki, J. Penzien and R.W. Clough - 1972 (PB 215 613)A19
- EERC 72-12 "SHAKE-A Computer Program for Earthquake Response Analysis of Horizontally Layered Sites," by P.B. Schnabel and J. Lysmer - 1972 (PB 220 207)A06
- EERC 73-1 "Optimal Seismic Design of Multistory Frames," by V.V. Bertero and H. Kamil - 1973
- EERC 73-2 "Analysis of the Slides in the San Fernando Dams During the Earthquake of February 9, 1971," by H.B. Seed, K.L. Lee, I.M. Idriss and F. Makdisi - 1973 (PB 223 402)A14

- EERC 73-3 "Computer Aided Ultimate Load Design of Unbraced Multistory Steel Frames," by M.B. El-Hafez and G.H. Powell 1973 (PB 248 315)A09
- EERC 73-4 "Experimental Investigation into the Seismic Behavior of Critical Regions of Reinforced Concrete Components as Influenced by Moment and Shear," by M. Celebi and J. Penzien - 1973 (PB 215 884)A09
- EERC 73-5 "Hysteretic Behavior of Epoxy-Repaired Reinforced Concrete Beams," by M. Celebi and J. Penzien - 1973 (PB 239 568)A03
- EERC 73-6 "General Purpose Computer Program for Inelastic Dynamic Response of Plane Structures," by A. Kanaan and G.H. Powell - 1973 (PB 221 260)A08
- EERC 73-7 "A Computer Program for Earthquake Analysis of Gravity Dams Including Reservoir Interaction," by P. Chakrabarti and A.K. Chopra - 1973 (AD 766 271)A04
- EERC 73-8 "Behavior of Reinforced Concrete Deep Beam-Column Subassemblages Under Cyclic Loads," by O. Küstü and J.G. Bouwkamp - 1973 (PB 246 117)A12
- EERC 73-9 "Earthquake Analysis of Structure-Foundation Systems," by A.K. Vaish and A.K. Chopra - 1973 (AD 766 272)A07
- EERC 73-10 "Deconvolution of Seismic Response for Linear Systems," by R.B. Reimer - 1973 (PB 227 179)A08
- EERC 73-11 "SAP IV: A Structural Analysis Program for Static and Dynamic Response of Linear Systems," by K.-J. Bathe, E.L. Wilson and F.E. Peterson - 1973 (PB 221 967)A09
- EERC 73-12 "Analytical Investigations of the Seismic Response of Long, Multiple Span Highway Bridges," by W.S. Tseng and J. Penzien - 1973 (PB 227 816)A10
- EERC 73-13 "Earthquake Analysis of Multi-Story Buildings Including Foundation Interaction," by A.K. Chopra and J.A. Gutierrez - 1973 (PB 222 970)A03
- EERC 73-14 "ADAP: A Computer Program for Static and Dynamic Analysis of Arch Dams," by R.W. Clough, J.M. Raphael and S. Mojtahedi - 1973 (PB 223 763)A09
- EERC 73-15 "Cyclic Plastic Analysis of Structural Steel Joints," by R.B. Pinkney and R.W. Clough - 1973 (PB 226 843)A08
- EERC 73-16 "QUAD-4: A Computer Program for Evaluating the Seismic Response of Soil Structures by Variable Damping Finite Element Procedures," by I.M. Idriss, J. Lysmer, R. Hwang and H.B. Seed - 1973 (PB 229 424)A05
- EERC 73-17 "Dynamic Behavior of a Multi-Story Pyramid Shaped Building," by R.M. Stephen, J.P. Hollings and J.G. Bouwkamp - 1973 (PB 240 718)A06
- EERC 73-18 "Effect of Different Types of Reinforcing on Seismic Behavior of Short Concrete Columns," by V.V. Bertero, J. Hollings, O. Küstü, R.M. Stephen and J.G. Bouwkamp - 1973
- EERC 73-19 "Olive View Medical Center Materials Studies, Phase I," by B. Bresler and V.V. Bertero - 1973 (PB 235 986)A06
- EERC 73-20 "Linear and Nonlinear Seismic Analysis Computer Programs for Long Multiple-Span Highway Bridges," by W.S. Tseng and J. Penzien - 1973
- EERC 73-21 "Constitutive Models for Cyclic Plastic Deformation of Engineering Materials," by J.M. Kelly and P.P. Gillis 1973 (PB 226 024)A03
- EERC 73-22 "DRAIN - 2D User's Guide," by G.H. Powell - 1973 (PB 227 016)A05
- EERC 73-23 "Earthquake Engineering at Berkeley - 1973," (PB 226 033)A11
- EERC 73-24 Unassigned
- EERC 73-25 "Earthquake Response of Axisymmetric Tower Structures Surrounded by Water," by C.Y. Liaw and A.K. Chopra 1973 (AD 773 052)A09
- EERC 73-26 "Investigation of the Failures of the Olive View Stairtowers During the San Fernando Earthquake and Their Implications on Seismic Design," by V.V. Bertero and R.G. Collins - 1973 (PB 235 106)A13
- EERC 73-27 "Further Studies on Seismic Behavior of Steel Beam-Column Subassemblages," by V.V. Bertero, H. Krawinkler and E.P. Popov - 1973 (PB 234 172)A06
- EERC 74-1 "Seismic Risk Analysis," by C.S. Oliveira - 1974 (PB 235 920)A06
- EERC 74-2 "Settlement and Liquefaction of Sands Under Multi-Directional Shaking," by R. Pyke, C.K. Chan and H.B. Seed 1974
- EERC 74-3 "Optimum Design of Earthquake Resistant Shear Buildings," by D. Ray, K.S. Pister and A.K. Chopra - 1974 (PB 231 172)A06
- EERC 74-4 "LUSH - A Computer Program for Complex Response Analysis of Soil-Structure Systems," by J. Lysmer, T. Udaka, H.B. Seed and R. Hwang - 1974 (PB 236 796)A05

- EERC 74-5 "Sensitivity Analysis for Hysteretic Dynamic Systems: Applications to Earthquake Engineering," by D. Ray 1974 (PB 233 213)A06
- EERC 74-6 "Soil Structure Interaction Analyses for Evaluating Seismic Response," by H.B. Seed, J. Lysmer and R. Hwang 1974 (PB 236 519)A04
- EERC 74-7 Unassigned
- EERC 74-8 "Shaking Table Tests of a Steel Frame - A Progress Report," by R.W. Clough and D. Tang - 1974 (PB 240 869)A03
- EERC 74-9 "Hysteretic Behavior of Reinforced Concrete Flexural Members with Special Web Reinforcement," by V.V. Bertero, E.P. Popov and T.Y. Wang - 1974 (PB 236 797)A07
- EERC 74-10 "Applications of Reliability-Based, Global Cost Optimization to Design of Earthquake Resistant Structures," by E. Vitiello and K.S. Pister - 1974 (PB 237 231)A06
- EERC 74-11 "Liquefaction of Gravelly Soils Under Cyclic Loading Conditions," by R.T. Wong, H.B. Seed and C.K. Chan 1974 (PB 242 042)A03
- EERC 74-12 "Site-Dependent Spectra for Earthquake-Resistant Design," by H.B. Seed, C. Ugas and J. Lysmer - 1974 (PB 240 953)A03
- EERC 74-13 "Earthquake Simulator Study of a Reinforced Concrete Frame," by P. Hidalgo and R.W. Clough - 1974 (PB 241 944)A13
- EERC 74-14 "Nonlinear Earthquake Response of Concrete Gravity Dams," by N. Pal - 1974 (AD/A 006 583)A06
- EERC 74-15 "Modeling and Identification in Nonlinear Structural Dynamics - I. One Degree of Freedom Models," by N. Distefano and A. Rath - 1974 (PB 241 548)A06
- EERC 75-1 "Determination of Seismic Design Criteria for the Dumbarton Bridge Replacement Structure, Vol. I: Description, Theory and Analytical Modeling of Bridge and Parameters," by F. Baron and S.-H. Pang - 1975 (PB 259 407)A15
- EERC 75-2 "Determination of Seismic Design Criteria for the Dumbarton Bridge Replacement Structure, Vol. II: Numerical Studies and Establishment of Seismic Design Criteria," by F. Baron and S.-H. Pang - 1975 (PB 259 408)A11 (For set of EERC 75-1 and 75-2 (PB 259 406))
- EERC 75-3 "Seismic Risk Analysis for a Site and a Metropolitan Area," by C.S. Oliveira - 1975 (PB 248 134)A09
- EERC 75-4 "Analytical Investigations of Seismic Response of Short, Single or Multiple-Span Highway Bridges," by M.-C. Chen and J. Penzien - 1975 (PB 241 454)A09
- EERC 75-5 "An Evaluation of Some Methods for Predicting Seismic Behavior of Reinforced Concrete Buildings," by S.A. Mahin and V.V. Bertero - 1975 (PB 246 306)A16
- EERC 75-6 "Earthquake Simulator Study of a Steel Frame Structure, Vol. I: Experimental Results," by R.W. Clough and D.T. Tang - 1975 (PB 243 981)A13
- EERC 75-7 "Dynamic Properties of San Bernardino Intake Tower," by D. Rea, C.-Y. Liaw and A.K. Chopra - 1975 (AD/A008 406) A05
- EERC 75-8 "Seismic Studies of the Articulation for the Dumbarton Bridge Replacement Structure, Vol. I: Description, Theory and Analytical Modeling of Bridge Components," by F. Baron and R.E. Hamati - 1975 (PB 251 539)A07
- EERC 75-9 "Seismic Studies of the Articulation for the Dumbarton Bridge Replacement Structure, Vol. 2: Numerical Studies of Steel and Concrete Girder Alternates," by F. Baron and R.E. Hamati - 1975 (PB 251 540)A10
- EERC 75-10 "Static and Dynamic Analysis of Nonlinear Structures," by D.P. Mondkar and G.H. Powell - 1975 (PB 242 434)A08
- EERC 75-11 "Hysteretic Behavior of Steel Columns," by E.P. Popov, V.V. Bertero and S. Chandramouli - 1975 (PB 252 365)A11
- EERC 75-12 "Earthquake Engineering Research Center Library Printed Catalog," - 1975 (PB 243 711)A26
- EERC 75-13 "Three Dimensional Analysis of Building Systems (Extended Version)," by E.L. Wilson, J.P. Hollings and H.H. Dovey - 1975 (PB 243 989)A07
- EERC 75-14 "Determination of Soil Liquefaction Characteristics by Large-Scale Laboratory Tests," by P. De Alba, C.K. Chan and H.B. Seed - 1975 (NUREG 0027)A08
- EERC 75-15 "A Literature Survey - Compressive, Tensile, Bond and Shear Strength of Masonry," by R.L. Mayes and R.W. Clough - 1975 (PB 246 292)A10
- EERC 75-16 "Hysteretic Behavior of Ductile Moment Resisting Reinforced Concrete Frame Components," by V.V. Bertero and E.P. Popov - 1975 (PB 246 388)A05
- EERC 75-17 "Relationships Between Maximum Acceleration, Maximum Velocity, Distance from Source, Local Site Conditions for Moderately Strong Earthquakes," by H.B. Seed, R. Murarka, J. Lysmer and I.M. Idriss - 1975 (PB 248 172)A03
- EERC 75-18 "The Effects of Method of Sample Preparation on the Cyclic Stress-Strain Behavior of Sands," by J. Mulilis, C.K. Chan and H.B. Seed - 1975 (Summarized in EERC 75-28)

- EERC 75-19 "The Seismic Behavior of Critical Regions of Reinforced Concrete Components as Influenced by Moment, Shear and Axial Force," by M.B. Atalay and J. Penzien - 1975 (PB 258 842)A11
- EERC 75-20 "Dynamic Properties of an Eleven Story Masonry Building," by R.M. Stephen, J.P. Hollings, J.G. Bouwkamp and D. Jurukovski - 1975 (PB 246 945)A04
- EERC 75-21 "State-of-the-Art in Seismic Strength of Masonry - An Evaluation and Review," by R.L. Mayes and R.W. Clough - 1975 (PB 249 040)A07
- EERC 75-22 "Frequency Dependent Stiffness Matrices for Viscoelastic Half-Plane Foundations," by A.K. Chopra, P. Chakrabarti and G. Dasgupta - 1975 (PB 248 121)A07
- EERC 75-23 "Hysteretic Behavior of Reinforced Concrete Framed Walls," by T.Y. Wong, V.V. Bertero and E.P. Popov - 1975
- EERC 75-24 "Testing Facility for Subassemblages of Frame-Wall Structural Systems," by V.V. Bertero, E.P. Popov and T. Endo - 1975
- EERC 75-25 "Influence of Seismic History on the Liquefaction Characteristics of Sands," by H.B. Seed, K. Mori and C.K. Chan - 1975 (Summarized in EERC 75-28)
- EERC 75-26 "The Generation and Dissipation of Pore Water Pressures during Soil Liquefaction," by H.B. Seed, P.P. Martin and J. Lysmer - 1975 (PB 252 648)A03
- EERC 75-27 "Identification of Research Needs for Improving Aseismic Design of Building Structures," by V.V. Bertero - 1975 (PB 248 136)A05
- EERC 75-28 "Evaluation of Soil Liquefaction Potential during Earthquakes," by H.B. Seed, I. Arango and C.K. Chan - 1975 (NUREG 0026)A13
- EERC 75-29 "Representation of Irregular Stress Time Histories by Equivalent Uniform Stress Series in Liquefaction Analyses," by H.B. Seed, I.M. Idriss, F. Makdisi and N. Banerjee - 1975 (PB 252 635)A03
- EERC 75-30 "FLUSH - A Computer Program for Approximate 3-D Analysis of Soil-Structure Interaction Problems," by J. Lysmer, T. Udaka, C.-F. Tsai and H.B. Seed - 1975 (PB 259 332)A07
- EERC 75-31 "ALUSH - A Computer Program for Seismic Response Analysis of Axisymmetric Soil-Structure Systems," by E. Berger, J. Lysmer and H.B. Seed - 1975
- EERC 75-32 "TRIP and TRAVEL - Computer Programs for Soil-Structure Interaction Analysis with Horizontally Travelling Waves," by T. Udaka, J. Lysmer and H.B. Seed - 1975
- EERC 75-33 "Predicting the Performance of Structures in Regions of High Seismicity," by J. Penzien - 1975 (PB 248 130)A03
- EERC 75-34 "Efficient Finite Element Analysis of Seismic Structure - Soil - Direction," by J. Lysmer, H.B. Seed, T. Udaka, R.N. Hwang and C.-F. Tsai - 1975 (PB 253 570)A03
- EERC 75-35 "The Dynamic Behavior of a First Story Girder of a Three-Story Steel Frame Subjected to Earthquake Loading," by R.W. Clough and L.-Y. Li - 1975 (PB 248 841)A05
- EERC 75-36 "Earthquake Simulator Study of a Steel Frame Structure, Volume II - Analytical Results," by D.T. Tang - 1975 (PB 252 926)A10
- EERC 75-37 "ANSR-I General Purpose Computer Program for Analysis of Non-Linear Structural Response," by D.P. Mondkar and G.H. Powell - 1975 (PB 252 386)A08
- EERC 75-38 "Nonlinear Response Spectra for Probabilistic Seismic Design and Damage Assessment of Reinforced Concrete Structures," by M. Murakami and J. Penzien - 1975 (PB 259 530)A05
- EERC 75-39 "Study of a Method of Feasible Directions for Optimal Elastic Design of Frame Structures Subjected to Earthquake Loading," by N.D. Walker and K.S. Pister - 1975 (PB 257 781)A06
- EERC 75-40 "An Alternative Representation of the Elastic-Viscoelastic Analogy," by G. Dasgupta and J.L. Sackman - 1975 (PB 252 173)A03
- EERC 75-41 "Effect of Multi-Directional Shaking on Liquefaction of Sands," by H.B. Seed, R. Pyke and G.R. Martin - 1975 (PB 258 781)A03
- EERC 76-1 "Strength and Ductility Evaluation of Existing Low-Rise Reinforced Concrete Buildings - Screening Method," by T. Okada and B. Bresler - 1976 (PB 257 906)A11
- EERC 76-2 "Experimental and Analytical Studies on the Hysteretic Behavior of Reinforced Concrete Rectangular and T-Beams," by S.-Y.M. Ma, E.P. Popov and V.V. Bertero - 1976 (PB 260 843)A12
- EERC 76-3 "Dynamic Behavior of a Multistory Triangular-Shaped Building," by J. Petrovski, R.M. Stephen, E. Gartenbaum and J.G. Bouwkamp - 1976
- EERC 76-4 "Earthquake Induced Deformations of Earth Dams," by N. Serff and H.B. Seed - 1976

- EERC 76-5 "Analysis and Design of Tube-Type Tall Building Structures," by H. de Clercq and G.H. Powell - 1976 (PB 252 220) A10
- EERC 76-6 "Time and Frequency Domain Analysis of Three-Dimensional Ground Motions, San Fernando Earthquake," by T. Kubo and J. Penzien (PB 260 556)A11
- EERC 76-7 "Expected Performance of Uniform Building Code Design Masonry Structures," by R.L. Mayes, Y. Omote, S.W. Chen and R.W. Clough - 1976
- EERC 76-8 "Cyclic Shear Tests on Concrete Masonry Piers," Part I - Test Results," by R.L. Mayes, Y. Omote and R.W. Clough - 1976 (PB 264 424)A06
- EERC 76-9 "A Substructure Method for Earthquake Analysis of Structure - Soil Interaction," by J.A. Gutierrez and A.K. Chopra - 1976 (PB 257 783)A08
- EERC 76-10 "Stabilization of Potentially Liquefiable Sand Deposits using Gravel Drain Systems," by H.B. Seed and J.R. Booker - 1976 (PB 258 820)A04
- EERC 76-11 "Influence of Design and Analysis Assumptions on Computed Inelastic Response of Moderately Tall Frames," by G.H. Powell and D.G. Row - 1976
- EERC 76-12 "Sensitivity Analysis for Hysteretic Dynamic Systems: Theory and Applications," by D. Ray, K.S. Pister and E. Polak - 1976 (PB 262 859)A04
- EERC 76-13 "Coupled Lateral Torsional Response of Buildings to Ground Shaking," by C.L. Kan and A.K. Chopra - 1976 (PB 257 907)A09
- EERC 76-14 "Seismic Analyses of the Banco de America," by V.V. Bertero, S.A. Mahin and J.A. Hollings - 1976
- EERC 76-15 "Reinforced Concrete Frame 2: Seismic Testing and Analytical Correlation," by R.W. Clough and J. Gidwani - 1976 (PB 261 323)A08
- EERC 76-16 "Cyclic Shear Tests on Masonry Piers, Part II - Analysis of Test Results," by R.L. Mayes, Y. Omote and R.W. Clough - 1976
- EERC 76-17 "Structural Steel Bracing Systems: Behavior Under Cyclic Loading," by E.P. Popov, K. Takanashi and C.W. Roeder - 1976 (PB 260 715)A05
- EERC 76-18 "Experimental Model Studies on Seismic Response of High Curved Overcrossings," by D. Williams and W.G. Godden - 1976
- EERC 76-19 "Effects of Non-Uniform Seismic Disturbances on the Dumbarton Bridge Replacement Structure," by F. Baron and R.E. Hamati - 1976
- EERC 76-20 "Investigation of the Inelastic Characteristics of a Single Story Steel Structure Using System Identification and Shaking Table Experiments," by V.C. Matzen and H.D. McNiven - 1976 (PB 258 453)A07
- EERC 76-21 "Capacity of Columns with Splice Imperfections," by E.P. Popov, R.M. Stephen and R. Philbrick - 1976 (PB 260 378)A04
- EERC 76-22 "Response of the Olive View Hospital Main Building during the San Fernando Earthquake," by S. A. Mahin, R. Collins, A.K. Chopra and V.V. Bertero - 1976
- EERC 76-23 "A Study on the Major Factors Influencing the Strength of Masonry Prisms," by N.M. Mostaghel, R.L. Mayes, R. W. Clough and S.W. Chen - 1976
- EERC 76-24 "GADFLER - A Computer Program for the Analysis of Pore Pressure Generation and Dissipation during Cyclic or Earthquake Loading," by J.R. Booker, M.S. Rahman and H.B. Seed - 1976 (PB 263 947)A04
- EERC 76-25 "Rehabilitation of an Existing Building: A Case Study," by B. Bresler and J. Axley - 1976
- EERC 76-26 "Correlative Investigations on Theoretical and Experimental dynamic Behavior of a Model Bridge Structure," by K. Kawashima and J. Penzien - 1976 (PB 263 388)A11
- EERC 76-27 "Earthquake Response of Coupled Shear Wall Buildings," by T. Srichatrapimuk - 1976 (PB 265 157)A07
- EERC 76-28 "Tensile Capacity of Partial Penetration Welds," by E.P. Popov and R.M. Stephen - 1976 (PB 262 899)A03
- EERC 76-29 "Analysis and Design of Numerical Integration Methods in Structural Dynamics," by H.M. Hilber - 1976 (PB 264 410)A06
- EERC 76-30 "Contribution of a Floor System to the Dynamic Characteristics of Reinforced Concrete Buildings," by L.J. Edgar and V.V. Bertero - 1976
- EERC 76-31 "The Effects of Seismic Disturbances on the Golden Gate Bridge," by F. Baron, M. Arikan and R.E. Hamati - 1976
- EERC 76-32 "Infilled Frames in Earthquake Resistant Construction," by R.E. Klingner and V.V. Bertero - 1976 (PB 265 892)A13

- UCB/EERC-77/01 "PLUSH - A Computer Program for Probabilistic Finite Element Analysis of Seismic Soil-Structure Interaction," by M.P. Romo Organista, J. Lysmer and H.B. Seed - 1977
- UCB/EERC-77/02 "Soil-Structure Interaction Effects at the Humboldt Bay Power Plant in the Ferndale Earthquake of June 7, 1975," by J.E. Valera, H.B. Seed, C.F. Tsai and J. Lysmer - 1977 (PB 265 795)A04
- UCB/EERC-77/03 "Influence of Sample Disturbance on Sand Response to Cyclic Loading," by K. Mori, H.B. Seed and C.K. Chan - 1977 (PB 267 352)A04
- UCB/EERC-77/04 "Seismological Studies of Strong Motion Records," by J. Shoja-Taheri - 1977 (PB 269 655)A10
- UCB/EERC-77/05 "Testing Facility for Coupled-Shear Walls," by L. Li-Hyung, V.V. Bertero and E.P. Popov - 1977
- UCB/EERC-77/06 "Developing Methodologies for Evaluating the Earthquake Safety of Existing Buildings," by No. 1 - B. Bresler; No. 2 - B. Bresler, T. Okada and D. Zisling; No. 3 - T. Okada and B. Bresler; No. 4 - V.V. Bertero and B. Bresler - 1977 (PB 267 354)A08
- UCB/EERC-77/07 "A Literature Survey - Transverse Strength of Masonry Walls," by Y. Omote, R.L. Mayes, S.W. Chen and R.W. Clough - 1977
- UCB/EERC-77/08 "DRAIN-TABS: A Computer Program for Inelastic Earthquake Response of Three Dimensional Buildings," by R. Guendelman-Israel and G.H. Powell - 1977 (PB 270 693)A07
- UCB/EERC-77/09 "SUBWALL: A Special Purpose Finite Element Computer Program for Practical Elastic Analysis and Design of Structural Walls with Substructure Option," by D.Q. Le, H. Peterson and E.P. Popov - 1977 (PB 270 567)A05
- UCB/EERC-77/10 "Experimental Evaluation of Seismic Design Methods for Broad Cylindrical Tanks," by D.P. Clough
- UCB/EERC-77/11 "Earthquake Engineering Research at Berkeley - 1976," - 1977
- UCB/EERC-77/12 "Automated Design of Earthquake Resistant Multistory Steel Building Frames," by N.D. Walker, Jr. - 1977
- UCB/EERC-77/13 "Concrete Confined by Rectangular Hoops Subjected to Axial Loads," by D. Zalinas, V.V. Bertero and E.P. Popov - 1977
- UCB/EERC-77/14 "Seismic Strain Induced in the Ground During Earthquakes," by Y. Sugimura - 1977
- UCB/EERC-77/15 "Bond Deterioration under Generalized Loading," by V.V. Bertero, E.P. Popov and S. Viathanatepa - 1977

- UCB/EERC-77/16 "Computer Aided Optimum Design of Ductile Reinforced Concrete Moment Resisting Frames," by S.W. Zagajeski and V.V. Bertero - 1977
- UCB/EERC-77/17 "Earthquake Simulation Testing of a Stopping Frame with Energy-Absorbing Devices," by J.M. Kelly and D.F. Tsztoo 1977
- UCB/EERC-77/18 "Inelastic Behavior of Eccentrically Braced Steel Frames under Cyclic Loadings," by C.W. Roeder and E.P. Popov - 1977
- UCB/EERC-77/19 "A Simplified Procedure for Estimating Earthquake-Induced Deformations in Dams and Embankments," by F.I. Makdisi and H.B. Seed - 1977
- UCB/EERC-77/20 "The Performance of Earth Dams during Earthquakes," by H.B. Seed, F.I. Makdisi and P. de Alba - 1977
- UCB/EERC-77/21 "Dynamic Plastic Analysis Using Stress Resultant Finite Element Formulation," by P. Lukkunapvasit and J.M. Kelly 1977
- UCB/EERC-77/22 "Preliminary Experimental Study of Seismic Uplift of a Steel Frame," by R.W. Clough and A.A. Huckelbridge - 1977
- UCB/EERC-77/23 "Earthquake Simulator Tests of a Nine-Story Steel Frame with Columns Allowed to Uplift," by A.A. Huckelbridge - 1977
- UCB/EERC-77/24 "Nonlinear Soil-Structure Interaction of Skew Highway Bridges," by M.-C. Chen and Joseph Penzien - 1977
- UCB/EERC-77/25 "Seismic Analysis of an Offshore Structure Supported on Pile Foundations," by D.D.-N. Liou - 1977
- UCB/EERC-77/26 "Dynamic Stiffness Matrices for Homogeneous Viscoelastic Half-Planes," by G. Dasgupta and A.K. Chopra - 1977
- UCB/EERC-77/27 "A Practical Soft Story Earthquake Isolation System," by J.M. Kelly and J.M. Eidinger - 1977
- UCB/EERC-77/28 "Seismic Safety of Existing Buildings and Incentives for Hazard Mitigation in San Francisco: An Exploratory Study," by A. J. Meltsner - 1977
- UCB/EERC-77/29 "Dynamic Analysis of Electrohydraulic Shaking Tables," by D. Rea, S. Abedi-Hayati and Y. Takahashi - 1977
- UCB/EERC-77/30 "An Approach for Improving Seismic-Resistant Behavior of Reinforced Concrete Interior Joints," by B. Galunic, V.V. Bertero and E.P. Popov - 1977

- UCB/EERC-78/01 "The Development of Energy-Absorbing Devices for Aseismic Base Isolation Systems," by J.M. Kelly and D.F. Tsztoo 1978
- UCB/EERC-78/02 "Effect of Tensile Prestrain on the Cyclic Response of Structural Steel Connections," by J.G. Bouwkamp and A. Mukhopadhyay - 1978
- UCB/EERC-78/03 "Experimental Results of an Earthquake Isolation System using Natural Rubber Bearings," by J.M. Eidinger and J.M. Kelly - 1978
- UCB/EERC-78/04 "Seismic Behavior of Tall Liquid Storage Tanks," by A. Niwa 1978
- UCB/EERC-78/05 "Hysteretic Behavior of Reinforced Concrete Columns Subjected to High Axial and Cyclic Shear Forces," by S.W. Zagajeski, V.V. Bertero and J.G. Bouwkamp - 1978
- UCB/EERC-78/06 "Inelastic Beam-Column Elements for the ANSR-I Program," by A. Riahi, D.G. Row and G.H. Powell - 1978
- UCB/EERC-78/07 "Studies of Structural Response to Earthquake Ground Motion," by O.A. Lopez and A.K. Chopra - 1978
- UCB/EERC-78/08 "A Laboratory Study of the Fluid-Structure Interaction of Submerged Tanks and Caissons in Earthquakes," by R.C. Byrd - 1978